AD_____

Award Number: W81XWH-07-2-0034

TITLE: Mass spectrometry to identify new biomarkers of nerve agent exposure

PRINCIPAL INVESTIGATOR: Oksana Lockridge Ph.D.

CONTRACTING ORGANIZATION: University of Nebraska Medical Center
Omaha, NE 55198-7835

REPORT DATE: April 2008

TYPE OF REPORT: Annual

PREPARED FOR: U.S. Army Medical Research and Materiel Command
Fort Detrick, Maryland 21702-5012

REPORT DOCUMENTATION PAGE

Form Approved
OMB No. 0704-0188

Public reporting burden for this collection of information is estimated to average 1 hour per response, including the time for reviewing instructions, searching existing data sources, gathering and maintaining the data needed, and completing and reviewing this collection of information. Send comments regarding this burden estimate or any other aspect of this collection of information, including suggestions for reducing this burden to Department of Defense, Washington Headquarters Services, Directorate for Information Operations and Reports (0704-0188), 1215 Jefferson Davis Highway, Suite 1204, Arlington, VA 22202-4302. Respondents should be aware that notwithstanding any other provision of law, no person shall be subject to any penalty for failing to comply with a collection of information if it does not display a currently valid OMB control number. **PLEASE DO NOT RETURN YOUR FORM TO THE ABOVE ADDRESS.**

1. REPORT DATE 30-04-2008	2. REPORT TYPE Annual	3. DATES COVERED 1 APR 2007 - 31 MAR 2008

4. TITLE AND SUBTITLE Mass spectrometry to identify new biomarkers of nerve agent exposure	5a. CONTRACT NUMBER
	5b. GRANT NUMBER W81XWH-07-2-0034
	5c. PROGRAM ELEMENT NUMBER

6. AUTHOR(S) Oksana Lockridge Ph.D. Email: olockrid@unmc.edu	5d. PROJECT NUMBER
	5e. TASK NUMBER
	5f. WORK UNIT NUMBER

7. PERFORMING ORGANIZATION NAME(S) AND ADDRESS(ES) University of Nebraska Medical Center Omaha, NE 55198-7835	8. PERFORMING ORGANIZATION REPORT NUMBER

9. SPONSORING / MONITORING AGENCY NAME(S) AND ADDRESS(ES) U.S. Army Medical Research and Materiel Command Fort Detrick, Maryland 21702-5012	10. SPONSOR/MONITOR'S ACRONYM(S)
	11. SPONSOR/MONITOR'S REPORT NUMBER(S)

12. DISTRIBUTION / AVAILABILITY STATEMENT
Approved for Public Release; Distribution Unlimited

13. SUPPLEMENTARY NOTES

14. ABSTRACT
Organophosphorus esters (OP) are known to make a covalent bond with the active site serine in the consensus sequence GXSXG of esterases and proteases. However, the site of attachment to proteins that have no active site serine is unknown. Human plasma as well as pure albumin, transferrin, tubulin, and synthetic peptides were treated with soman, sarin, DFP, chlorpyrifos oxon, dichlorvos, and FP-biotin. The site of covalent attachment of OP was determined by fragmentation in the QTRAP mass spectrometer. It was found that OP made a covalent bond with tyrosine in every protein and synthetic peptide tested. The reactive tyrosines were near an arginine or lysine. OP-tyrosine adducts were stable and did not undergo aging. In conclusion, a new OP binding motif has been identified. Recognition of this new OP binding motif may lead to an explanation of noncholinergic effects of OP and of chronic illness from low dose exposure.

15. SUBJECT TERMS
 mass spectrometry, organophosphorus nerve agent binding motif, detection, biomarker,

16. SECURITY CLASSIFICATION OF:			17. LIMITATION OF ABSTRACT	18. NUMBER OF PAGES	19a. NAME OF RESPONSIBLE PERSON USAMRMC
a. REPORT U	b. ABSTRACT U	c. THIS PAGE U	UU	89	19b. TELEPHONE NUMBER *(include area code)*

Standard Form 298 (Rev. 8-98)
Prescribed by ANSI Std. Z39.18

Table of Contents

Li B, Nachon F, Froment MT, Verdier L, Debouzy JC, Brasme B, Gillon E, Schopfer LM, Masson P (2008) Binding and hydrolysis of soman by human serum albumin. *Chem Res Toxicol* 21: 421-431.

ABBREVIATIONS

amu	atomic mass unit
BChE	butyrylcholinesterase
CAM	carbamidomethylated cysteine
CHCA	alpha-cyano 4-hydoxycinnamic acid; matrix for MALDI
CPO	chlorpyrifos oxon
DFP	diisopropylfluorophosphate
FENTA	ferric nitrilotriacetate
FPB	FP-biotin
FP-biotin	biotin-tagged organophosphorus agent; 10-fluoroethoxyphosphinyl-N-biotinamidopentyldecanamide
HPLC	high performance liquid chromatography
LC/MS/MS	liquid chromatography coupled to tandem mass spectrometry
MALDI-TOF	matrix assisted laser desorption ionization-time of flight mass spectrometer
MS/MS	tandem mass spectrometry in which the mass of a molecule is determine in the first MS and the masses of the fragments are determined in the second MS
m/z	mass to charge ratio
OP	organophosphorus toxicant
PAGE	polyacrylamide gel electrophoresis
PVDF	polyvinylidene fluoride membrane for protein blots
SDS	sodium dodecyl sulfate
TFA	trifluoroacetic acid
UCSF	University of California San Francisco
Y	single letter code for tyrosine

INTRODUCTION

There is overwhelming evidence that the acute toxicity of organophosphorus nerve agents and pesticides (OP) is due to inhibition of acetylcholinesterase. The OP binds covalently to the active site serine to make an irreversible adduct. The OP-modified acetylcholinesterase is incapable of performing its physiological function of hydrolyzing the neurotransmitter acetylcholine. Excess acetylcholine overstimulates receptors, initiating a cascade of reactions that results in uncontrolled seizures and respiratory arrest (McDonough and Shih, 1997).

The active site serine of acetylcholinesterase is located in a conserved sequence GlyXSerXGly common to all serine esterases and serine proteases.

What is not understood is why some people suffer chronic illness from a dose of OP too low to inhibit acetylcholinesterase. The implication is that OP reactive proteins exist that are more sensitive than acetylcholinesterase to OP. When we began this work we assumed that these highly reactive proteins would have serine at the active site. But when we searched for these proteins using a biotinylated OP we consistently found proteins that had no active site serine. At first we suspected that the avidin beads had nonspecifically bound these proteins and that we were looking at artifacts. To convince ourselves that a protein like tubulin actually binds OP, we studied OP binding to pure tubulin. We used mass spectrometry to identify the OP binding site. The labeled amino acid was tyrosine. We studied other pure proteins, and finally synthetic peptides. A consistent pattern emerged of OP binding to tyrosine.

We believe that we have identified a new motif for OP binding to proteins. This report presents the evidence for our conclusion that OP bind not only to serine hydrolases but also to proteins that contain an activated tyrosine.

APPROVED STATEMENT OF WORK
Technical Objectives for the entire project.
1) To identify the proteins in human plasma that covalently bind soman. The method for identification is mass spectrometry.
2) To verify the identity of selected proteins as soman targets, by a second method, for example enzyme activity assays.
3) To determine nerve agent targets that react with a low dose of soman. Multiple Reaction Monitoring assays will be made on previously identified soman-binding proteins, after reacting plasma with low doses of soman.

Project Milestones
Year 1
1. The fragmentation of soman-labeled trypsin gives product
     ions of 179, 95, 79, 77 and 63 m/z in negative ion mode, and
     product ions of 181, 97, and 85m/z in positive ion mode.

2. The fragmentation of soman-labeled albumin gives the same
     product ions as soman-labeled trypsin except that there are
     more 77 m/z and fewer 95 m/z ions in negative ion mode.

3. MALDI-TOF analysis of FP-biotinylated proteins in human
     plasma shows the presence of positive control ions, 3503 m/z
     for the tryptic peptide of BChE and 984 m/z for the tryptic
     peptide of albumin, as well as additional ions.

4. LC/MS/MS of FP-biotinylated peptides derived from human
     plasma finds peptides that contain product ions of 227, 312,
     and 329 m/z.

5. Analysis of fragmentation patterns gives the sequence of 1
     to 20 FP-biotinylated peptides, and thereby reveals the
     identity of the proteins that were labeled by FP-biotin. It
     is assumed that these will also be labeled by soman.

Milestones 1 and 2
1. The fragmentation of soman-labeled trypsin gives product ions of 179, 95, 79, 77 and 63 m/z in negative ion mode, and product ions of 181, 97, and 85m/z in positive ion mode.
2. The fragmentation of soman-labeled albumin gives the same product ions as soman-labeled trypsin except that there are more 77 m/z and fewer 95 m/z ions in negative ion mode.
Relation to statement of work.   Results for milestones 1 and 2 are reported.

Binding and hydrolysis of soman by human serum albumin

Li B, Nachon F, Froment MT, Verdier L, Debouzy JC, Brasme B, Gillon E, Schopfer LM, Lockridge O, Masson P.

ABSTRACT
Human plasma and fatty acid free human albumin were incubated with soman at pH 8.0 and 25 °C. Four methods were used to monitor the reaction of albumin with soman: progressive inhibition of the aryl acylamidase activity of albumin, the release of fluoride ion from soman, 31P NMR, and mass spectrometry. Inhibition (phosphonylation) was slow with a bimolecular rate constant of 15 ± 3 M^{-1} min^{-1}. MALDI-TOF and tandem mass spectrometry of the soman-albumin adduct showed that albumin was phosphonylated on tyrosine 411. No secondary dealkylation of the adduct (aging) occurred. Covalent docking simulations and 31P NMR experiments showed that albumin has no enantiomeric preference for the four stereoisomers of soman. Spontaneous reactivation at pH 8.0 and 25 °C, measured as regaining of aryl acylamidase activity and decrease of covalent adduct (pinacolyl methylphosphonylated albumin) by NMR, occurred at a rate of 0.0044 h^{-1}, indicating that the adduct is quite stable ($t1/2 = 6.5$ days). At pH 7.4 and 22 °C, the covalent soman-albumin adduct, measured by MALDI-TOF mass spectrometry, was more stable ($t_{1/2} = 20$ days). Though the concentration of albumin in plasma is very high (about 0.6 mM), its reactivity with soman (phosphonylation and phosphotriesterase activity) is too slow to play a major role in detoxification of the highly toxic organophosphorus compound soman. Increasing the bimolecular rate constant of albumin for organophosphates is a protein engineering challenge that could lead to a new class of bioscavengers to be used against poisoning by nerve agents. Soman-albumin adducts detected by mass spectrometry could be useful for the diagnosis of soman exposure.

A pdf file of this publication is attached.

Milestones 3, 4, and 5
3. MALDI-TOF analysis of FP-biotinylated proteins in human plasma shows the presence of
     positive control ions, 3503 m/z for the tryptic peptide of BChE and 984 m/z for the tryptic
     peptide of albumin, as well as additional ions.
4. LC/MS/MS of FP-biotinylated peptides derived from human plasma finds peptides that
     contain product ions of 227, 312, and 329 m/z.
5. Analysis of fragmentation patterns gives the sequence of 1 to 20 FP-biotinylated peptides, and
     thereby reveals the identity of the proteins that were labeled by FP-biotin. It is assumed that
     these will also be labeled by soman.
Relation to statement of work.   Results for milestones 3, 4, and 5 are reported.

Five tyrosines and two serines in human albumin are labeled by the organophosphorus agent FP-biotin

ABSTRACT

Tyrosine 411 of human albumin is an established site for covalent attachment of FP-biotin,
diisopropylfluorophosphate, chlorpyrifos oxon, soman, sarin, and dichlorvos. This work
investigated the hypothesis that other residues in albumin could be modified by
organophosphorus agents (OP). Human plasma was aggressively treated with FP-biotin; plasma
proteins were separated into high and low abundant portions using a proteome partitioning
antibody kit, and the proteins were digested with trypsin.   The FP-biotinylated tryptic peptides
were isolated by binding to monomeric avidin beads. The major sites of covalent attachment
identified by mass spectrometry were Y138, Y148, Y401, Y411, Y452, S232 and S287 of human
albumin. Prolonged treatment of pure human albumin with chlorpyrifos oxon labeled Y138,
Y150, Y161, Y401, Y411 and Y452. To identify the most reactive residue, albumin was treated
for 2 h with DFP, FP-biotin, chlorpyrifos oxon, or soman, digested with trypsin or pepsin and
analyzed by mass spectrometry. The most reactive residue was always Tyr 411.
Diethylphosphate-labeled Tyr 411 was stable for months at pH 7.4. These results will be useful
in the development of specific antibodies to detect OP exposure, and to engineer albumin for use
as an OP scavenger.

INTRODUCTION

Albumin has been reported to covalently bind diisopropylfluorophosphate (DFP), sarin, soman,
cyclosarin, tabun, FP-biotin, chlorpyrifos oxon, and dichlorvos (Schwartz, 1982; Hagag et al.,
1983; Li et al., 2007; Williams et al., 2007; Li et al., 2008) and to hydrolyze chlorpyrifos oxon,
paraoxon (Sultatos et al., 1984) and O-hexyl O-2,5-dichlorophenyl phosphoramidate (Sogorb
and Vilanova, 2002).   Mass spectrometry has identified Tyrosine 411 of human albumin as the
site for covalent attachment of organophosphorus (OP) nerve agents and OP pesticides (Li et al.,

2007). A second site for covalent attachment of soman was suggested by experiments that found more fluoride ion released than could be accounted for by one site in albumin (Li et al., 2008). Pretreatment of albumin with decanoate, a lipid that binds to the Tyr 411 subdomain, inhibited incorporation of 91% of ^{3}H-DFP, leaving open the possibility that 9% of the ^{3}H-DFP bound to other sites (Means and Wu, 1979). In the present work, crystallization trials of chlorpyrifos oxon (CPO)-labeled human albumin yielded gelatinous soft amorphous crystals further suggesting the likelihood that more than one site was labeled and that labeling was not uniform. The goal of this study was to determine if sites in addition to Tyr 411 could make a covalent bond with OP, and to identify the labeled residues.

EXPERIMENTAL PROCEDURES

Materials. 10-Fluoroethoxyphosphinyl-N-biotinamidopentyldecanamide (FP-biotin, MW 592.32) was custom synthesized in the laboratory of Dr. Charles M. Thompson at the University of Montana, Missoula, MT (Schopfer et al., 2005). FP-biotin was dissolved in methanol and stored at -80˚C. Chlorpyrifos oxon (ChemService Inc. West Chester, PA; MET-674B) was dissolved in ethanol and stored at -80˚C. Diisopropylfluorophosphate (DFP), a liquid with a concentration of 5.73 M, was from Sigma (D0879). Soman from CEB (Vert-le-Petit, France) was dissolved in isopropanol. Proteome Partitioning Kit, ProteomeLab IgY-12 High Capacity in Spin Column format contains IgY antibodies directed against the 12 most abundant proteins in human plasma (Beckman Coulter #A24331 S0510903). Cibacron blue 3GA agarose (Sigma, C1535) binds 10-20 mg of human albumin per mL of gel. Porcine trypsin (Promega, Madison, WI; V5113 sequencing grade modified trypsin) at a concentration of 0.4 µg/µL in 50 mM acetic acid was stored at -80˚C. Pepsin (Sigma, St. Louis, MO; P6887 from porcine gastric mucosa) was dissolved in 10 mM HCl to make a 1 mg/mL solution, and stored at -80˚C. Monomeric avidin agarose beads (#20228) were from Pierce Co. NeutrAvidin agarose beads (#29202) were from Thermo Scientific (Rockford, IL). Fatty acid free human albumin (Fluka 05418) was from Sigma/Aldrich.

Separation of low and high abundance proteins in human plasma. 200 µl of human plasma (collected in EDTA anticoagulant) were fractionated into low and high abundance proteins by processing 20 µL of plasma at a time on the Beckman Coulter Proteome IgY Spin column depletion kit. The yield of high abundance proteins was 400 µL with a protein concentration of 12 µg/µL. Of this, 123 µL was labeled with FP-biotin, 123 µL was used as a negative control, and the remainder was used for determination of protein concentration.

High abundance proteins labeled with FP-biotin, digested with trypsin, and purified on monomeric avidin. The high abundance fraction of plasma has albumin as its major component. A 123 µL aliquot of the high abundance fraction was treated with 1.25 µL of 20 mM FP-biotin for 48 h at 37˚C at pH 8.0. The final FP-biotin concentration was 200 µM. Excess FP-biotin was removed by dialysis against 2 x 4 L of 10 mM ammonium bicarbonate.

Proteins, in 8 M urea, were reduced with 5 mM dithiothreitol and alkylated with 40 mM iodoacetamide. The samples were diluted to reduce the concentration of urea to 2 M. Proteins were digested with a 1:50 ratio of trypsin to protein at 37˚C overnight. The trypsin was inactivated by heating the sample in a boiling water bath for 10 min. It was necessary to inactivate trypsin because trypsin could have destroyed the avidin protein used in the next step.

FP-biotinylated peptides were purified by binding to 0.5 mL of monomeric avidin beads. Nonspecifically bound peptides were washed off with high salt buffers. The column was washed with water to remove salts, and FP-biotinylated peptides were eluted with 10% acetic acid. The eluate was dried in a vacuum centrifuge in preparation for mass spectrometry.

The negative control was human plasma treated with everything except FP-biotin.

Depletion of albumin on Cibacron Blue, labeling with FP-biotin, digestion with trypsin, and purification on NeutrAvidin. An albumin depleted plasma sample was prepared by binding 0.6 mL human plasma to 2 mL of Cibacron Blue and collecting the protein that eluted in 10 mL of 10 mM TrisCl pH 8.0, containing 0.3 M NaCl. The protein was desalted, concentrated to 0.5 mL and labeled with 100 µM FP-biotin at 37˚C for 16 h in 10 mM ammonium bicarbonate. The labeled protein was denatured in 8 M urea, reduced with dithiothreitol, carbamidomethylated with iodoacetamide, and desalted on a spin column. The yield was 2000 µg in 500 µL. The entire sample was digested with 40 µg of trypsin (Promega) at 37˚C overnight. The FP-biotinylated tryptic peptides were bound to 0.1 mL NeutrAvidin beads, washed with high salt buffers and water, and eluted with 45% acetonitrile, 0.1% formic acid.

Mass spectrometry on QSTAR elite and QTRAP 2000. Five micrograms of the high abundance FP-biotinylated peptides purified with monomeric avidin beads were analyzed on the QSTAR elite LC/MS/MS system with ProteinPilot 2.0 software at the Applied Biosystems laboratories (Framingham, MA).

A second 5 µg aliquot from the same protein preparation, a negative control sample, and the NeutrAvidin purified peptides were analyzed by LC/MS/MS on the QTRAP 2000 mass spectrometer (Applied Biosystems) at the University of Nebraska Medical Center with Analyst 1.4.1 software. The digest was dried in a vacuum centrifuge and dissolved in 5% acetonitrile, 0.1% formic acid to make 0.5 µg/µL. A 10 µL aliquot was injected into the HPLC nanocolumn (#218MS3.07515 Vydac C18 polymeric rev-phase, 75 µm i.d. x 150 mm long; P.J. Cobert Assoc, St. Louis, MO). Peptides were separated with a 90 min linear gradient from 0% to 60% acetonitrile at a flow rate of 0.3 µL/min and electrosprayed through a nanospray fused silica emitter (360 µm o.d., 75 µm i.d., 15 µm taper, New Objective) directly into the QTRAP 2000, a hybrid quadrupole linear ion trap mass spectrometer. An ion-spray voltage of 1900 volts was maintained between the emitter and the mass spectrometer. Information-dependent acquisition was used to collect MS, enhanced MS and MS/MS spectra for the 3 most intense peaks in each cycle, having a charge of +1 to +4, a mass between 400 and 1700 m/z, and an intensity >10,000 counts per sec. All spectra were collected in the enhanced mode, i.e. using the trap function. Precursor ions were excluded for 30 seconds after one MS/MS spectrum had been collected. The collision cell was pressurized to 40 µTorr with pure nitrogen. Collision energies between 20 and 40 eV were determined automatically by the software, based on the mass and charge of the precursor ion. The mass spectrometer was calibrated on selected fragments from the MS/MS spectrum of Glu-Fibrinopeptide B. MS/MS spectra were submitted to Mascot for identification of labeled peptides and amino acids (Perkins et al., 1999).

Mass spectrometry by MALDI-TOF-TOF 4800. 0.5 µL of essentially salt-free samples were spotted on a MALDI target plate, air dried, and overlaid with 0.5 µL of 10 mg/mL alpha-cyano-4-hydroxy cinnamic acid in 50% acetonitrile, 0.1% trifluoroacetic acid. MS spectra were acquired using a MALDI-TOF-TOF 4800 (Applied Biosystems), with a laser power of 3000

volts, in positive reflector mode. Each spectrum was the average of 500 laser shots. The mass spectrometer was calibrated against des-Arg-Bradykinin (904.468 Da), Angiotensin 1 (1296.685 Da), Glu-Fibrinopeptide B (1570.677 Da) and neurotensin (1672.918 Da) (Cal Mix 1 from Applied Biosystems).

Percent OP-labeled Tyr 411 monitored by MALDI-TOF. A 5 µL aliquot of albumin was diluted with 5 µL of 1% trifluoroacetic and digested with 2 µL of 1 mg/mL porcine pepsin for 1-2 h at 37˚C. The digest was diluted with 50% acetonitrile, 0.1% trifluoroacetic acid to give a final protein concentration of about 0.5 mg/mL. A 0.5 µL aliquot was spotted on the MALDI target plate, dried, and overlaid with 0.5 µL of 10 mg/mL alpha-cyano-4-hydroxy cinnamic acid. MS spectra were acquired with the laser set at 3000 volts. Percent OP-labeled Tyr 411 was calculated by dividing the cluster area of the labeled peptide by the sum of the cluster areas for the unlabeled and labeled peaks. The unlabeled peptides were VRYTKKVPQVSTPTL (1717.0 amu) and LVRYTKKVPQVSTPTL (1830.1 amu). After covalent bond formation with CPO these masses increased by 136 amu to become 1853.0 and 1966.1 amu.

Prolonged treatment of albumin with chlorpyrifos oxon. At the time we prepared CPO-labeled human albumin for crystallization trials, we knew that Tyr 411 was labeled by CPO, and had no reason to suspect that other residues might also be labeled. Chlorpyrifos oxon dissolved in ethanol was added to an albumin solution in 10 mM ammonium bicarbonate pH 8.3, 0.01% sodium azide in 6 additions over a one month period.

   Labeling efficiency was poor when the albumin concentration was 500 mg/mL, so the albumin was diluted to 35 mg/mL, and then to 5 mg/mL and finally to 1 mg/mL. The final ratio was 7.7 µmoles of albumin to 146 µmoles of CPO. During the one month labeling time, the decision to add more CPO was based on the percent Tyr 411 labeled. No further additions of CPO were made after 85% of the Tyr 411 had been labeled. The majority of the labeled albumin was dialyzed against 10 mM potassium phosphate pH 7.0, 0.01% azide and concentrated to 200 mg/mL for crystallization trials. A small aliquot was processed for LC/MS/MS analysis in the QTRAP mass spectrometer.

Crystallization conditions. Crystals were obtained by vapor diffusion using sitting drops composed of 3 µL of protein with 1.5 µL precipitant solution containing 25 -38% PEG 3350, 50 mM potassium phosphate pH 7.0 and 100 mM ammonium acetate. Similar looking crystals were also obtained when the precipitant solution contained 0.17 M ammonium sulfate, 85 mM MES pH 6.5, 26% PEG 5000MME and 15% glycerol.

Identification of the most reactive residues. The conditions reported to label one mole of albumin with one mole of DFP were used (Means and Wu, 1979). Human albumin (1.8 mg/mL) in 10 mM TrisCl pH 8.0 was treated with a 20-fold molar excess of DFP for 2 h at room temperature. The reaction was stopped by the addition of solid urea to 8 M and boiling for 10 min in the presence of 10 mM dithiothreitol. Free sulfhydryl groups were alkylated with iodoacetamide. The carbamidomethylated albumin was dialyzed against 2 x 4 L of 10 mM ammonium bicarbonate and digested with trypsin. Tryptic peptides were subjected to LC/MS/MS on the QTRAP 2000.

   The experiment was repeated with FP-biotin, soman, and chlorpyrifos oxon. A 15 µM solution of albumin in 10 mM TrisCl pH 8.0 was treated with 150 µM FP-biotin or 150 µM

11

soman or 150 µM CPO for 2 h at 22˚C. Samples with intact disulfides were digested with pepsin and analyzed by MALDI-TOF. Carbamidomethylated tryptic peptides were analyzed by LC/MS/MS. Tryptic peptides labeled with FP-biotin were also purified on monomeric avidin beads eluted with 50% acetonitrile, 0.1% formic acid and analyzed by MALDI-TOF-TOF.

Stability of CPO-labeled Tyr 411. The stability of CPO-labeled Tyr 411 in human albumin was tested at pH 1.5, 7.4, and 8.3 after incubation for up to seven months at 22˚C and -80˚C. Albumin labeled on 97% of Tyr 411 with diethylphosphate was prepared by incubating 1 mg/mL human albumin (15.6 µM) in 10 mM TrisCl pH 8.0, 0.01% sodium azide with 118 µM CPO for 2.5 days at 22˚C. Excess CPO was removed by dialysis of the 8.5 mL solution against 2 x 4 L of 10 mM ammonium bicarbonate pH 8.3, 0.01% azide.

pH 1.5. The pH of 2.6 mL of the dialyzed CPO-albumin was adjusted to pH 1.5 by adding 2.6 mL of 1% trifluoroacetic acid. Half of the sample was stored at room temperature, and half was divided into 40 µL aliquots and stored at -80˚C.

pH 7.4. The pH was adjusted to pH 7.4 by dialyzing 3.3 mL of the CPO-albumin preparation against 4.5 L of 10 mM potassium phosphate pH 7.4, 0.01% azide. To avoid freeze-thaw artifacts, samples intended for storage at -80˚C were divided into 20 µL aliquots so that each tube was thawed only once.

pH 8.3. The pH of 2.6 mL of CPO-albumin was brought to pH 8.3 by dialysis against 10 mM ammonium bicarbonate, 0.01% sodium azide, pH 8.3. Samples to be stored at -80˚C were divided into 65 tubes each containing 20 µL.

After various times, a tube was removed from -80˚C storage and the entire contents digested with pepsin. Samples stored at room temperature were also digested with pepsin. The digests were analyzed by MALDI-TOF and % labeled Tyr 411 was calculated from cluster areas as described above.

The sample stored at -80˚C in pH 7.4 buffer was analyzed by LC/MS/MS to determine whether sites in addition to Tyr 411 were labeled. The CPO-albumin was denatured, reduced, carbamidomethylated, and digested with trypsin in preparation for LC/MS/MS. The diethylphosphate group was found on Tyr 411 and Tyr 138.

RESULTS
The structures of the organophosphorus agents are shown in Figure 1.1.

Soman M_r 182.2
added mass 162.2 for $C_7H_{15}O_2P$

DFP M_r 184.1
added mass 164.1 for $C_6H_{13}O_3P$

Chlorpyrifos oxon M_r 334.5
added mass 136.0 for $C_4H_9O_3P$

FP-biotin M_r 592.3
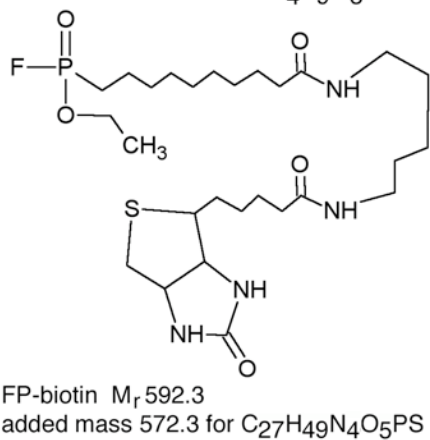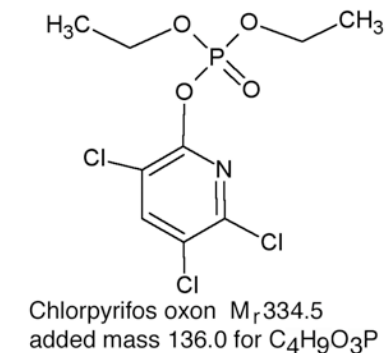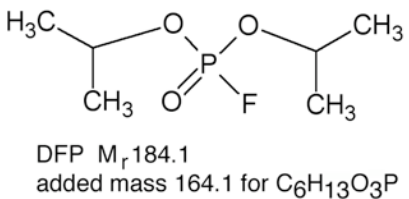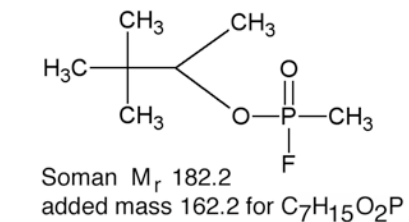added mass 572.3 for $C_{27}H_{49}N_4O_5PS$

Figure 1.1. Structures of organophosphorus agents.

Five tyrosines and two serines in human albumin were labeled with FP-biotin including Tyr 138, Tyr 148, Tyr 401, Tyr 411, Tyr 452, Ser 232, and Ser 287 (Table 1.1).

Table 1.1. FP-biotinylated human albumin tryptic peptides identified by LC/MS/MS.

Start - End	Mr	Sequence	FP-biotinylated
137-144	1627.9	KY*LYEIAR	Y138
138-144	1499.8	Y*LYEIAR	Y138
145-159	2471.3	RHPY*FYAPELLFFAK	Y148
145-160	2627.4	RHPY*FYAPELLFFAKR	Y148
146-159	2315.2	HPY*FYAPELLFFAK	Y148
146-160	2471.3	HPY*FYAPELLFFAKR	Y148
226-233	1452.7	AEFAEVS*K	S232
287-313	3546.6	S*HCIAEVENDEMPADLPSLAADFVESK	S287
390-402	2230.0	QNCELFEQLGEY*K	Y401
411-413	983.5	Y*TK	Y411
445-466	3246.6	RMPCAEDY*LSVVLNQLCVLHEK	Y452
446-466	3090.5	MPCAEDY*LSVVLNQLCVLHEK	Y452

Residue numbers in accession # gi: 3212456 are for the mature albumin protein, and do not include the 24 amino acid signal peptide. The added mass from FP-biotin is 572.3 amu. Cysteines were carbamidomethylated, thus adding a mass of 57 amu.

Supporting MS/MS spectra for these assignments are in Figures 1.2-1.5. A peptide labeled with FP-biotin always had ions at 227, 312, and 329 atomic mass units (amu) resulting from fragmentation of FP-biotin (Schopfer et al., 2005). Two ions characteristic of covalent binding of FP-biotin to the hydroxyl group of tyrosine are the immonium ion of tyrosine-FP-biotin at 708 amu and its partner ion at 691 amu, produced by loss of NH_3. The 708 and 691 amu masses are prominent in Figures 1.2A and 1.2B, but barely visible in Figures 1.3A and 1.3B. An additional complexity in Figure 1.2A is the presence of ions that had lost a 329 or 227 amu fragment from FP-biotin.

The masses in Figure 1.2A are consistent with the sequence YTK where the added mass of 572 amu from FP-biotin is on Tyr. The complete y-ion series (y1, 147.0 amu, Lys; y2, 248.4 amu, LysThr; and singly-charged, FP-biotinylated parent ion) is present. Peaks at 227.2, 312.4, 329.4, 691.3, and 708.5 amu are indicative of the presence of FP-biotinylated tyrosine. The remainder of the major peaks are consistent with various FP-biotinylated tyrosine fragments missing pieces of the FP-biotin moiety.

Peptide YLYEIAR has two tyrosines. A complete y-ion series (y1 to y5) indicates that the FP-biotin label is on the N-terminal Tyr. Only the first tyrosine was labeled. Additional evidence for labeling on Tyr 138 rather than on Tyr 140 was the presence of the a2 ion at 821.4 amu, the b2 ion at 849.2 amu and the $a2^{++}$ ion at 411.4 m/z (Figure 1.2B). If the FP-biotin had been attached to Tyr 140, the masses would have been a2=249, b2=277, and $a2^{++}$ =125 amu. Peaks at 226.3, 312.4, 329.3, 708.2 and 691.3 amu confirm the presence of FP-biotinylated tyrosine in the peptide.

Analysis of the missed cleavage peptide KYLYEIAR supports labeling on Tyr 138 (data not shown).
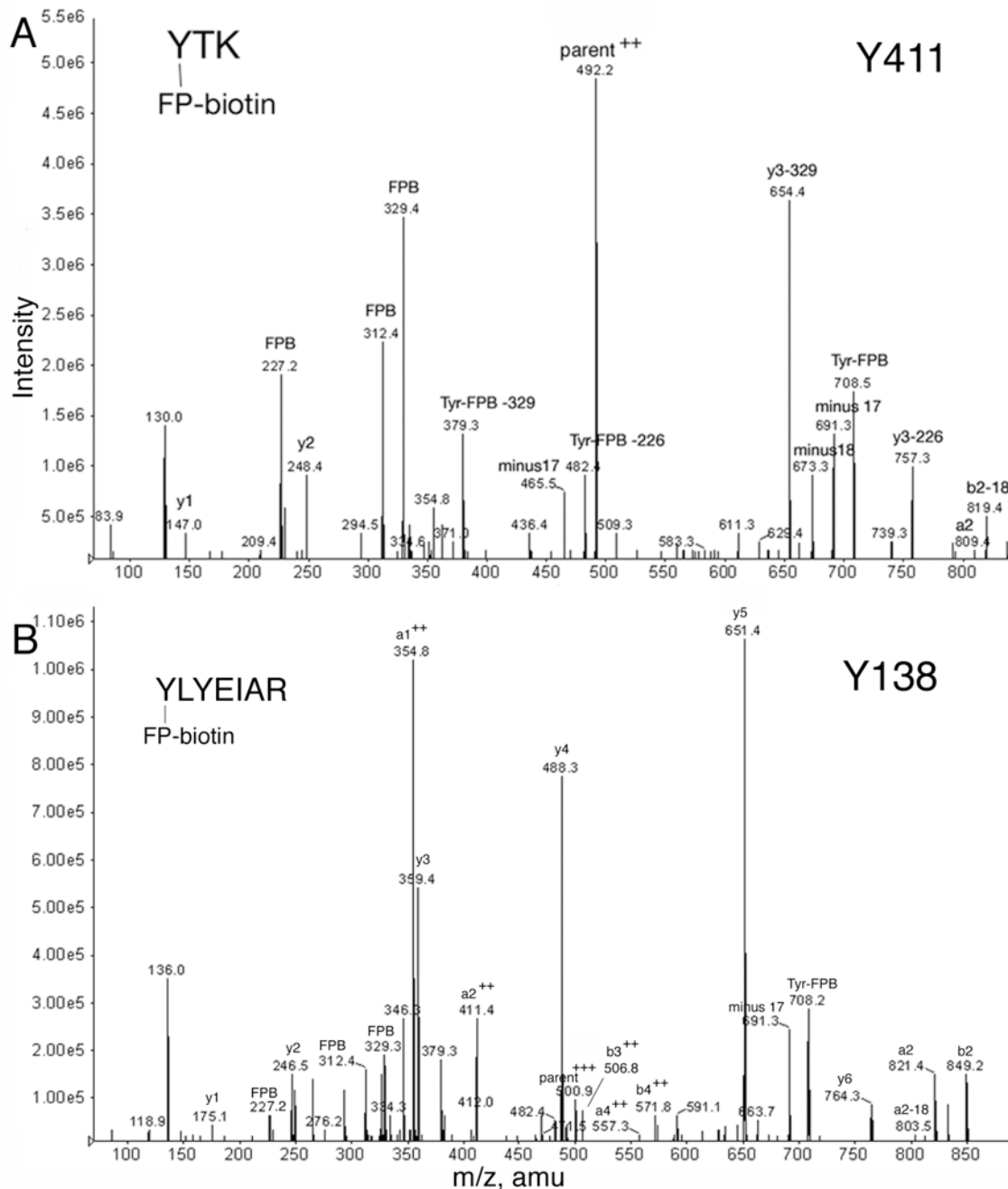
Figure 1.2. MS/MS spectra of albumin peptides labeled with FP-biotin on Tyrosine. A) Tyr 411 in peptide YTK, and B) Tyr 138 in peptide YLYEIAR are covalently modified by FP-biotin. The characteristic fragments of FP-biotin at 227.2, 312.4, and 329.3 amu are present. Ions characteristic of FP-biotin modification on Tyrosine are the immonium ion at 708 amu and the immonium ion minus 17 at 691 amu. Support for modification of the first tyrosine rather than the second in YLYEIAR is the mass of ions a2, b2, and a2^{++}. The doubly charged parent ion in A had a mass of 492.2 amu. The triply charged parent ion in B had a mass of 500.9 m/z.

Peptide HPYFYAPELLFFAK in Figure 1.3A also has two tyrosines. Evidence for labeling on Tyr 148 rather than on Tyr 150 is the presence of the b4 ion at 1118.5 amu, the a4^{++} ion at 545.4 amu and the b4^{++} ion at 559.3 m/z. The total mass of the b4 fragment (1117.6 amu) is equal to the fragment HPYF (545 amu) plus the added mass from FP-biotin (572 amu). Of the four residues in the b4 fragment, Tyr 148 is the most reasonable candidate for labeling. Fragment masses for b5 and b6 also support labeling of Tyr 148 rather than Tyr 150. An extensive y-ion series (y1-y8) supports the assignment of this peptide. Masses at 227.3, 312.2 and 329.4, 691.2, and 708.5 amu indicate the presence of FP-biotinylated tyrosine.

A similar analysis was made for peptides RHPYFYAPELLFFAK and HPYFYAPELLFFAKR, which differ from HPYFYAPELLFFAK by virtue of missed cleavages (data not shown).

Peptide QNCELFEQLGEYK in Figure 1.3B is FP-biotinylated on Tyr 401 as demonstrated by the y2 ion at 882.5 amu, the y3 ion at 1011.5 amu, the y4 ion at 1068.5 amu, and the y5 ion at 1181.8 amu. The y2 mass is equal to the sum of Lys (147 amu), Tyr (163 amu) and the added mass of FP-biotin (572 amu). A variety of larger, multiply-charged y-ion fragments support the labeling assignment. Prominent b-ion fragments confirm the identity of the peptide. Fragments at 227.2, 312.2, and 329.3 amu indicate the presence of FP-biotin in the peptide.
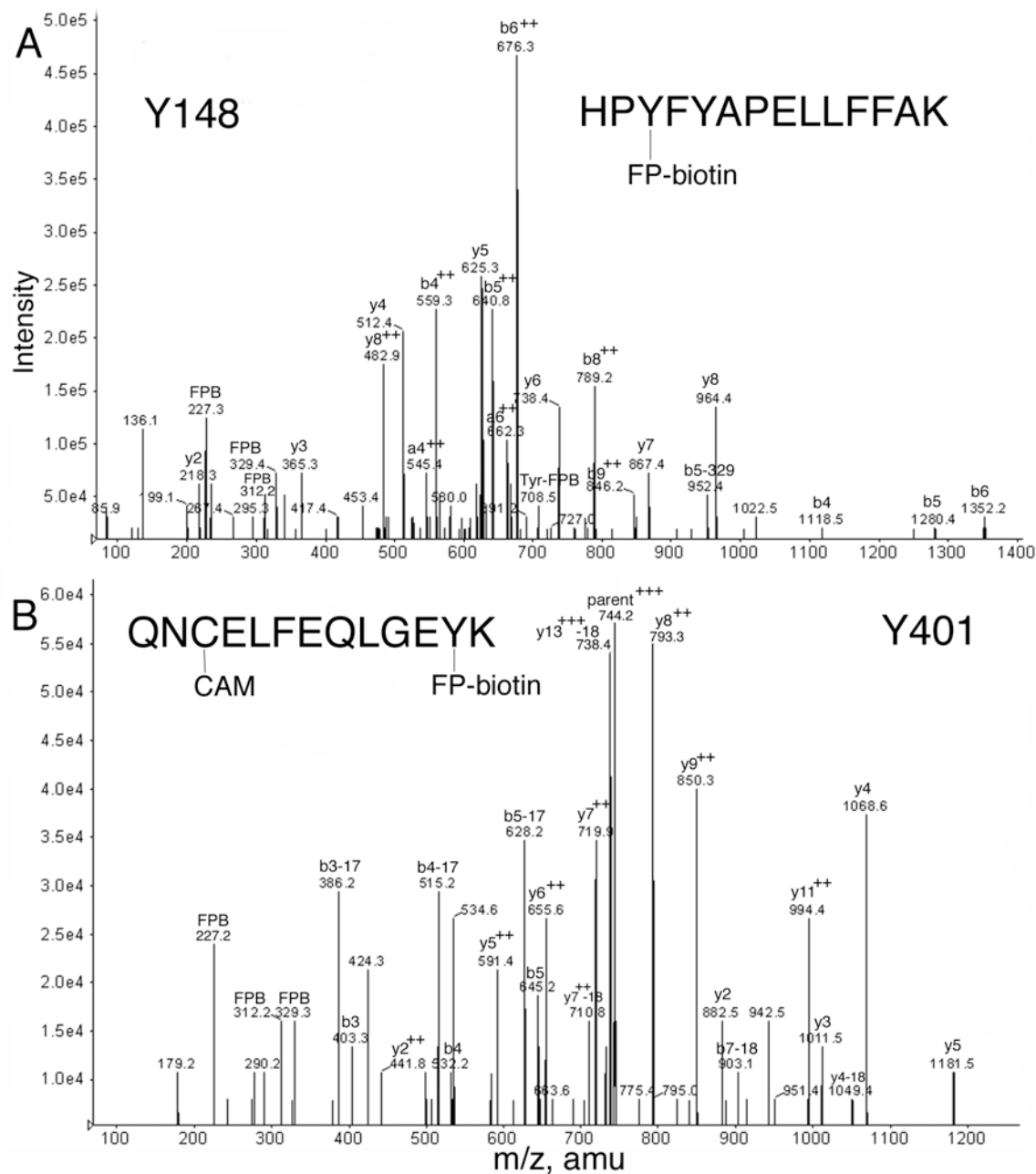
Figure 1.3. MS/MS spectra of albumin peptides labeled with FP-biotin on Tyrosine. A) Tyr 148 in peptide HPYFYAPELLFFAK, and B) Tyr 401 in peptide QNCELFEQLGEYK are covalently modified by FP-biotin. The quadruply charged parent ion in A has a mass of 579.7 m/z. The triply charged parent ion in B has a mass of 744.2 m/z.

Peptide MPCAEDYLSVVLNQLCVLHEK in Figure 1.4 is FP-biotinylated on Tyr 452. The best evidence in support of this interpretation is the doubly-charged mass at 720.4 m/z which is consistent with the b7 ion plus the added mass from FP-biotin. The b7 ion consists of MPCAEDY. Of these residues, only Tyr 452 is a reasonable candidate for FP-biotinylation. The b8^{++}, b9^{++} and b10^{++} ions support this interpretation. The y-series (y3-y10) supports identification of this peptide. Masses at 227.2, 312.2, 329.4, 691.4, and 708.4 amu indicate the presence of FP-biotinylated tyrosine in this peptide.

A missed cleavage form of this peptide, RMPCAEDYLSVVLNQLCVLHEK was also analyzed and the results support labeling of Tyr 452 (data not shown).
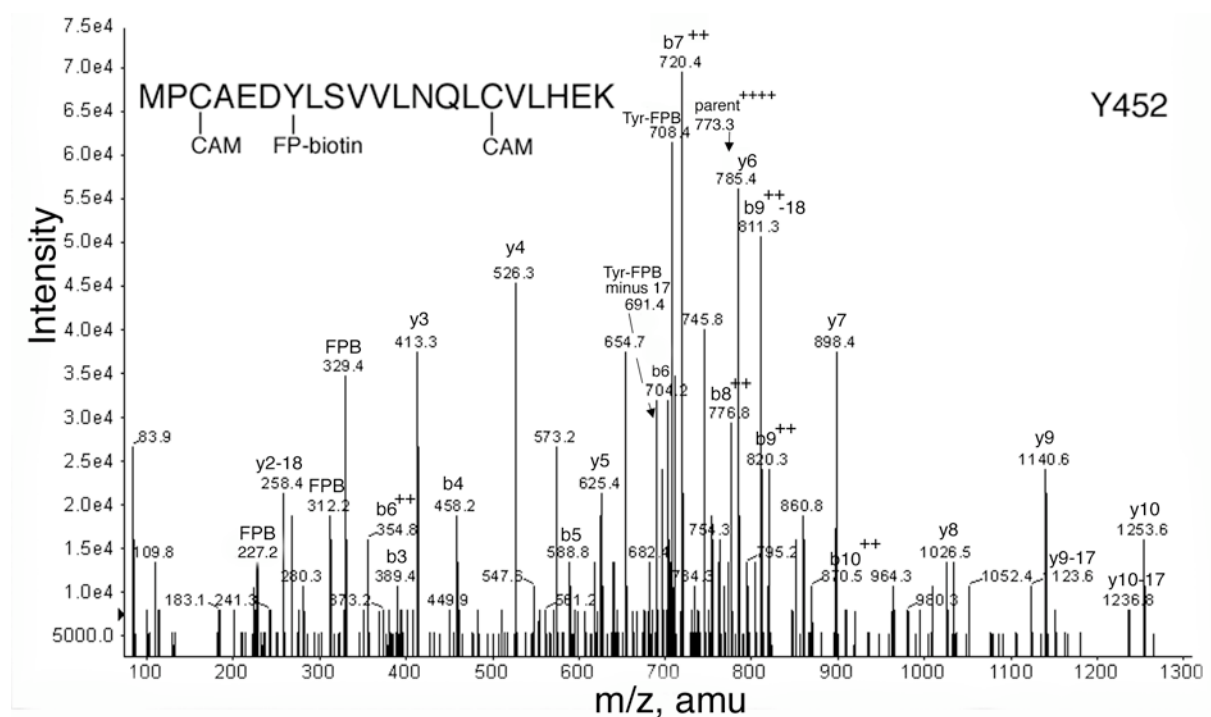

Figure 1.4. MS/MS spectrum of albumin peptide labeled with FP-biotin on Tyrosine 452. The quadruply charged parent ion has a mass of 773.3 m/z. The carbamidomethylated cysteine is indicated as CAM.

Peptide SHCIAEVENDEMPADLPSLAADFVESK in Figure 1.5 is FP-biotinylated on Ser 287. Existence of an FP-biotinylated serine is indicated by the major peak at 591.4 amu. This is a characteristic mass from FP-biotin that appears as the result of beta-type elimination of FP-biotin from a serine adduct, during collision induced dissociation in the mass spectrometer (Schopfer et al., 2005). The complimentary peptide fragment arising from this fragmentation contains a dehydroalanine in place of serine. The masses of a b-series (b5-b8, 609.4, 680.3, 729.3 and 908.5 amu) containing a dehydroalanine residue support the elimination of FP-biotin from serine. Of the residues in the b5 fragment (SHCIA), serine at position 287 is a candidate for FP-biotinylation. The cysteine might have been considered as a target for labeling, but the

overall mass of the fragment is consistent with carbamidomethylation on the cysteine. A y-ion series (y4-y15) supports the identification of the peptide. Additional support for the presence of FP-biotin in the peptide comes from characteristic masses at 312.1 and 329.2 amu. Absence of the characteristic mass at 227 amu is common for FP-biotinylated serine.
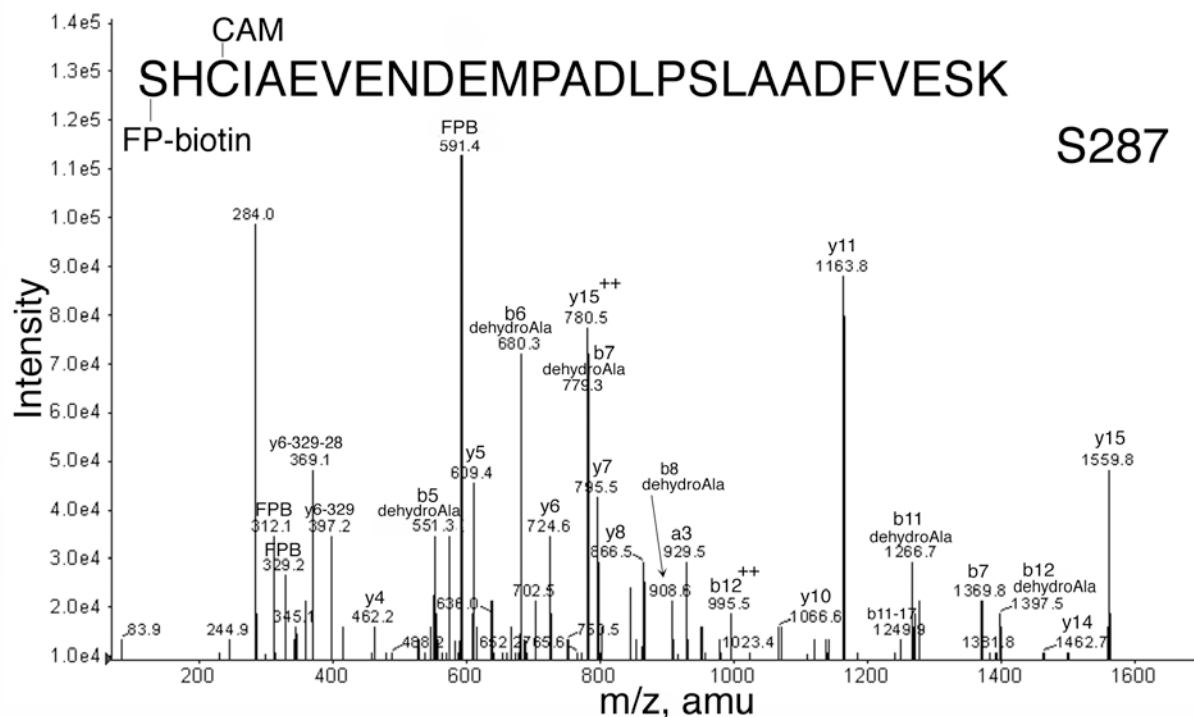
Figure 1.5. MS/MS spectrum of albumin peptide labeled with FP-biotin on Ser 287. The triply charged parent ion has a mass of 1183.8 m/z. The carbamidomethylated (CAM) peptide carried the FP-biotin tag on Ser 287. The evidence for modification on serine is the presence of a b-ion series for the dehydroalanine form of the peptide. The 591.4 amu ion is FP-biotin released from serine where the fluoride ion has been replaced by a hydroxyl group. Release of the entire OP accompanied by formation of dehydroalanine is a characteristic of OP bound to serine.
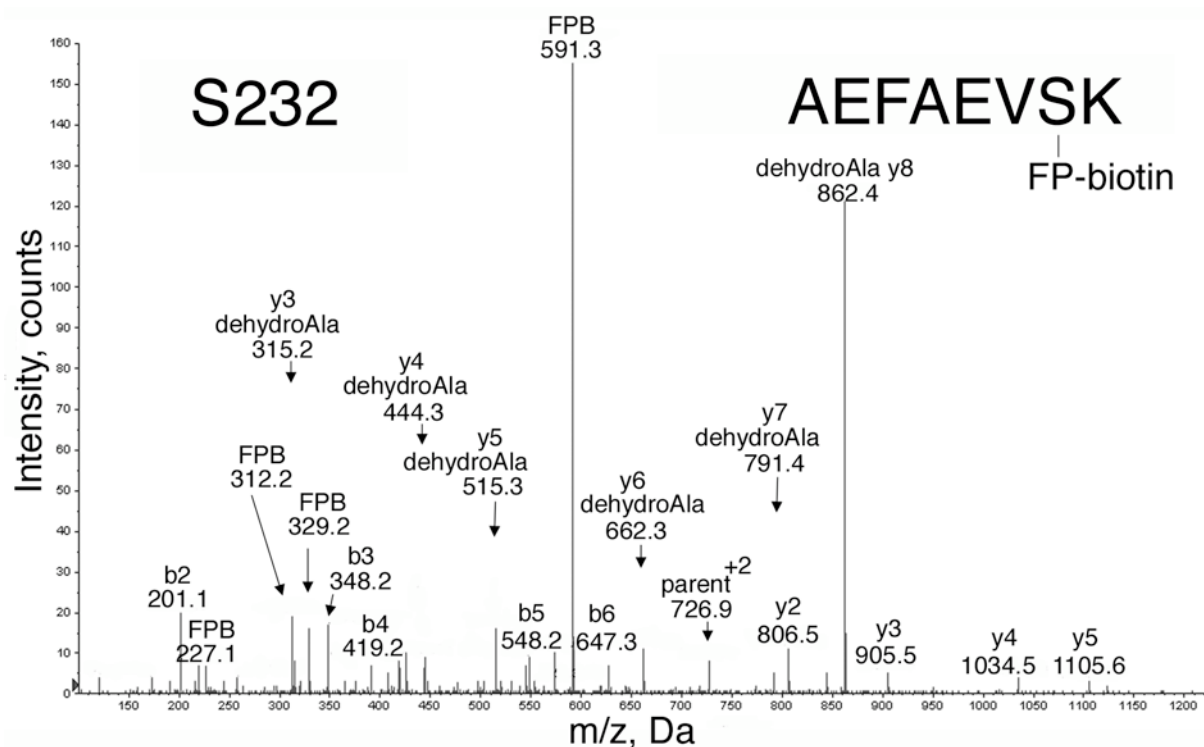
Figure 1.6. MS/MS spectrum of albumin peptide labeled with FP-biotin on Ser 232.   This spectrum was acquired on the QSTAR elite mass spectrometer. The doubly charged parent ion is at 726.9 amu. The peak at 591.3 is FP-biotin released from serine, carrying a hydroxyl group in place of fluorine. Four y-ions (y2, y3, y4, y5) carry FP-biotin on serine, whereas 6 y-ions (dehydroAla y3-y8) have lost FP-biotin as well as a molecule of water, thus converting Serine to dehydroAlanine.

      The MS/MS spectrum for peptide AEFAEVSK labeled by FP-biotin on Ser 232 is in Figure 1.6. The b- and y-ion masses support the assigned sequence. Peaks not assigned by Mascot included 6 dehydroalanine fragments as well as the 591 amu ion of FP-biotin, and the 227, 312, and 329 amu fragments of FP-biotin. These additional peaks strongly support the conclusion that Ser 232 of albumin was labeled by FP-biotin. This labeled peptide was present in very low abundance as indicated by the fact that it was detected by the QSTAR elite, but not by the QTRAP 2000 mass spectrometer.
      No FP-biotinylated peptides were found in the control plasma that had not been treated with FP-biotin.

Crystals of CPO-albumin. Soft amorphous crystals were obtained by vapor diffusion in high PEG conditions that were previously reported for preparation of other human serum albumin crystals (Carter et al., 1989; Curry et al., 1998; Sugio et al., 1999). These crystals were obtained from extensive screening using the Classics, PEGs and Cryo crystal screens from Qiagen, and Index from Hampton Research. Similar crystals were obtained following optimization around the preliminary hit conditions. The crystals were difficult to mount due to their jelly like texture

and were not useful for structural studies. We succeeded in mounting a few crystals, though most had no discernable diffraction spots and the best diffracting crystals had only a few spots in the proximity of the beamstop, at about 30Å. The poor crystal quality suggests that the protein was not homogeneously labeled.

Albumin residues labeled by chlorpyrifos oxon. Prolonged labeling of albumin with chlorpyrifos oxon, for crystallization trials, resulted in labeling of 6 tyrosines: Y138, Y150, Y161, Y401, Y411, and Y452. Table 1.2. Four of these sites were also labeled by FP-biotin (Y138, Y401, Y411, and Y452). The HPYFYAPELLFFAK peptide was labeled on Tyr 150 by chlorpyrifos oxon, whereas it was labeled on Tyr 148 by FP-biotin. A new peptide YKAAFTECCQAADK was labeled by chlorpyrifos oxon and not by FP-biotin.

Table 1.2. Chlorpyrifos oxon labeled human albumin peptides.

Start - End	Mr	Sequence	CPO-labeled
138-144	1062.5	Y*LYEIAR	Y138
146-159	1877.9	HPYFY*APELLFFAK	Y150
161-174	1797.8	Y*KAAFTECCQAADK	Y161
390-402	1791.8	QNCELFEQLGEY*K	Y401
409-423	1758.9	VRY*TKKVPQVSTPTL	Y411
446-466	2653.2	MPCAEDY*LSVVLNQLCVLHEK	Y452

Tyr 411 reacts most readily with OP. The finding that 7 tyrosines and 2 serines make a covalent bond with OP led to the question of which amino acid reacts most readily with OP. To answer this question we duplicated the conditions reported to label one molar equivalent of human albumin with DFP (Means and Wu, 1979). MALDI-TOF analysis of pepsin-digested, DFP-treated human albumin suggested that 80% of Tyr 411 was labeled with DFP. MS/MS analysis of a tryptic digest of carbamidomethylated DFP-treated albumin confirmed that Tyr 411 in peptide Y*TK was labeled. In addition, less than 10% of peptide EFNAETFTFHADICT*LS*EK was labeled (on residues T515 and S517).

Albumin treated with FP-biotin for 2 h and digested with pepsin had 52% of its Tyr 411 labeled in peptide VRY*TKKVPQVSTPTRL as calculated by MALDI-TOF mass spectrometry. The carbamidomethylated, trypsin digested preparation analyzed by LC/MS/MS confirmed that Tyr 411 in peptide Y*TK was labeled with FP-biotin. Peptide HPY*FYAPELLFFAK was labeled on Tyr 148 with FP-biotin, but to less than 10%. A third method to identify FP-biotinylated peptides was purification on monomeric avidin beads followed by MALDI-TOF-TOF analysis. This method yielded only one FP-biotinylated peptide, the Y*TK peptide labeled on Tyr 411.

Soman-treated albumin (150 μM soman for 2 h) analyzed by MALDI-TOF and LC/MS/MS yielded only one labeled peptide. The soman was on Tyr 411.

Albumin treated with chlorpyrifos oxon for 2 h before digestion with pepsin or trypsin and analyzed by MALDI-TOF and LC/MS/MS was labeled on Tyr 411. Approximately 30% of the Tyr 411 sites were labeled in peptides VRY*TKKVPQVSTPTL and LVRY*TKKVPQVSTPTL. In addition, less than 5% of Thr 566 in peptide ET*CFAEEGKK and less than 5% of Thr 236 and Thr 239 in peptide LVT*DLT*KVHTECCHGDLLECADDR were labeled. We conclude that Tyr 411 is the most OP reactive residue in human albumin.

        Support for the conclusion that Tyr 411 is the most OP reactive residue in albumin comes from (Williams et al., 2007). They incubated the albumin fraction of human plasma with radiolabeled sarin, digested with trypsin, purified the radiolabeled peptides by HPLC, and analyzed by LC/MS/MS. A single radiolabeled peptide was isolated. Its sequence was YTK with the isopropyl methylphosphonyl group on tyrosine.

Unstable OP-Ser and OP-Thr, but stable OP-Tyr. It was noted that serine and threonine residues were labeled in addition to tyrosine when samples had been incubated at pH 8.0-8.3 for 2 to 48 h, but were not found in samples incubated at pH 8.3 for a month. In contrast, OP-labeled tyrosines were found even after 1 month incubation at pH 8.3. Our stability study of CPO-labeled albumin confirmed that the Tyr 411 adduct was stable (Figure 1.7). We interpret these results to mean that OP-labeled serine and threonine adducts are unstable compared to OP-labeled tyrosine.
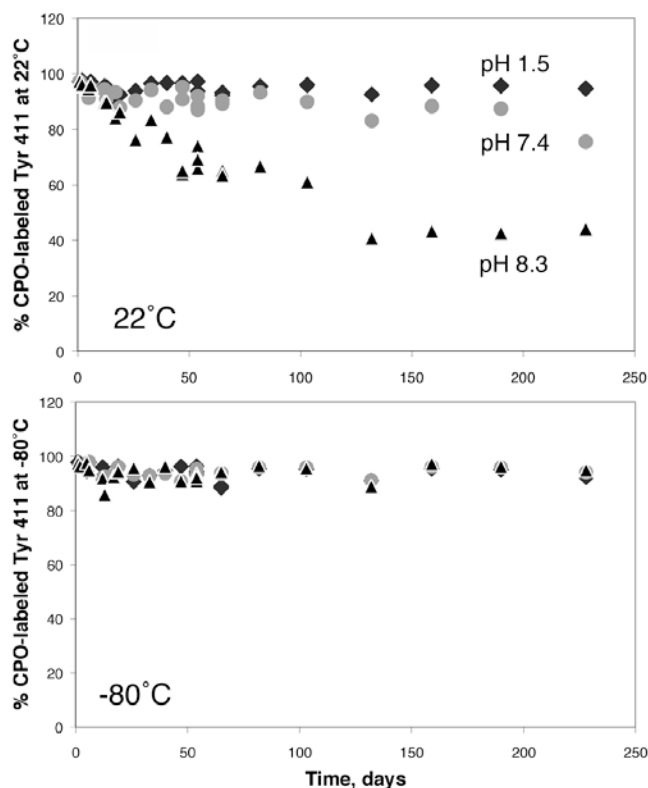

Figure 1.7. Stability of the diethylphosphate adduct of human albumin on Tyr 411. Albumin was treated with CPO to achieve 97% labeling of Tyr 411. Excess CPO was removed by dialysis. The pH of the dialyzed albumin was adjusted to 1.5, 7.4, and 8.3. CPO-albumin samples were stored at 22°C and -80°C. After various times of storage, samples were digested with pepsin and % labeling of Tyr 411 was calculated from cluster areas of labeled and unlabeled peptides in the MALDI-TOF mass spectrometer. CPO-labeled Tyr 411 was stable at pH 1.5 and 7.4 when CPO-albumin was stored at 22°C (top panel), and it was stable at all pH values when CPO-albumin was stored at -80°C (bottom panel). Storage of CPO-albumin at pH 8.3 at 22°C resulted in release of half of the diethylphosphate group from Tyr 411 after 3.6 months.

Surface location of OP reactive residues.   The crystal structure in Figure 1.8 shows the 5 tyrosines and 2 serines that become labeled by FP-biotin. These residues are located on the surface of the albumin molecule where they are available for reaction with OP.

Human albumin has 18 Tyrosines and 24 Serines, but only 5 Tyrosines and 2 serines made a covalent bond with FP-biotin. Their special reactivity may be explained by a nearby arginine or lysine that stabilizes the ionized hydroxyl of tyrosine or serine.
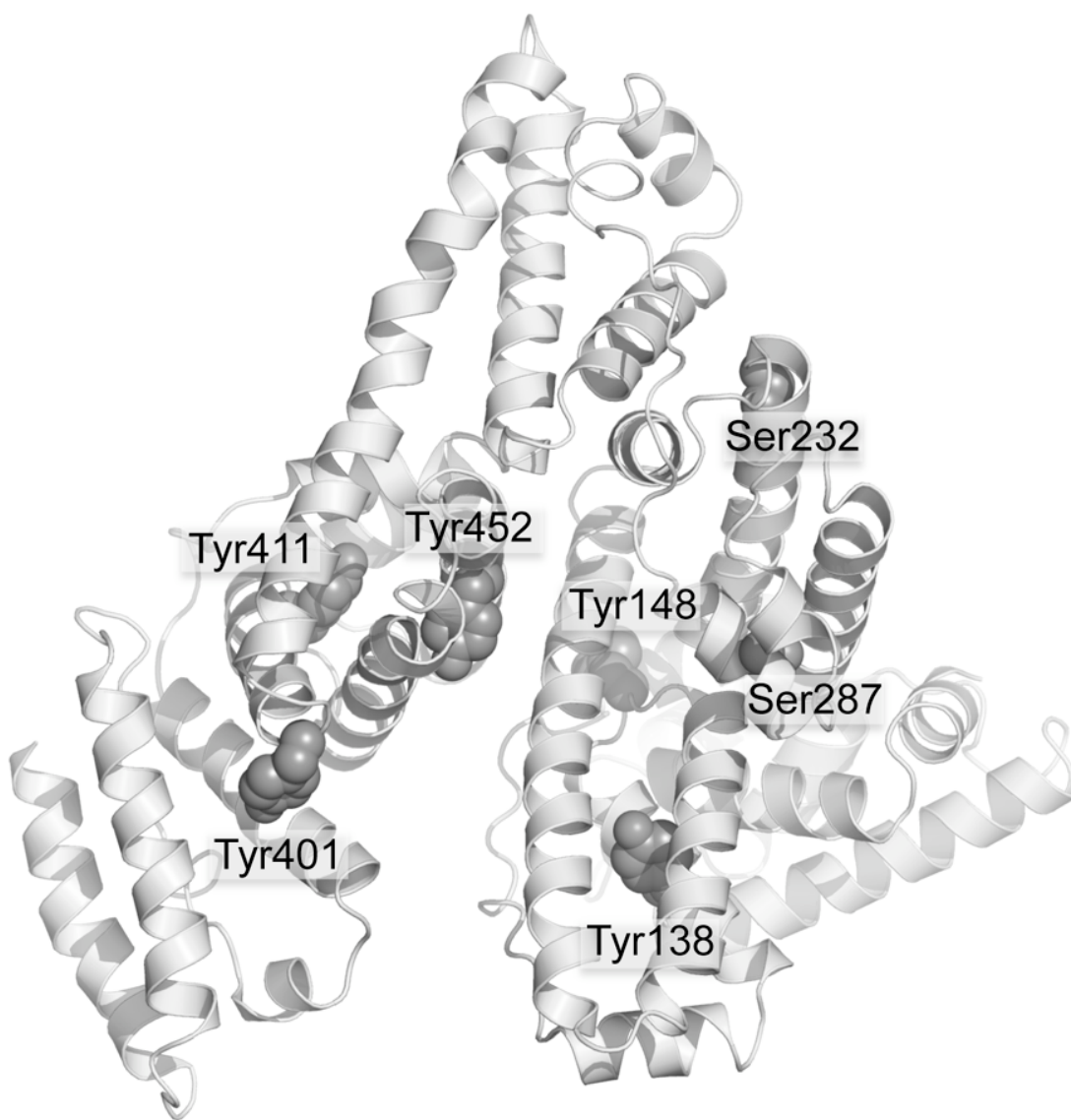

Figure 1.8. Crystal structure of human albumin showing surface location of Tyr 138, Tyr 148, Tyr 401, Tyr 411, Tyr 452, Ser 232, and Ser 287. The residues are shown as space-filled structures. The picture was made with PyMol software using the structure in PDB code 1bm0 (Sugio et al., 1999).

DISCUSSION

Many OP-reactive residues in human albumin. Though Tyr 411 is the most OP reactive residue in human albumin, an additional 8 amino acids were labeled when the OP concentration was high and the reaction time was prolonged. The reaction with FP-biotin at pH 8.0 resulted in the labeling of 5 tyrosines and two serines in albumin. Chlorpyrifos oxon labeled 6 tyrosines (two of which were different from those labeled by FP-biotin) and no serines.

The pKa of the tyrosine hydroxyl group is 10.1 and of the serine hydroxyl group is approximately 16, based on comparison to ethanol (Ballinger and Long, 1960). In the absence of special activation, less than 1% of the tyrosines and less than 0.000001% of the serines would be expected to be ionized at pH 8.0. Ionized forms react preferentially with OP, so the reactivity of tyrosine and especially of serine with OP would be expected to be poor at pH 8. The special reactivity of Tyr 411 suggests that the pKa of this particular tyrosine has been lowered. Means and Wu identified an OP reactive residue in albumin that had a pKa of 8.3 (Means and Wu, 1979). It is likely that Tyr 411 corresponds to that residue.

Albumin as an OP scavenger. Our results show that albumin is an OP scavenger, undergoing a covalent reaction with OP. As such, albumin contributes to detoxication of OP. A significant amount of OP can be bound by albumin because the concentration of albumin in serum is high (≈0.6 mM), even though the rate of reaction with OP is slow (Li et al., 2008).

Tyrosines with an abnormally low pKa are involved directly or indirectly in the catalytic activity of numerous enzymes including glutathione S-transferase (Atkins et al., 1993), asparaginase (Derst et al., 1994), beta-lactamases (Lamotte-Brasseur et al., 2000), and old yellow enzyme (Kohli and Massey, 1998). Lowering the pKa of tyrosines in albumin by modifying their environment, either by mutagenesis or by chemical modification of vicinal residues, would increase the reactivity of albumin with OP. Specific nitration of tyrosine by tetranitromethane was found to lower the pKa of tyrosine to 6.8 (Cuatrecasas et al., 1968). Another nitration reagent of tyrosine, peroxynitrite was found to increase the catalytic activity of a few enzymes (Ji et al., 2006). Thus, specific nitration of tyrosine residues in albumin could also lead to a gain in reactivity of this protein, increasing its scavenging properties.

No aging of OP-tyrosine adducts. When soman or DFP are bound to acetylcholinesterase or butyrylcholinesterase the OP lose an alkyl group in a process called aging (Jansz et al., 1959; Michel et al., 1967; Millard et al., 1999; Nachon et al., 2005). An aged soman-labeled peptide would have an added mass of 78 rather than 162; an aged DFP-labeled peptide would have an added mass of 122 rather than 164; an aged CPO-labeled peptide would have an added mass of 108 rather than 136. Masses corresponding to aged OP-labeled peptides were not found in MS scans. We conclude that albumin OP adducts on tyrosine do not age.

Support for this conclusion comes from the work of others (Adams et al., 2004; Williams et al., 2007). Human albumin covalently labeled with soman or sarin, and treated with sodium fluoride to release the OP, yielded intact soman and sarin. Soman-tyrosine adducts isolated from nerve agent treated guinea pigs contained the pinacolyl group of soman.

The absence of aging is a special advantage for OP-albumin as a biomarker because it allows for a more precise identification of the OP. In contrast, soman and sarin exposure cannot be distinguished when the biomarker is cholinesterase, where aging of OP adducts occurs rapidly.

24

OP labeling of albumin in living animals. Guinea pigs treated with the nerve agents soman, sarin, cyclosarin, or tabun have nerve agent-labeled albumin in their blood (Williams et al., 2007). The OP are bound to tyrosine. The tabun-tyrosine and soman-tyrosine adducts were detected in blood 7 days post exposure, indicating that the adducts are stable. The adducts had not undergone aging and had not been released from tyrosine by treatment of the guinea pigs with oxime. These are characteristic features of OP adducts on albumin. Mice treated with a nontoxic dose of FP-biotin by intraperitoneal injection had FP-biotinylated albumin in blood and muscle (Peeples et al., 2005). These examples show that OP bind covalently to albumin under physiological conditions and that OP-albumin adducts could therefore be useful as biomarkers of OP exposure (Carter et al., 2007). Low OP doses make a covalent bond with Tyr 411, but other tyrosines may also be modified.

Stability of OP-Tyr. The CPO-adduct on Tyr 411 was stable for several months at pH 7.4 and 22˚C. CPO-labeled tyrosine adducts were found after a month of treating albumin at pH 8.3. However OP-Ser and OP-Thr adducts were found only if treatment was brief (2-48h) and if peptides were immediately generated and analyzed in the mass spectrometer. This result indicates that OP-Ser and OP-Thr adducts are unstable compared to OP-Tyr adducts. Instability of OP-Ser adducts suggests it may be difficult to make antibodies against OP-labeled serine peptides because they may spontaneously lose the OP label after they are injected into an animal. In contrast, antibodies against OP-labeled tyrosine peptides have a good chance of being successfully produced because the OP-tyrosine bond is stable at pH 7.4.

Significance. Our results suggest that OP exposure could be monitored by mass spectrometry of OP-albumin adducts or with antibodies against OP-albumin adducts. The surface location of the OP-binding sites in albumin suggests that these epitopes may be available for reaction with antibodies. This is in distinct contrast with acetylcholinesterase and butyrylcholinesterase where the OP binding site is buried deep within the molecule making it unavailable to antibodies. The studies described here support investigation into whether albumin could be engineered to become a more efficient OP scavenger.

Additional progress on Milestones 3, 4, and 5

Tyrosines of human and mouse transferrin covalently labeled by organophosphorus agents; a new motif for OP binding to proteins that have no active site serine

ABSTRACT

Background: Our goal is to identify proteins in plasma labeled by organophosphorus agents (OP). In vitro experiments identified transferrin as being OP labeled. The expectation from the literature is that OP-reactive proteins have an active site serine. Since transferrin does not have an active site serine, the site of covalent OP attachment was unknown.

Methods: Pure human and mouse transferrin were treated with 10-50 fold molar excess of FP-biotin, chlorpyrifos oxon, diisopropylfluorophosphate, dichlorvos, sarin, and soman. Tryptic peptides were separated by liquid chromatography and analyzed by mass spectrometry. The OP were found to bind to tyrosine. An OP binding motif for tyrosine was tested by measuring OP binding to a peptide that contained positively charged Arg adjacent to Tyr. Possible disruption of transferrin function due to OP binding was tested by titration with ferric ion.

Results: Tyr 238 and Tyr 574 in human transferrin and Tyr 238, Tyr 319, Tyr 429, Tyr 491, and Tyr 518 in mouse transferrin were labeled by OP. Transferrin labeled on Tyr 238 and Tyr 574 with FP-biotin bound the normal two moles of ferric ion per mole of human transferrin. The tyrosine in a small synthetic peptide RYTR made a covalent bond with DFP, CPO, and dichlorvos at pH 8.0. Peptide SYSM also bound OP on Y, but only at high concentrations of OP.

Conclusions: A new motif for OP binding to tyrosine has been demonstrated. The OP-reactive tyrosine reacts more readily with OP when tyr is activated by interaction with Arg or Lys. It is suggested that many proteins in addition to those already identified may be modified by OP on tyrosine, and that tyrosine modification may be involved in developmental and/or behavioral OP toxicity.

INTRODUCTION

We have previously shown that many proteins in plasma react with the organophosphorus agent (OP) FP-biotin (Peeples et al., 2005). Our goal is to identify these proteins. The proteins that react most rapidly with FP-biotin and with other OP are enzymes in the serine hydrolase family, for example butyrylcholinesterase in human plasma, acetylcholinesterase in red blood cells and brain, acylpeptide hydrolase, fatty acid amide hydrolase, arylformamidase, and neuropathy target esterase-lysophospholipase (Richards et al., 2000; Casida and Quistad, 2004). The residue that is labeled in these enzymes is the active site serine which appears in the consensus sequence GXSXG. However, proteins with no consensus active site serine constitute another group of OP-reactive proteins, where OP binds to tyrosine. Papain and bromelain bind DFP on tyrosine (Murachi et al., 1965; Chaiken and Smith, 1969). Mass spectrometry has allowed identification of OP-binding to tyrosines in albumin and tubulin (Li et al., 2007; Grigoryan et al., 2008; Li et al., 2008). The present report adds transferrin to this list. Analysis of the reactive peptides from these proteins shows that a new motif of OP binding is beginning to emerge.

Our strategy uses FP-biotin, initially, to label the OP-reactive proteins in plasma. Through the use of the fluorescent probe Streptavidin-Alexa 680 and the biotin tag, the proteins that are OP-reactive in serum can be visualized. The biotin tag also provides a means for purification of the labeled proteins and peptides by binding to avidin-agarose beads. The FP-biotin labeled proteins and peptides are identified by mass spectrometry. It is relatively simple to identify a protein by mass spectrometry because only a few peptides from a protein suffice. However, it is often difficult to find a specific labeled peptide. Convincing proof that a protein is OP-labeled comes only from identifying the labeled peptide and the amino acid in that peptide that is modified by OP. To provide this proof we label pure protein with OP, digest with trypsin, separate and enrich the OP-labeled peptides by reverse phase HPLC, and determine the peptide sequence and site of attachment by collision induced dissociation in the mass spectrometer.

Not all OP are expected to bind covalently to a particular protein. Toxicity testing has shown that toxic symptoms differ depending on the identity of the OP (Moser, 1995; Pope, 1999). Therefore we treated human and mouse transferrin with 6 different OP. Human transferrin bound 4 OP, mouse transferrin bound 3 OP of those six. No evidence for soman or sarin binding to either human or mouse transferrin was found.

The common feature in the motif for OP-reactive tyrosines is the presence of a positively charged arginine or lysine within 5 residues of the tyrosine. The generality of this OP binding motif was tested with two synthetic peptides, both containing tyrosine, but only one containing nearby arginines. Tyrosine formed a covalent bond with OP in both peptides, but the reaction proceeded more readily with RYTR than with SYSM.

EXPERIMENTAL PROCEDURES

Materials. FP-biotin (Mr 592.32) was custom synthesized in the laboratory of Dr. Charles Thompson at the University of Montana, Missoula, MT. A 2 mM FP-biotin solution in dimethyl sulfoxide was stored at -80°C. Chlorpyrifos oxon (ChemService Inc. West Chester, PA; MET-674B) was dissolved in ethanol and stored at -80°C. Dichlorvos (ChemService Inc.; PS-89) was dissolved in methanol. Soman and sarin from CEB (Vert-le-Petit, France) were dissolved in isopropanol. Immun-Blot PVDF membrane for protein blotting, 0.2 μm (162-0177) and Affi-gel blue (153-7301), a crosslinked agarose bead with covalently attached Cibacron Blue F3GA dye, were from Bio-Rad Laboratories, Hercules, CA. Streptavidin Alexa Fluor 680 (S-21378) was from Molecular Probes, Eugene, OR. Porcine trypsin (Promega, Madison, WI; V5113

27

sequencing grade modified trypsin) at a concentration of 0.4 μg/μL in 50 mM acetic acid was stored at -80°C. Immobilized tetrameric avidin-agarose beads (Pierce 20219) and immobilized monomeric avidin-agarose beads (Pierce 20228) were used to purify FP-biotinylated proteins as well as FP-biotinylated peptides. Human butyrylcholinesterase was purified from outdated human plasma as described (Lockridge et al., 2005) and labeled with FP-biotin as described (Peeples et al., 2005). Mouse plasma was from strain 129Sv mice. Human holo-transferrin (T0665), human apo-transferrin (T4382), mouse apo-transferrin (T0523), bovine holo-transferrin (T1408), human alpha 2-macroglobulin (M6159), human alpha 1-antitrypsin (A9024), human complement C3 (C2910), nitrilotriacetic acid (N9877), Coomassie blue R250 (Brilliant Blue R), and diisopropylfluorophosphate (D0879, a liquid with a concentration of 5.73 M) were from Sigma, St. Louis, MO. ProbeQuant G50 micro column was from Amersham (27-5335-01). Peptide RYTK was custom synthesized and purified to >95% by Genscript Corp., Piscataway, NJ. Peptide SYSM (20621) was from AnaSpec, Inc. (San Jose, CA). Alpha-cyano-4-hydroxy cinnamic acid, Glu Fibrinopeptide B, and Cal Mix 1 were from Applied Biosystems (MDS Sciex, Foster City, CA).

Blot of FP-biotin labeled proteins from a nondenaturing PAGE gel. 200 μL of human or mouse serum was treated with 100 μM FP-biotin for 24 h at 37°C. 10-30 μL aliquots were subjected to gel electrophoresis on nondenaturing polyacrylamide gradient gels, 4-22.5%, cast in a Hoefer gel apparatus. The PAGE gels were 0.75 mm thick, 15 cm wide, and 12 cm high. Nondenaturing gels were used because albumin separates from other plasma proteins on a nondenaturing gel, but not on an SDS gel. Proteins were electrophoretically transferred to a PVDF membrane using a Bio-Rad Trans-blot apparatus. The blot was hybridized with a fluorescent probe, Streptavidin Alexa Fluor 680, as described (Peeples et al., 2005). Fluorescence intensity was captured in the Odyssey Infrared Imaging System (LiCor).

Blot of FP-biotin labeled proteins from an SDS PAGE gel. Purified bovine holo-transferrin (76-81 kDa), human alpha 2-macroglobulin (tetramer 720 kDa; monomer 179 kDa), human alpha 1-antitrypsin (52 kDa), and human complement C3 (115 and 70 kDa) were dissolved in phosphate buffered saline to a concentration of 500 pmol in 50 μL. Proteins were treated with 100 μM FP-biotin at 37°C for 20 h. Control samples were treated with dimethyl sulfoxide but no FP-biotin. Unreacted FP-biotin was removed by passing the samples through a G50 spin column. Samples were boiled in the presence of dithiothreitol and SDS and loaded on a 4-22.5% polyacrylamide gradient SDS gel. After electrophoresis, some gels were stained for protein with Coomassie blue R250. For other gels, the protein was transferred to a PVDF membrane where the biotin tag was detected with Streptavidin Alexa Fluor 680, as described (Peeples et al., 2005). The amount of protein loaded on the Coomassie stained gel ranged from 3.5 to 70 μg, and that on the gel used for transfer to PVDF ranged from 1.5 to 30 μg.

Isolation of FP-biotin labeled proteins with avidin-agarose beads. Plasma was depleted of albumin by chromatography on Affi-gel blue because albumin reacts extensively with FP-biotin and can deplete the FP-biotin pool making reaction with other proteins more difficult. The albumin depleted plasma was treated with 100 μM FP-biotin for 24 h at 37°C, and dialyzed to remove excess FP-biotin. The FP-biotinylated proteins were purified by binding to tetrameric avidin-agarose beads and separated by SDS gel electrophoresis as described (Peeples et al., 2005).

Purification of FP-biotin-labeled peptides. In some experiments the FP-biotin-labeled peptides rather than FP-biotin-labeled proteins were purified by binding to monomeric avidin-agarose beads. After washing with 1 M NaCl in pH 8.0 buffer, followed by water washes to desalt the column, the peptides were released with 10% acetic acid.

Reaction of pure transferrin with OP. A 1 mg/mL solution of human or mouse transferrin in 0.1 M TrisCl pH 8.5, or in phosphate buffered saline, or in 10 mM TrisCl pH 8.5, 0.01% sodium azide was treated with 0.5 mM OP at 37°C for 16 hours. The accession numbers in the SwissProt database are P02787 for human and Q921I1 for mouse transferrin. Their molecular weight is about 75,000 after subtraction of the 19 amino acid signal peptide.

Tryptic peptides for mass spectrometry. Three protocols were used to prepare peptides for mass spectrometry. 1) Proteins in SDS PAGE gel slices were digested with trypsin. The peptides were extracted from the gel and analyzed by LC/MS/MS as described (Peeples et al., 2005). This protocol was used only for the preliminary experiments where the data are not shown. 2) Pure proteins in solution were denatured in 8 M urea, reduced with 10 mM dithiothreitol at pH 8, carbamidomethylated with 50 mM iodoacetamide, and desalted by dialysis against 10 mM ammonium bicarbonate. The carbamidomethylated proteins were digested with trypsin at a ratio of 50:1 (wt/wt) at 37° for 16 hours. Peptides were separated offline by reverse phase HPLC on a 100 x 4.60 mm Phenomenex C18 column eluted with a 60 min gradient from 0 to 60% acetonitrile versus 0.1% trifluoroacetic acid at a flow rate of 1 mL/min. Fractions were analyzed by MALDI-TOF mass spectrometry to locate the OP-labeled peptides. Selected samples were dried, dissolved in 50% acetonitrile, 0.1% formic acid and infused into the QTRAP 4000 mass spectrometer for MS/MS analysis. Peptides were infused into the mass spectrometer when the mass of the parent ion was known. 3) Trypsin digested pure protein was analyzed s second way to allow for the possibility that the mass of the parent ion was unknown. The offline HPLC step was omitted, and peptides were separated on a nanocolumn whose output was electrosprayed into the QTRAP 2000 mass spectrometer. MS/MS spectra were acquired for 3 peptides every 2.8 seconds.

Reaction of model peptides with OP. Peptides RYTR (0.17 mM) and SYSM (0.17 mM) in 10 mM ammonium bicarbonate pH 8.3 were treated with 0.1, 0.2, or 1 mM DFP, CPO, or dichlorvos for 16 h at 37°C. Aliquots were spotted on a MALDI target plate, overlaid with CHCA matrix, and analyzed by MALDI-TOF as well as by MALDI-TOF-TOF mass spectrometry and by LC/MS/MS on the QTRAP 2000.

MALDI-TOF mass spectrometry. All peptide samples were screened by MALDI-TOF before they were analyzed in the QTRAP mass spectrometer because MALDI-TOF is a quick way to obtain peptide masses and thereby a suggestion of whether an OP-labeled peptide is present. Salt-free peptides were spotted on a target plate in 0.5 μL aliquots, allowed to dry, and overlaid with 10 mg/mL CHCA matrix in 50% acetonitrile, 0.1% trifluoroacetic acid. Mass spectra were acquired with the MALDI-TOF-TOF 4800 mass spectrometer (Applied Biosystems, MDS Sciex, Foster City, CA). Each scan is the sum of 500 laser shots - 50 shots were taken at one location on the spot and then the laser automatically moved to a new location to avoid burning out the sample. Laser intensity was adjusted to obtain maximum signal intensity without exceeding the

saturation limit. The mass spectrometer was calibrated against Cal Mix 1 (des-Arg Bradykinin, Glu Fibrinopeptide B, angiotensin I and neurotensin).

LC/MS/MS on a Tandem quadrupole mass spectrometer. Tryptic digests of OP-labeled human and mouse transferrin were analyzed by this method. A 10 μL aliquot of peptides in 5% acetonitrile, 0.1% formic acid, at a concentration of about 2 pmol/μL, was injected into the HPLC nanocolumn (#218MS3.07515 Vydac C18 polymeric rev-phase, 75 micron ID x 150 mm long; P.J. Cobert Assoc, St. Louis, MO). Peptides were separated with a 90 min linear gradient from 0% to 60% acetonitrile at a flow rate of 0.3 μL/min and electrosprayed through a nanospray emitter (fused silica, 360 micron OD x 75 micron ID x 15 micron taper; New Objective) directly into the mass spectrometer. Mass spectra, high resolution mass spectra, and product ion spectra (MS/MS) were acquired on a QTRAP 2000 triple quadrupole linear ion trap mass spectrometer (Applied Biosystems) using the trap (enhanced sensitivity) mode. An ion-spray voltage of 1900 volts was maintained between the emitter and the mass spectrometer. Information-dependent acquisition was used to acquire data for the 3 most intense peaks in each cycle, having a charge of +1 to +4, a mass between 200 and 1700 m/z, and an intensity >10,000 cps. Precursor ions were excluded for 30 seconds after one MS/MS spectrum had been collected. The collision cell was pressurized to 40 μTorr with pure nitrogen and collision energies between 20 and 40 eV were determined automatically by the Analyst 1.4.1 software, based on the mass and charge of the precursor ion. The mass spectrometer was calibrated using fragment ions generated from collision-induced dissociation of Glu fibrinopeptide B (Sigma). The MS/MS data were processed using Analyst 1.4.1 software and submitted to Mascot for identification of peptide sequences modified by OP on Tyr, Ser, or Thr (Perkins et al., 1999).

Infusion in the QTRAP 4000 mass spectrometer. HPLC purified OP-labeled human and mouse transferrin tryptic peptides were analyzed by this method when the mass of the parent ion was known from MALDI-TOF experiments. Peptides were dissolved in 50% acetonitrile, 0.1% formic acid to a concentration of 2-6 pmol/μL. Peptides were infused into the QTRAP 4000 (Applied Biosystems, Foster City, CA) mass spectrometer at a flow rate of 0.3 μL/min through an 8 μm emitter (#FS360-50-8-D, New Objective) via a 25 μL Hamilton syringe mounted on a Harvard pump. 500 MS/MS spectra were accumulated for each parent ion.

Binding of ferric ion to transferrin. The normal function of transferrin is iron transport through the blood. Binding of ferric ion is a measure of the functional viability. Titration of transferrin with ferric ion was performed as described (Welch and Skinner, 1989). A 1 mg/mL solution of apo-human transferrin was prepared in 0.1 M TrisCl pH 8.5 containing 5 mM Na_2CO_3. Half of the transferrin solution was incubated with 100 μM FP-biotin at 37°C for 16 h, resulting in the labeling of Tyr 238 and Tyr 574. The other half was the unlabeled control. Protein concentration was determined with the CB-X protein assay kit (Genotech, St. Louis, MO; #786-12X). FP-biotin-labeled as well as control apo-transferrin were titrated with ferric nitrilotriacetate (FENTA) to determine the stoichiometry of ferric ion binding. Each 1 mL solution of transferrin was titrated by sequential additions of 5 μL of 1 mM FENTA. Binding was monitored by following the change in absorbance at 470 nm.

RESULTS
Human and mouse plasma proteins that bind FP-biotin. The blots in Figures 2.1A and 2.1B show at least 12 bands in both human and mouse plasma that bind FP-biotin (Figures 2.1A and 2.1B lanes 7, 8, 9). The most intense band in human plasma is FP-biotin-labeled albumin. The most intense band in mouse plasma contains two proteins: FP-biotin-labeled carboxylesterase ES1 and FP-biotin-labeled albumin (Figure 2.1B lanes 7, 8, 9). A major difference between human and mouse plasma is that only mouse plasma contains carboxylesterase (Li et al., 2005). Albumin, ES1 carboxylesterase, and butyrylcholinesterase have previously been identified as proteins in mouse plasma that bind FP-biotin (Peeples et al., 2005).

The search for additional OP-reactive proteins in plasma led to preliminary identification of human transferrin. This preliminary identification resulted from LC/MS/MS mass spectral analysis of an in-gel, tryptic digest of a band from an SDS PAGE gel. Data were acquired on the QTRAP 2000 mass spectrometer. Proteins applied to this gel had been labeled with FP-biotin and purified with avidin-agarose (data not shown). Mass spectra identified transferrin, but not the labeled peptide.

To confirm that transferrin was actually labeled by FP-biotin, pure human and mouse transferrin treated with FP-biotin were visualized on a blot hybridized with Streptavidin Alexa Fluor 680. Lane 3 in Figures 2.1A and 2.1B shows an intense band for FP-biotinylated transferrin, thus confirming that human and mouse transferrin bind FP-biotin.
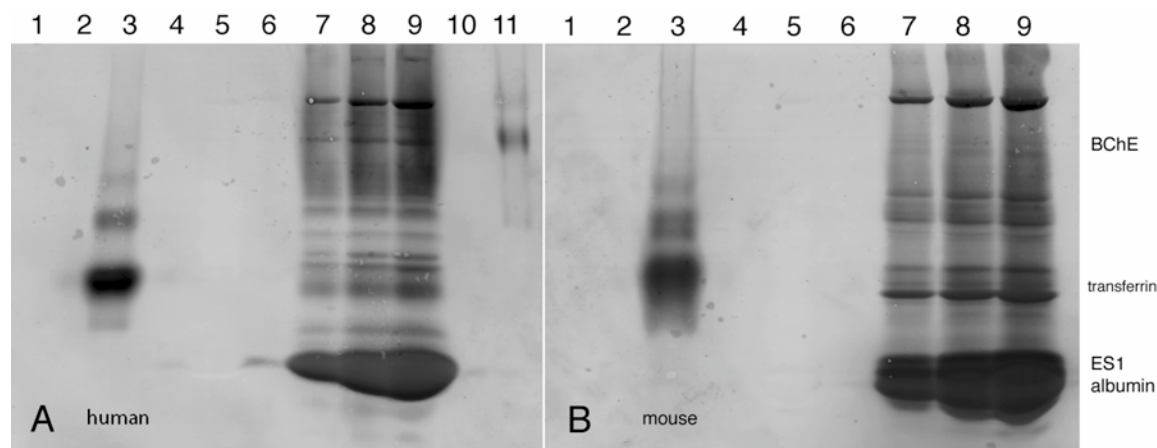

Figure 2.1. Blots showing FP-biotin-reactive proteins in human (A) and mouse (B) plasma. The blots were made by transferring FP-biotin treated protein from nondenaturing, polyacrylamide gels onto PVDF membranes and hybridizing with the fluorescent probe Streptavidin Alexa Fluor 680. A1, 20 μg human transferrin; A2, blank; A3, 20 μg FP-biotinylated human transferrin; A4, blank; A5, 5 μL human plasma; A6, blank; A7, 3.3 μL FP-biotinylated human plasma; A8, 6.6 μL FP-biotinylated human plasma; A9, 9.9 μL FP-biotinylated human plasma; A10, blank; A11, 1 pmole FP-biotinylated human butyrylcholinesterase (BChE). B1, 20 μg mouse transferrin; B2, blank; B3, 20 μg FP-biotinylated mouse transferrin; B4, blank; B5, 5 μL mouse plasma; B6, blank; B7, 5 μL FP-biotinylated mouse plasma; B8, 10 μL FP-biotinylated mouse plasma; B9, 15 μL FP-biotinylated mouse plasma. ES1 carboxylesterase in mouse plasma does not separate well from albumin on a nondenaturing gel. Human plasma does not contain carboxylesterase.

The preliminary LC/MS/MS mass spectral experiments also showed alpha-2-macroglobulin, alpha-1-antitrypsin, and complement C3 as proteins in human plasma that could be labeled with FP-biotin (data not shown). As with transferrin, the FP-biotinylated plasma proteins had been purified on avidin-agarose beads, separated by SDS gel electrophoresis, digested with trypsin, and analyzed by LC/MS/MS. The labeled peptides from these proteins were not found in these preliminary experiments. To confirm that these proteins made a covalent bond with FP-biotin, highly purified preparations of the proteins were treated with FP-biotin and subjected to SDS gel electrophoresis. The labeled proteins were transferred from the gel to PVDF membrane. The membrane was hybridized with Streptavidin Alexa Fluor 680 (Figure 2.2B). A second gel, containing higher quantities of protein, was stained with Coomassie blue R250 (Figure 2.2A). Figure 2.2 (lanes 2, 4, 6, 8) shows that control proteins, not treated with FP-biotin, have a Coomassie stained band in panel A, but no fluorescent band in panel B. On the other hand, proteins treated with FP-biotin (lanes 1, 3, 5, 7) have a band in panel A as well as in panel B. The blot confirms that human alpha-1-antitrypsin, human complement C3, human alpha-2-macroglobulin, and bovine holo-transferrin covalently bind FP-biotin.

No further results were obtained for alpha-1-antitrypsin, complement C3, and alpha-2-macroglobulin. The site for covalent attachment of FP-biotin in these proteins is unknown.
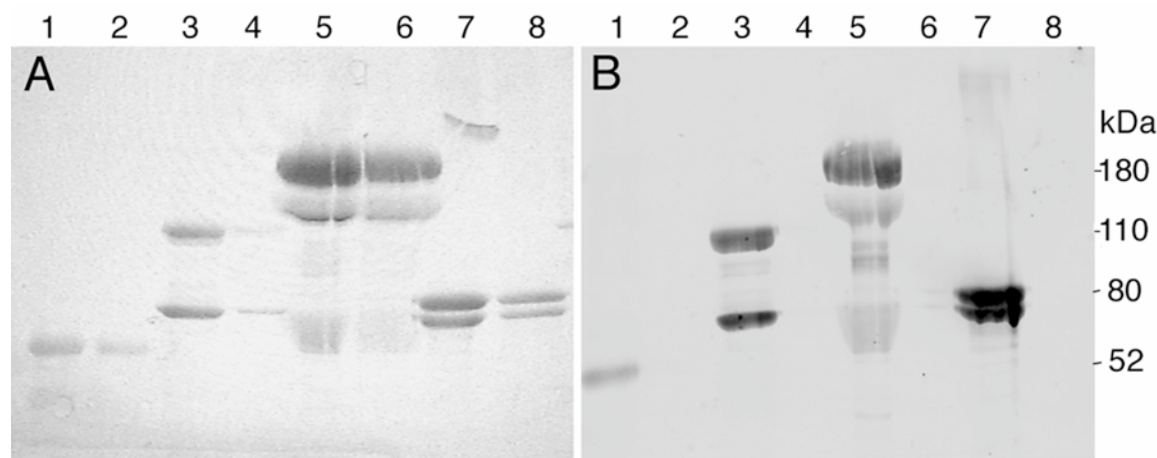

Figure 2.2. Covalent binding of FP-biotin to human alpha-1-antitrypsin, human complement C3, human alpha-2-macroglobulin, and bovine holo-transferrin. A) Coomassie stained SDS gel. B) Blot hybridized with Streptavidin Alexa Fluor 680 to visualize FP-biotinylated proteins transferred to PVDF membrane from the gel. Lane 1, FP-biotinylated alpha-1-antrypsin; lane 2, unlabeled alpha-1-antitrypsin; lane 3, FP-biotinylated complement C3; lane 4, unlabeled complement C3; lane 5, FP-biotinylated alpha-2-macroglobulin; lane 6, unlabeled alpha-2-macroglobulin; lane 7, FP-biotinylated transferrin; lane 8, unlabeled transferrin.

Tyr 238 and Tyr 574 of human transferrin bind OP. FP-biotinylated, carbamidomethylated (CAM) tryptic peptides of human transferrin were purified on monomeric avidin beads and their masses determined by MALDI-TOF mass spectrometry. Every peak in the MALDI-TOF spectrum was fragmented with the MALDI-TOF-TOF feature of the mass spectrometer. The MS/MS scans were examined for the presence of ions characteristic of FP-biotin at 227, 312, and

329 amu (Schopfer et al., 2005). A peptide that fragmented to yield these ions was definitely labeled with FP-biotin. Additional information about the peptide was obtained in the QTRAP 4000 mass spectrometer.

Two FP-biotin-labeled peptides were identified. The MS/MS spectrum in Figure 2.3A shows that FP-biotin is covalently attached to tyrosine in peptide KPVDEY*K. The parent ion mass (726 m/z, doubly charged) is equal to the peptide mass plus the added mass from FP-biotin (572 amu). Fragments at 227.3, 312.5 and 329.5 amu are characteristic for the presence of FP-biotin. Absence of a mass at 591 amu suggests the FP-biotin is bound to tyrosine (Schopfer et al., 2005). The masses at 708.8 and 691.6 amu are commonly seen in the fragmentation spectrum of FP-biotinylated tyrosine and are consistent with the immonium ion of FP-biotinylated tyrosine and its deamino counterpart (unpublished observations). The y-ion series (y2-y6) is consistent with FP-biotin attached to the C-terminal peptide, YK. Of these two residues, tyrosine is the most likely candidate for carrying the label. Were the lysine to have been labeled, experience argues that trypsin would not have recognized that lysine as a cleavage site. The b-ion series (b1-b5) supports the identification of the peptide.

The spectrum in Figure 2.4A shows that FP-biotin is covalently attached to tyrosine in peptide KPVEEY*ANCHLAR. The parent ion mass (541.4 m/z, quadruply charged) is consistent with the mass of the peptide plus the added mass of FP-biotin. The characteristic fragments at 227.3, 312.6, 329.6, 708.7 and 691.6 amu along with the absence of a fragment at 591 amu are indicative of FP-biotin bound to a tyrosine in this peptide. Minor fragments at 1248.6, 1378.0 and 1507.0 amu are consistent with FP-biotinylated peptides y8-y10 that have lost 328 amu during collision induced dissociation in the mass spectrometer. 328 amu is the neutral counterpart of the 329 amu characteristic fragment from FP-biotin. The y-ion series (y1-y7) and the b-ion series (b1-b5) account for all the residues in the peptide except for the tyrosine which appears to carry the FP-biotin label.

The labeled tyrosines are Tyr 238 and Tyr 574, when numbering is for the mature human transferrin protein (MacGillivray et al., 1982) from which the 19 amino acid signal peptide has been deleted (Swiss Prot accession #P02787). Both holo- and apo-human transferrin bound FP-biotin.

Human transferrin also covalently bound DFP, chlorpyrifos oxon, and dichlorvos on Tyr 238 and Tyr 574, as shown in Figures 2.3 and 2.4, panels B, C, and D. Analyses of the spectra support the labeling of these tyrosines. Details are given in the figure legends.

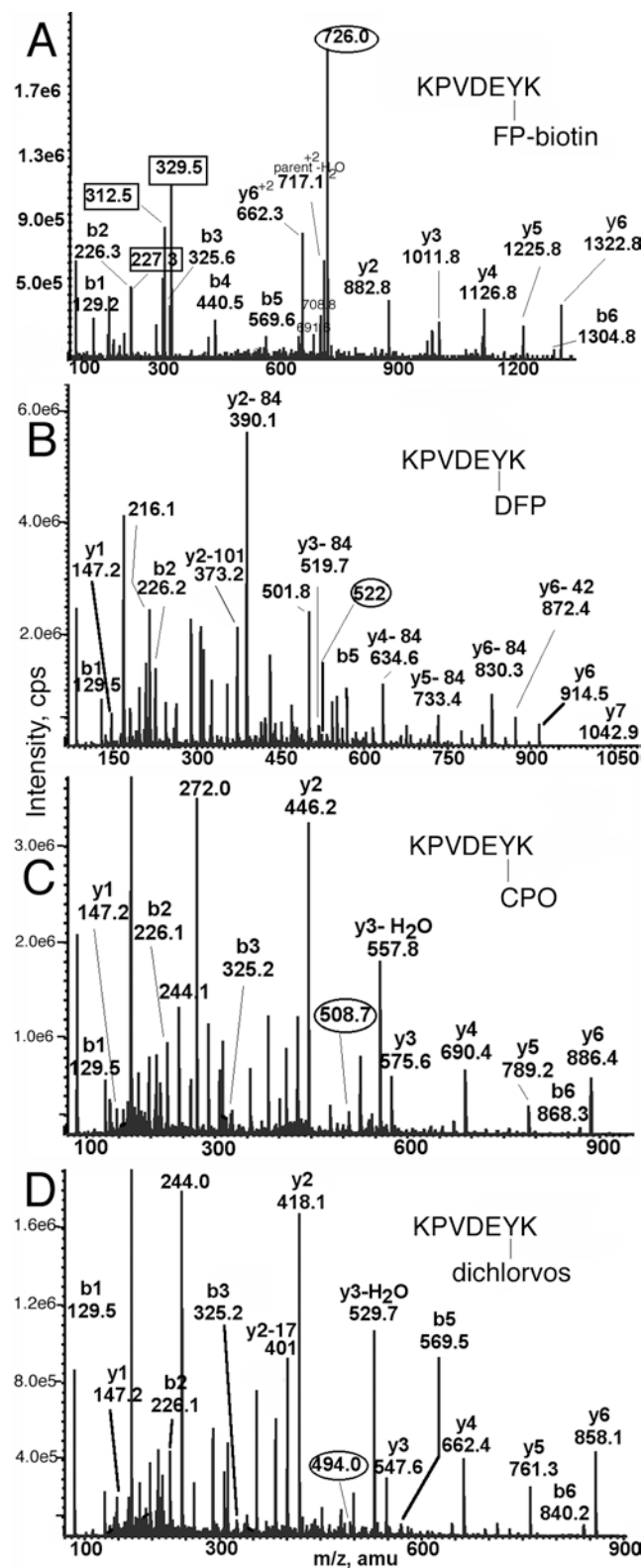No evidence of covalent binding of soman or sarin to transferrin was found.

Figure 2.3. MS/MS spectra of OP labeled Tyr 238 in peptide KPVDEYK of human transferrin. Mass spectra were acquired on the QTRAP 4000 mass spectrometer by infusion. The b and y ion masses in all panels are consistent with OP covalently bound to Tyr 238; the added mass

from FP-biotin is 572 amu, from DFP is 164 amu, from chlorpyrifos oxon is 136 amu, and from dichlorvos is 108 amu. A) The doubly charged parent ion of the FP-biotin labeled peptide is at 726.0 m/z. Masses enclosed in boxes at 227.3, 312.5, and 329.5 amu are fragments of FP-biotin. The immonium ion of FP-biotinylated tyrosine is at 708.8 amu. Its partner ion at 691.6 amu has lost 17 amu. B) The doubly charged parent ion of the DFP-labeled peptide is at 522.0 m/z. Loss of one or both isopropyl groups during collision induced dissociation yields y-ions minus 42 or minus 84 amu, confirming the presence of diisopropylphosphate. Loss of both isopropyl groups is the most common observation (Li et al., 2007; Grigoryan et al., 2008). The y-ion series (y1 and y2-84 through y6-84) indicates that tyrosine is labeled. The delta mass (242.9 amu) between y1 (147.2 amu) and y2-84 (390.1 amu) is consistent with the appearance of tyrosine phosphate at fragment y2 (163 amu for tyrosine and 80 amu for phosphate). The mass at 373.2 amu is the y2 ion minus 101 amu, representing loss of two isopropyl groups as well as ammonia. The mass at 501.8 m/z is the doubly charged parent ion minus one isopropyl group. The mass at 216.1 amu is consistent with the phosphotyrosine immonium ion. C) The doubly charged parent ion of the chlorpyrifos oxon-labeled peptide is at 508.7 m/z. The y-ion series (y1-y6) shows the presence of all residues. The mass difference (299.0 amu) between y1 (147.2 amu) and y2 (446.2 amu) clearly shows the diethoxyphosphate on tyrosine in fragment y2 (163 amu for tyrosine and 136 amu for diethoxyphosphate). The mass at 244.1 amu is consistent with the monoethoxyphosphotyrosine immonium ion. The mass at 272.0 amu is consistent with the diethoxyphosphotyrosine immonium ion. D) The doubly charged parent ion of the dichlorvos-labeled peptide is at 494.0 m/z. The y-ion series (y1-y6) shows the presence of all residues. The mass difference (270.9 amu) between y1 (147.2 amu) and y2 (418.1 amu) clearly shows the dimethoxyphosphate on tyrosine in fragment y2 (163 amu for tyrosine and 108 amu for dimethoxyphosphate). The mass at 244.0 amu is consistent with dimethoxyphosphotyrosine immonium ion.
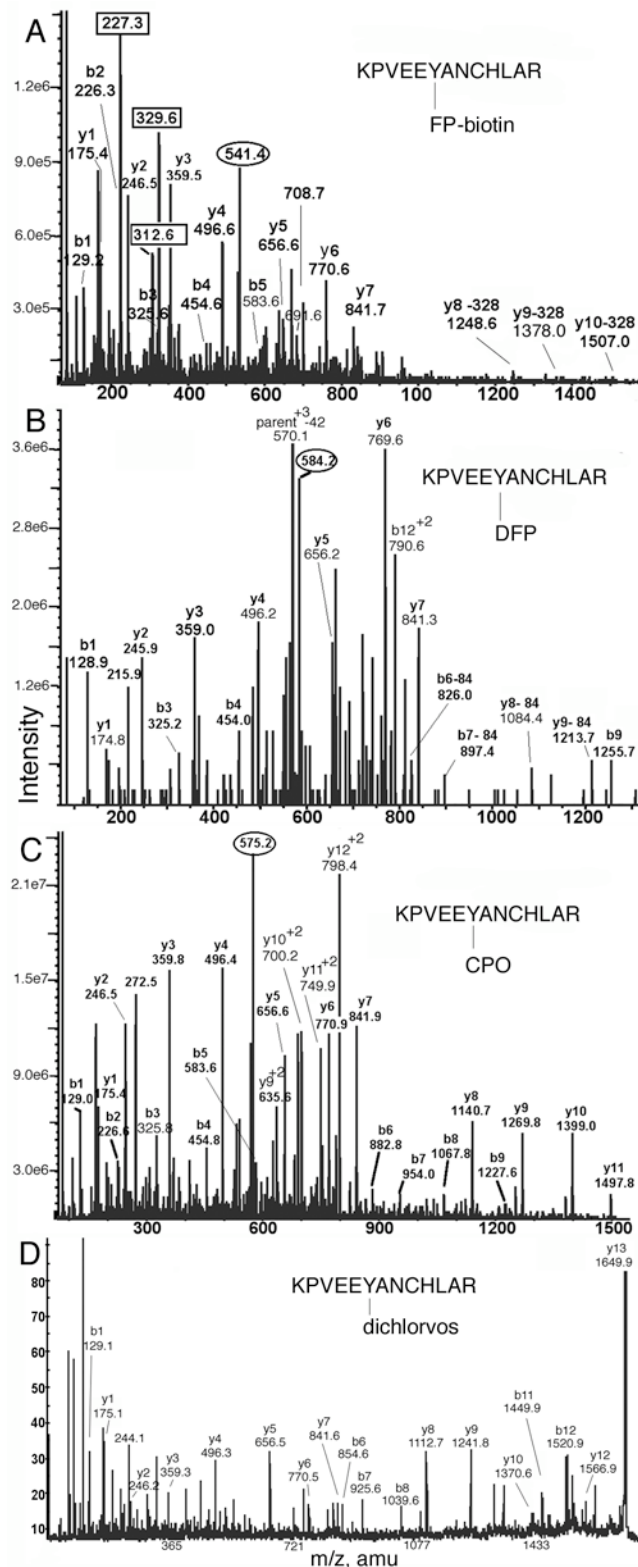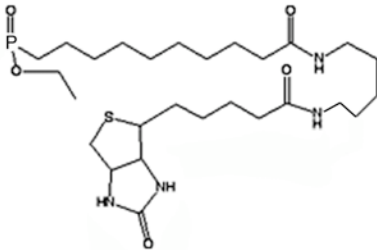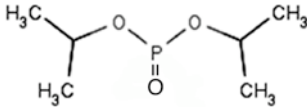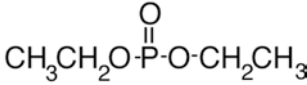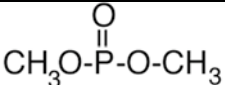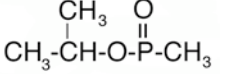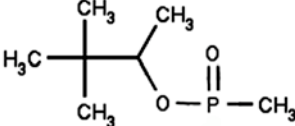
Figure 2.4. MS/MS spectra of OP labeled Tyr 574 in peptide KPVEEYANCHLAR of human transferrin. Mass spectra were acquired on the QTRAP 4000 mass spectrometer by infusion. The b and y ion masses in all panels are consistent with OP covalently bound to Tyr 574; the added mass from FP-biotin is 572 amu, from DFP is 164 amu, from chlorpyrifos oxon is 136 amu, and

from dichlorvos is 108 amu. A) The quadruply charged parent ion of the FP-biotin labeled peptide is at 541.4 m/z. Masses enclosed in boxes at 227.3, 312.6, and 329.6 amu, are fragments of FP-biotin. The immonium ion of FP-biotinylated tyrosine is at 708.7 amu. Its partner ion at 691.6 amu has lost 17 amu. Three y-ions have lost 328 amu from FP-biotin. B) The triply charged parent ion of the DFP-labeled peptide is at 584.2 m/z. Loss of one or both isopropyl groups yields ions minus 42 or minus 84 amu. The y-ion series (y1-y7) supports the identification of the peptide and indicates that the OP label is not in that portion of the peptide. The delta mass (243.2 amu) between y7 (841.3 amu) and y8-84 (1084.4 amu) fits with the appearance of tyrosine-phosphate in fragment y8 (163 amu for tyrosine and 80 amu for phosphate). The presence of tyrosine-phosphate is expected for tyrosine-diisopropylphosphate that has lost both isopropyl groups. Masses at 1213.7 (y9-84), 826.0 (b6-84) and 897.4 amu (b7-84) support this assignment. The mass at 215.9 amu is consistent with the phosphotyrosine immonium ion. C) The triply charged parent ion of the chlorpyrifos oxon-labeled peptide is at 575.2 m/z. The y-ion series (y1-y11) shows a delta mass (299.4 amu) between y7 (841.3 amu) and y8 (1140.7 amu) that is consistent with the appearance of tyrosine-diethoxyphosphate at fragment y8 (163 amu for tyrosine and 136 amu for diethoxyphosphate). This is supported by the b-ion series (b1-b9) which shows the appearance of the same tyrosine as tyrosine-diethoxyphosphate at fragment b6. The mass at 272.5 amu is consistent with the diethoxyphosphotyrosine immonium ion. D) The singly charged parent ion of the dichlorvos-labeled peptide is at 1694.9 m/z. This is a MALDI-TOF-TOF spectrum, whereas the spectra in A-C were acquired in the QTRAP mass spectrometer. The y-ion series (y1-y10) shows a delta mass (271.1 amu) between y7 (841.6 amu) and y8 (1112.7 amu) which is consistent with the appearance of tyrosine-dimethoxyphosphate at fragment y8 (163 amu for tyrosine and 108 amu for dimethoxyphosphate). The mass at 244.1 amu is consistent with dimethoxyphosphotyrosine immonium ion.

Mouse transferrin labeled on Tyr 238, Tyr 319, Tyr 429, Tyr 491, Tyr 518. Five tyrosines in mouse transferrin were labeled by FP-biotin and chlorpyrifos oxon (Table 2.1). Two tyrosines were labeled by DFP. No residues were labeled by dichlorvos. Both holo- and apo- mouse transferrin bound FP-biotin (data not shown).

Table 2.1. Mouse transferrin (Swiss Prot accession #Q921I1) labeled with OP.

OP	added mass	structure of added mass	labeled peptide	OP-Tyr
FP-biotin	572		KPVDQY*EDCYLAR	Y238
			LYLGHNY*VTAIR	Y319
			GY*YAVAVVK	Y429
			FDEFFSQGCAPGY*EK	Y491
			EEYNGY*TGAFR	Y518
DFP	164		KPVDQY*EDCYLAR	Y238
			GY*YAVAVVK	Y429
CPO	136		KPVDQY*EDCYLAR	Y238
			LYLGHNY*VTAIR	Y319
			GY*YAVAVVK	Y429
			FDEFFSQGCAPGY*EK	Y491
			EEYNGY*TGAFR	Y518
dichlorvos	108		none	none
sarin	120			
soman	162			

No aging. Aging of OP-modified acetylcholinesterase and butyrylcholinesterase involves the loss of an alkyl group from the OP. For example, soman-inhibited acetylcholinesterase loses the pinacolyl group during aging so that the added mass for aged soman is 72 rather than 162 amu. No evidence for aging of the OP-tyrosine adducts of transferrin was found.

Motif for OP binding to Tyrosine. Comparison of the sequences of the 7 transferrin peptides that bind OP shows no definite consensus sequence around the tyrosine to which the OP binds. What the peptides do have in common is the presence of a positively charged Arginine or Lysine within 1-5 amino acids from the labeled tyrosine.   Figure 2.5 suggests a histidine may also participate in activation of tyrosine. These positively charged residues probably interact with the phenolic hydroxyl group of tyrosine to lower the pKa. Tyrosines with a lower pKa value would be better nucleophiles and thus be better able to attack OP.
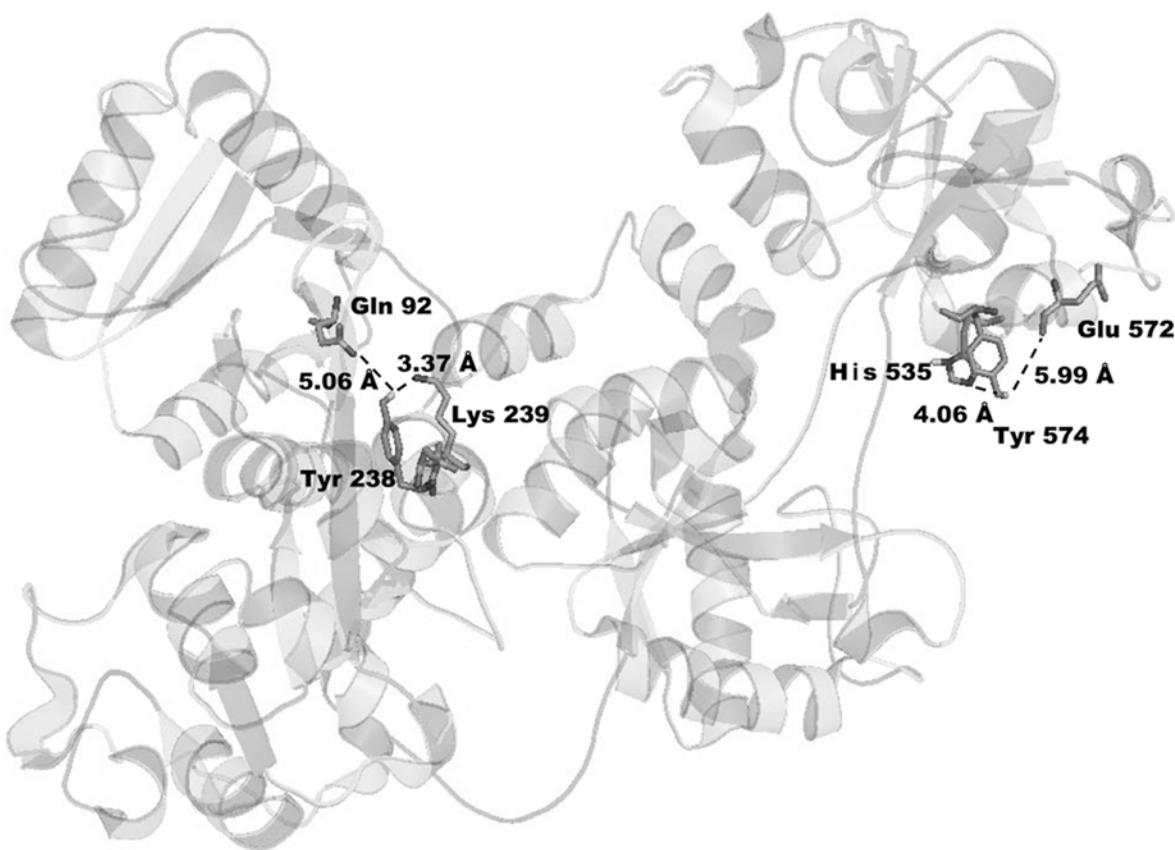
Figure 2.5. OP-labeled Tyr 238 and Tyr 574 in the crystal structure of human apo-transferrin (PDB code 2hav).   The phenolic hydroxyl of Tyr 238 is 3.37 Å from the amine of Lys 239 and 5.06 Å from Gln 92.   The phenolic hydroxyl of Tyr 574 is 4.06 Å from the imidazole nitrogen of His 535 and 5.99 Å from oxygen in the carbonyl of Glu 572 (Wally et al., 2006).

Peptide RYTR covalently binds OP. The hypothesis was tested that a positively charged amino acid located near a tyrosine could activate tyrosine, enabling it to covalently bind OP. Incubation of peptide RYTR with 0.1, 0.2, or 1 mM CPO, dichlorvos, or DFP in pH 8.3 buffer at 37°C for 16 hours resulted in covalent labeling of tyrosine (Figure 2.6). 37% of a 170 μM solution of RYTR was labeled by 1 mM DFP, 24% by 1 mM CPO, and 21% by 1 mM dichlorvos. MS/MS spectra showed that the OP-labeled residue in peptide RYTR was tyrosine. In contrast, peptide SYSM was labeled only by DFP and not by dichlorvos or CPO. MS/MS spectra showed that the OP-labeled residue in SYSM was tyrosine. Peptide SYSM ionized poorly in the MALDI-TOF, giving a weak signal with large standard deviation.   It was concluded that tyrosines in general could be labeled by OP, but that the most reactive tyrosines were within hydrogen-bonding distance of a positively charged arginine or lysine.
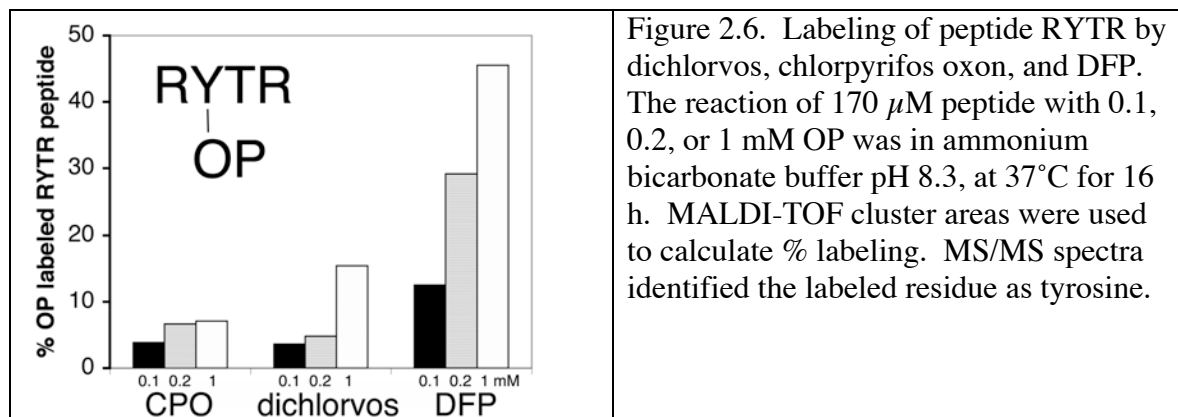
Figure 2.6. Labeling of peptide RYTR by dichlorvos, chlorpyrifos oxon, and DFP. The reaction of 170 μM peptide with 0.1, 0.2, or 1 mM OP was in ammonium bicarbonate buffer pH 8.3, at 37°C for 16 h. MALDI-TOF cluster areas were used to calculate % labeling. MS/MS spectra identified the labeled residue as tyrosine.

Function of transferrin is not disrupted by OP binding. It was unknown whether covalent binding of an OP to transferrin affected the ability of transferrin to bind ferric ions. Tyrosines 95, 188, 426, and 517 are involved in the binding of ferric ions in human transferrin (Sargent et al., 2005).

Human apo-transferrin, labeled with FP-biotin on Tyr 238 and Tyr 574, as well as control apo-transferrin were titrated with ferric nitriloacetate to determine binding stoichiometry. Figure 2.7 shows that both transferrin preparations bound approximately 2 moles of ferric ion per mole of transferrin, a result in agreement with the known number of ferric ion binding sites in transferrin (Bates and Schlabach, 1973). It was concluded that modification of human transferrin by FP-biotin did not interfere with binding of ferric ion.
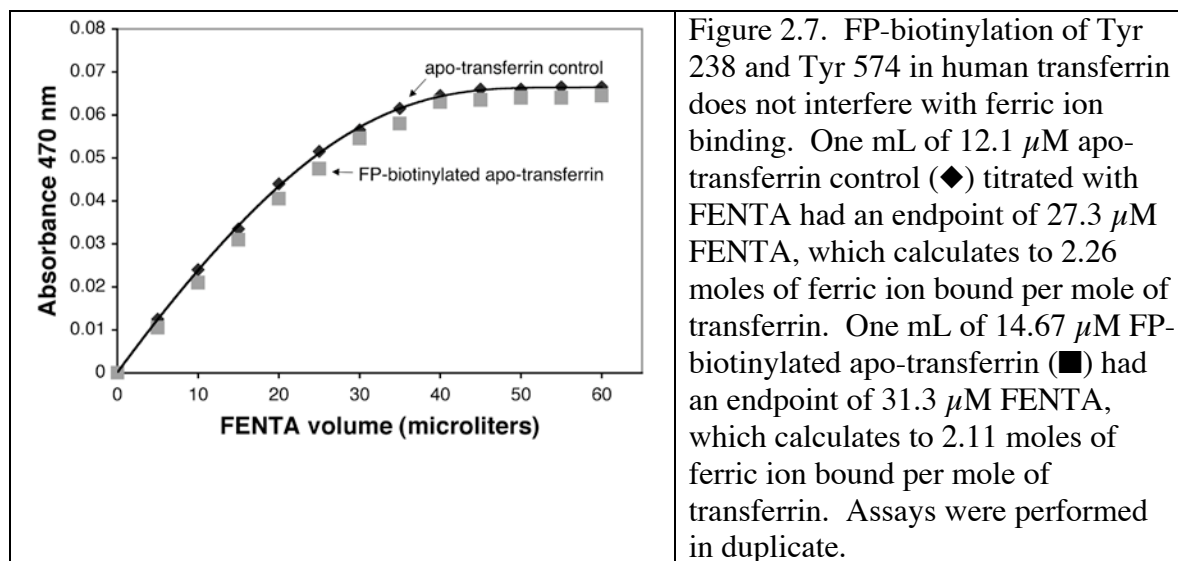

Figure 2.7. FP-biotinylation of Tyr 238 and Tyr 574 in human transferrin does not interfere with ferric ion binding. One mL of 12.1 μM apo-transferrin control (◆) titrated with FENTA had an endpoint of 27.3 μM FENTA, which calculates to 2.26 moles of ferric ion bound per mole of transferrin. One mL of 14.67 μM FP-biotinylated apo-transferrin (■) had an endpoint of 31.3 μM FENTA, which calculates to 2.11 moles of ferric ion bound per mole of transferrin. Assays were performed in duplicate.

DISCUSSION
Serine hydrolases are not the only OP binding proteins in human plasma. Our expectation when we started this project was that OP-labeled proteins would all be serine esterases and serine proteases. We expected butyrylcholinesterase to be the dominant OP-binding protein in human plasma (Fidder et al., 2002; Van Der Schans et al., 2004). Our results show that this expectation was not met. OP bind not only to serine esterases and serine proteases, but also to proteins that

have an activated tyrosine. Using mass spectrometry, we have conclusively demonstrated OP binding to 18 tyrosines in five proteins: human albumin (Li et al., 2007), alpha- and beta-tubulin (Grigoryan et al., 2008), human transferrin and mouse transferrin. In addition we have shown that human alpha-1-antitrypsin, human complement C3, human alpha-2-macroglobulin covalently bind FP-biotin, though the site of attachment is unknown. Tyrosine in small synthetic peptides was also the site of attachment of OP.

New OP binding motif. The OP binding motif in the serine hydrolase family is GXSXG where OP is covalently bound to serine. Though OP binding to Tyr 411 of human albumin has long been recognized, OP binding to tyrosine as a general phenomenon has not been appreciated. Our results show that OP binding to tyrosine is not confined to Tyr 411 of albumin, but is found on many tyrosines in many proteins. Even the small peptide RYTR made a covalent bond with OP. The chief requirement for OP binding to tyrosine appears to be a nearby positively charged arginine or lysine.

It is anticipated that many more proteins than those we have already identified can be modified by OP. Proteins with no active site serine that have, however, been implicated in OP-induced neurodevelopmental and behavioral toxicity, or immunosuppression could be modified on tyrosine, for example neurotransmitter receptors (Katz et al., 1997; Pope, 1999; Bomser and Casida, 2001; Quistad et al., 2002; Aldridge et al., 2003; Smulders et al., 2004; Lein and Fryer, 2005), proteins in the adenylyl cyclase signaling cascade (Song et al., 1997), cyclic AMP response element binding protein (Schuh et al., 2002), immune function proteins (Kassa et al., 2003), and kinesin in the axonal transport system (Gearhart et al., 2007; Prendergast et al., 2007; Terry et al., 2007).

Biomarkers of OP exposure. Our in vitro conditions used high concentrations of OP that would not be found during in vivo poisoning. It is unknown whether live animals treated with a nonlethal dose of OP would have OP-labeled transferrin. However, it is known that mice treated with a nontoxic dose of FP-biotin (Peeples et al., 2005) and guinea pigs treated with sarin, soman, cyclosarin, and tabun have OP-labeled albumin in their blood (Williams et al., 2007). Thus, tyrosine-modified proteins could serve as biomarkers for OP exposure. The serine hydrolases, acetylcholinesterase, butyrylcholinesterase, and acylpeptide hydrolase have been shown to serve as biomarkers of OP exposure in mice and rats (Richards et al., 2000; Quistad et al., 2005).

Significance. Our findings may have application to diagnosis and treatment of OP exposure. Proteins that have no active site serine may serve as biomarkers of exposure. In the future it may be possible to develop antibodies to the new OP-labeled biomarkers to use for screening OP exposure. Synthetic peptides containing arginine, lysine, and tyrosine may find application as scavengers to clear the body of OP. The recognition that tyrosines are labeled by OP may aid in understanding the mechanism by which OP cause neurodevelopmental toxicity and cognitive impairment.

Additional progress on Milestones 3, 4, and 5

Mass spectrometry identifies covalent binding of soman, sarin, chlorpyrifos oxon, diisopropyl fluorophosphate, and FP-biotin to tyrosines on tubulin; OP-binding to tubulin may explain cognitive deficits associated with OP exposure

ABSTRACT

Chronic low dose exposure to organophosphorus poisons (OP) results in cognitive impairment. Studies in rats have shown that OP interfere with microtubule polymerization. Since microtubules are required for transport of nutrients from the nerve cell body to the nerve synapse, it has been suggested that disruption of microtubule function could explain the learning and memory deficits associated with OP exposure. Tubulin is a major constituent of microtubules. We tested the hypothesis that OP bind to tubulin by treating purified bovine tubulin with sarin, soman, chlorpyrifos oxon, diisopropylfluorophosphate, and 10-fluoroethoxyphosphinyl-N-biotinamidopentyldecanamide (FP-biotin). Tryptic peptides were isolated and analyzed by mass spectrometry. It was found that OP bound to tyrosine 83 of alpha tubulin in peptide TGTYR, tyrosine 59 in beta tubulin peptide YVPR, tyrosine 281 in beta tubulin peptide GSQQYR, and tyrosine 159 in beta tubulin peptide EEYPDR. The OP reactive tyrosines are located either near the GTP binding site or within loops that interact laterally with protofilaments. It is concluded that OP bind covalently to tubulin, and that this binding could explain cognitive impairment associated with OP exposure.

INTRODUCTION

Acute toxicity from organophosphorus poisons (OP) is mainly due to inhibition of acetylcholinesterase (Maxwell et al., 2006). However, low dose exposure that causes minimal inhibition of AChE and no obvious cholinergic symptoms has been linked to memory loss, sleep disorder, depression, learning and language impairment, and decreased motor skills in humans (Stephens et al., 1995; London et al., 2005; Roldan-Tapia et al., 2005). Rats treated with low doses of chlorpyrifos have behavioral deficits in a water-maze hidden platform task and in prepulse inhibition (Terry et al., 2007). The mechanism to explain cognitive deficits from low dose exposure is thought to be inhibition of fast axonal transport (Terry et al., 2007). Axonal transport was impaired in sciatic nerves isolated from chlorpyrifos treated rats (Terry et al., 2003; Terry et al., 2007). Transport of nutrients to nerve endings is accomplished via microtubules that

serve as the highway on which kinesin molecules carry their cargo (Gearhart et al., 2007). When microtubule function is disrupted, neurons lose viability.   Microtubules are polymers of alpha and beta tubulin. Prendergast et al have shown that polymerization of tubulin is inhibited by low doses of chlorpyrifos and diisopropyl fluorophosphate DFP (Prendergast et al., 2007). The goal of the present work was to identify the amino acid residues modified by reaction of tubulin with OP. Mass spectrometry identified 4 covalent binding sites, all of them tyrosines.

METHODS

Materials. Bovine tubulin (TL238) >99% pure, isolated from bovine brain, was from Cytoskeleton, Inc (Denver, CO). This tubulin preparation contains both alpha and beta-tubulin. Chlorpyrifos oxon (MET-674B) was from Chem Service Inc. (West Chester, PA). 10-Fluoroethoxyphosphinyl-N-biotinamidopentyldecanamide (FP-biotin) was custom synthesized in the laboratory of Dr. Charles M. Thompson at the University of Montana, Missoula, MT (Schopfer et al., 2005). Diisopropylfluorophosphate (D0879) was from Sigma/Aldrich (St. Louis, MO). The nerve agents sarin and soman were from CEB (Vert-le-Petit, France). Sequencing grade modified porcine trypsin (V5113) was from Promega (Madison, WI). Slide-A-Lyzer 7K dialysis cassettes (No. 66370) and ImmunoPure immobilized monomeric avidin (#20228) were from Pierce Biotechnology Inc. (Rockford, IL).

OP-labeled tubulin tryptic peptides. Bovine tubulin (2 mg/mL) was dissolved in either 50 mM ammonium bicarbonate pH 8.3 or in 80 mM PIPES, 0.5 mM EGTA, 0.25 mM $MgCl_2$ buffer pH 6.9, or in 10 mM TrisCl pH 8.0. The 0.5 mL of 2 mg/mL tubulin (40 µM) was treated with a 20-fold molar excess of FP-biotin dissolved in dimethyl sulfoxide, or a 200-fold molar excess of diisopropyl fluorophosphate (DFP), or a 20-fold molar excess of chlorpyrifos oxon (CPO) dissolved in dimethyl sulfoxide, or a 5-fold molar excess of soman and sarin dissolved in isopropanol. The reaction mixtures were incubated at 37˚C for 16 to 24 hours. The proteins were denatured by boiling in a water bath for 10 min. Excess OP was removed by dialysis against 10 mM ammonium bicarbonate. The 1 mg of dialyzed tubulin was digested with 0.02 mg of Promega trypsin at 37˚C for 16 hours.

Purification of FP-biotinylated peptides on monomeric avidin beads. The trypsin-digested, FP-biotinylated tubulin was boiled for 10 min to denature trypsin. This prevented digestion of avidin protein by trypsin. The digest was loaded on a 1 mL column of monomeric avidin beads. The column was washed with 20 mL of 1 M TrisCl pH 8.5 to wash off unbound peptides, followed by 20 mL of 0.1 M TrisCl pH 8.5, and 20 mL of 10 mM ammonium bicarbonate. Salts were washed off with 20 mL water, before the peptides were eluted with 10 mL of 10% acetic acid. One mL fractions were collected.

HPLC purification. Peptides intended for infusion on the Q-Trap mass spectrometer were purified by reverse phase HPLC. The advantage of offline HPLC purification was the large amount of peptide sample that could be loaded on the C18 column (Phenomenex Prodigy 5 micron ODS size 100 x 4.60 mm). Peptides from a 1 mg tubulin digest were eluted with a gradient that started with 100% of 0.1% trifluoroacetic acid and increased to 60% acetonitrile/40% 0.1% trifluoroacetic acid in 60 min on a Waters 625 LC system. Fractions of 1 mL were collected, analyzed by MALDI-TOF mass spectrometry, and dried in a SpeedVac.

MALDI-TOF mass spectrometry. The MALDI-TOF-TOF 4800 mass spectrometer (Applied Biosystems) was used for analysis of tryptic peptides prior to more rigorous analysis with the Q-Trap. This mass spectrometer was also used for analysis of tryptic peptides. A 0.5 µL sample was spotted on a 384 well Opti-TOF plate (P/N 1016491, Applied Biosystems) and the air dried spot was overlaid with 0.5 µL of 10 mg/mL a-cyano-4-hydroxycinnamic acid dissolved in 50% acetonitrile, 0.1% trifluoroacetic acid. Mass spectra were collected in positive ion reflector mode on a MALDI-TOF-TOF 4800 mass spectrometer (Applied Biosystems, Foster City, CA). The final spectrum was the average of 500 laser shots. Masses were calibrated using CalMix 5 (Applied Biosystems).

Q-Trap 4000 mass spectrometry. Peptides from selected HPLC fractions were dissolved in 100 µL of 50% acetonitrile, 0.1% formic acid and infused into the Q-Trap 4000 linear ion trap mass spectrometer (Applied Biosystems) via a nanospray source, using a continuous flow head, a flow rate of 0.30 µL/min, and an ion spray potential of 1900 volts. Spray was through a distal coated silica tip emitter FS360-75-15-D (New Objective, Woburn, MA). Mass spectra were obtained using the trap function at 4000 amu/sec with dynamic fill to determine the filling time for the trap. One hundred to 350 spectra were averaged. Peptide fragmentation also employed the trap. MS/MS spectra were obtained by collision induced dissociation at a nitrogen gas pressure of 40 µTorr and a collision energy of 30-60 volts. The spectrometer was calibrated on selected fragments from the MS/MS spectrum of [Glu]-fibrinopeptide B.

RESULTS

Strategy for identifying labeled residues in tubulin. The strategy is to first use FP-biotin to label tubulin. FP-biotinylated peptides are easy to find because the biotin tag gives a signature fragmentation pattern. Masses of 227, 312, and 329 amu are always present in the MS/MS scan of an FP-biotin labeled peptide (Schopfer et al., 2005). We use the MS/MS function of the MALDI-TOF-TOF mass spectrometer to screen for FP-biotin labeled peptides. Then we use the Q-Trap 4000 mass spectrometer to fragment the peptides for de novo sequencing to identify the site of covalent attachment of FP-biotin.

In a second phase, the protein is labeled with other OP. In the first round of screening for peptides labeled with these other OP, the assumption is made that the sites labeled by FP-biotin are also labeled by other OP. This assumption allows one to calculate theoretical OP-peptide masses and to look for the presence of these masses in the HPLC-fractionated, tryptic digest using the MALDI-TOF-TOF mass spectrometer. However, this assumption may not hold for all OP. Therefore a second strategy is used. Peptide masses observed in the MS scan for OP-labeled peptides are compared with theoretical masses for unlabeled peptides. The list of theoretical masses is generated with Protein Prospector software (UCSF). This free software is available at http://prospector.ucsf.edu. Candidates for OP-labeled peptides are chosen when their masses are equal to the sum of the known peptide mass and the added mass from the OP. These putative, OP-labeled peptides are further tested by CID fragmentation in the Q-Trap 4000 mass spectrometer, followed by manual de novo sequencing to identify the site of covalent OP attachment.

Four tubulin peptides are labeled by OP. The structures of the OP studied in the present
report are shown in Figure 3.1. A portion of each OP and the phenolic proton from the labeled
tyrosine are displaced when the OP makes a covalent bond with tubulin, so that the mass added
to tubulin is less than the mass of the OP. The added masses are 120 amu for sarin, 136 amu for
CPO, 162 amu for soman, 164 amu for DFP, and 572 amu for FP-biotin. The leaving group is
fluoride ion for sarin, soman, DFP and FP-biotin, and is 3,5,6-trichloro-2-(O)-pyridine for CPO.

Figure 3.1. OP structures.

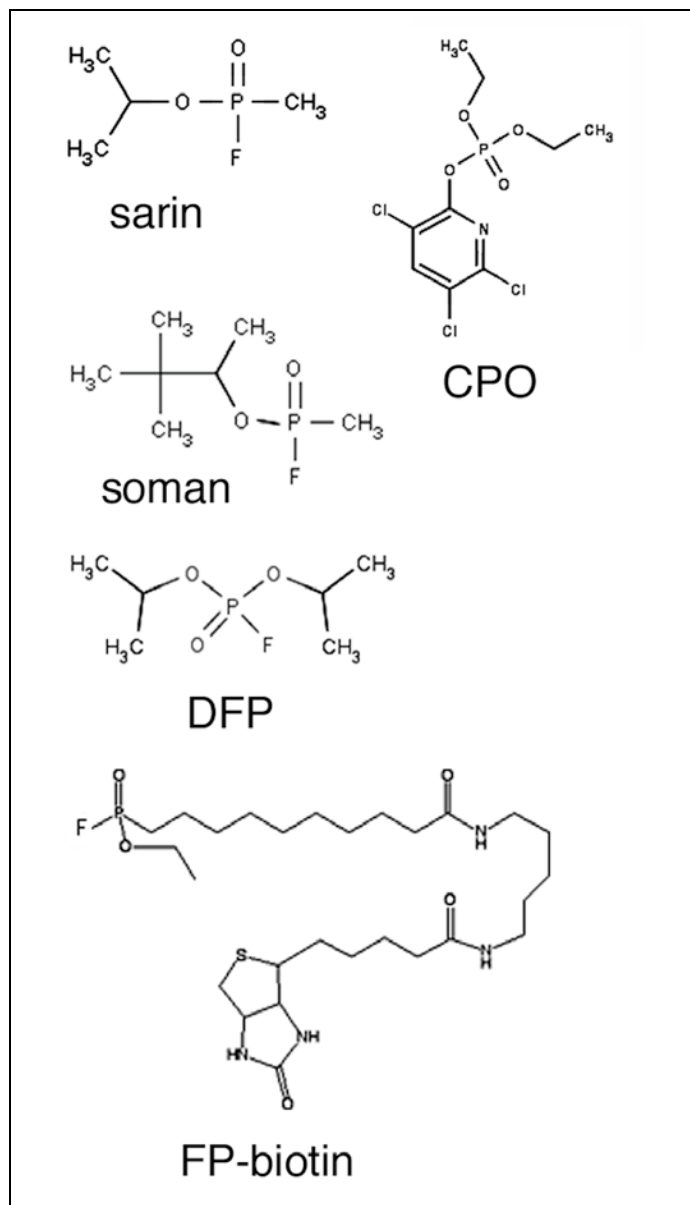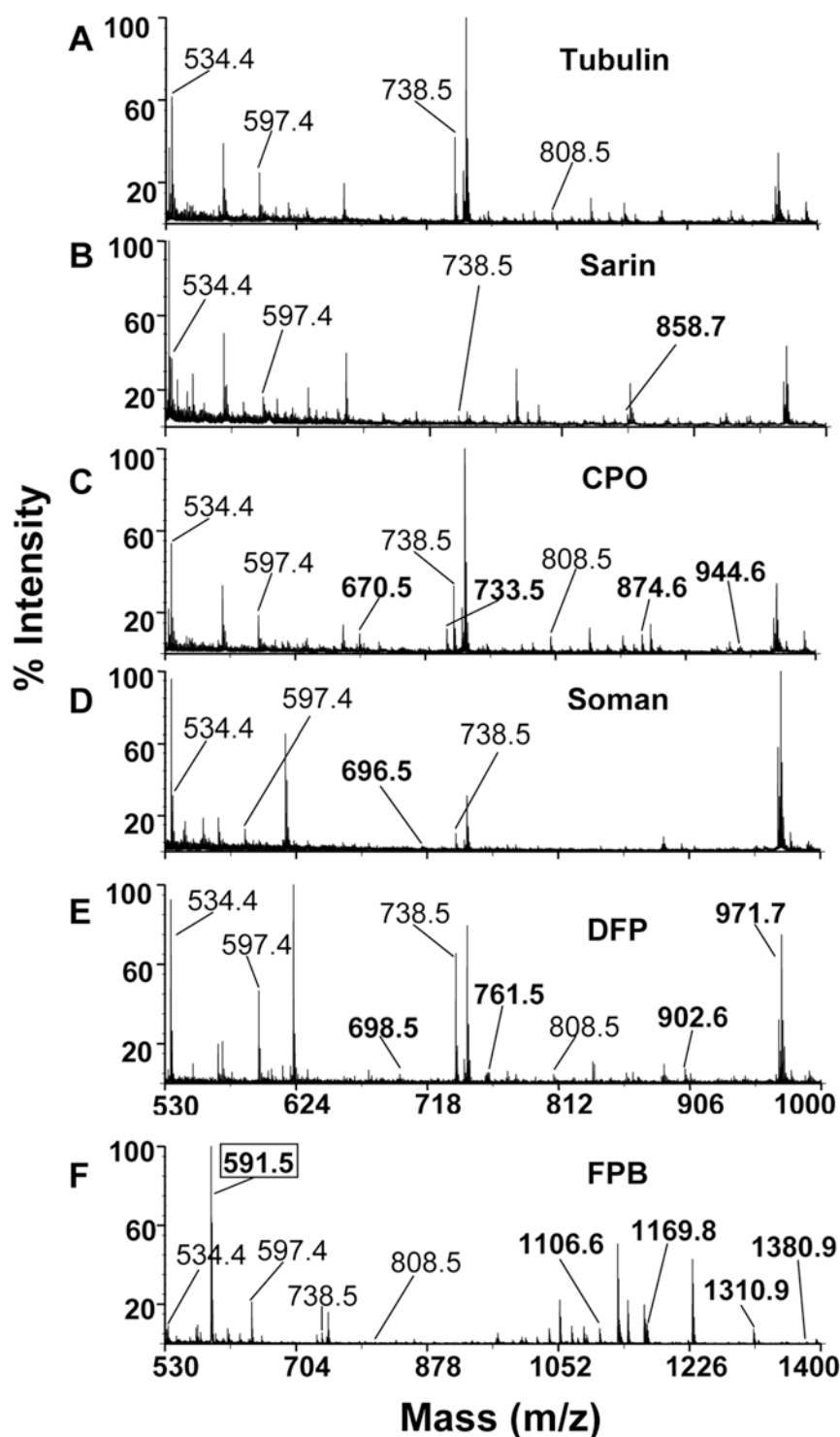Figure 3.2. Mass spectra of tryptic peptides of bovine tubulin, before and after labeling with OP. Peptides from A) control bovine tubulin, B) sarin treated tubulin, C) CPO treated tubulin, E) DFP treated tubulin, D) soman treated tubulin, F) FP-biotin treated tubulin. OP-labeled peptide masses are in bold. One peptide was labeled with sarin and soman; 4 peptides were labeled with CPO, DFP, and FP-biotin.

Figure 3.2 shows the tubulin tryptic peptides that are targets for OP-labeling, before (panel A) and after treatment with OP (panels B-F). The peaks at 534.4, 597.4, 738.5 and 808.5 m/z in panel A are unlabeled peptides with the sequences YVPR, TGTYR, GSQQYR, and EEYPDR. After treatment of tubulin with OP, new peaks appear whose masses correspond to some of the expected, theoretical masses for OP-labeled peptides (Table 3.1).

Table 3.1. Theoretical masses of bovine tubulin tryptic peptides covalently labeled by OP.

tubulin chain	sequence	mass, m/z	+120 sarin	+136 CPO	+162 soman	+164 DFP	+572 FP-biotin
alpha	TGTYR	597.3	717.3	733.3	759.3	761.3	1169.3
beta	YVPR	534.3	654.3	670.3	696.3	698.3	1106.3
beta	GSQQYR	738.4	858.4	874.4	900.4	902.4	1310.4
beta	EEYPDR	808.3	928.3	944.3	970.3	972.3	1380.3

Accession # gi: 73586894 for alpha-tubulin and gi: 75773583 for beta-tubulin NCBInr database.

Unlabeled active site peptides were present in each digest, indicating that modification by OP was incomplete. The relative amount of labeled and unlabeled peptide was calculated from isotope cluster areas. The results are summarized in Table 3.2. FP-biotin, DFP, and CPO reacted with all 4 peptides, whereas sarin and soman reacted with only one peptide. Soman and sarin concentrations were significantly lower than the concentrations of the other OP during the labeling reaction, which might explain why fewer peptides were labeled.

Table 3.2. Percent of each peptide labeled by OP.

	% labeled				
sequence	sarin	CPO	soman	DFP	FP-biotin
TGTYR		43		7	70
YVPR		19	2	6	54
GSQQYR	54	23		13	66
EEYPDR		21		12	62

Tyrosine covalently modified by OP. Collision induced fragmentation in the Q-Trap mass spectrometer conclusively identified the amino acid sequence of each labeled peptide and the residue covalently modified by OP. The MS/MS spectra in Figures 3.3, 3.4, 3.5, and 3.6 show the y ions of each unlabeled peptide (panel A), and the same peptide after covalent modification by sarin, CPO, soman, DFP, and FP-biotin (panels B-F). The masses exactly fit the indicated sequence and fit the interpretation that the OP is attached to tyrosine (Table 3.3). Ions at 214, 216, 244, and 272 m/z provide additional evidence that the OP bind to tyrosine (see figure legends for details).

Table 3. 3. OP-labeled tyrosines in bovine tubulin.

| tubulin	sequence	OP- Tyr	location in crystal structure
alpha	TGTYR	Tyr 83	loop between H2 and S3
beta	YVPR	Tyr 59	part of the loop between H1-S2; makes lateral contact between protofilaments (Lowe et al., 2001)
beta	GSQQYR	Tyr 281	part of the M loop between S7 and H9; makes lateral contact between protofilaments (Lowe et al., 2001)
beta	EEYPDR	Tyr 159	at the C-terminus of helix H4: residues 157-176 bind ribose of GTP (Nogales et al., 1998)
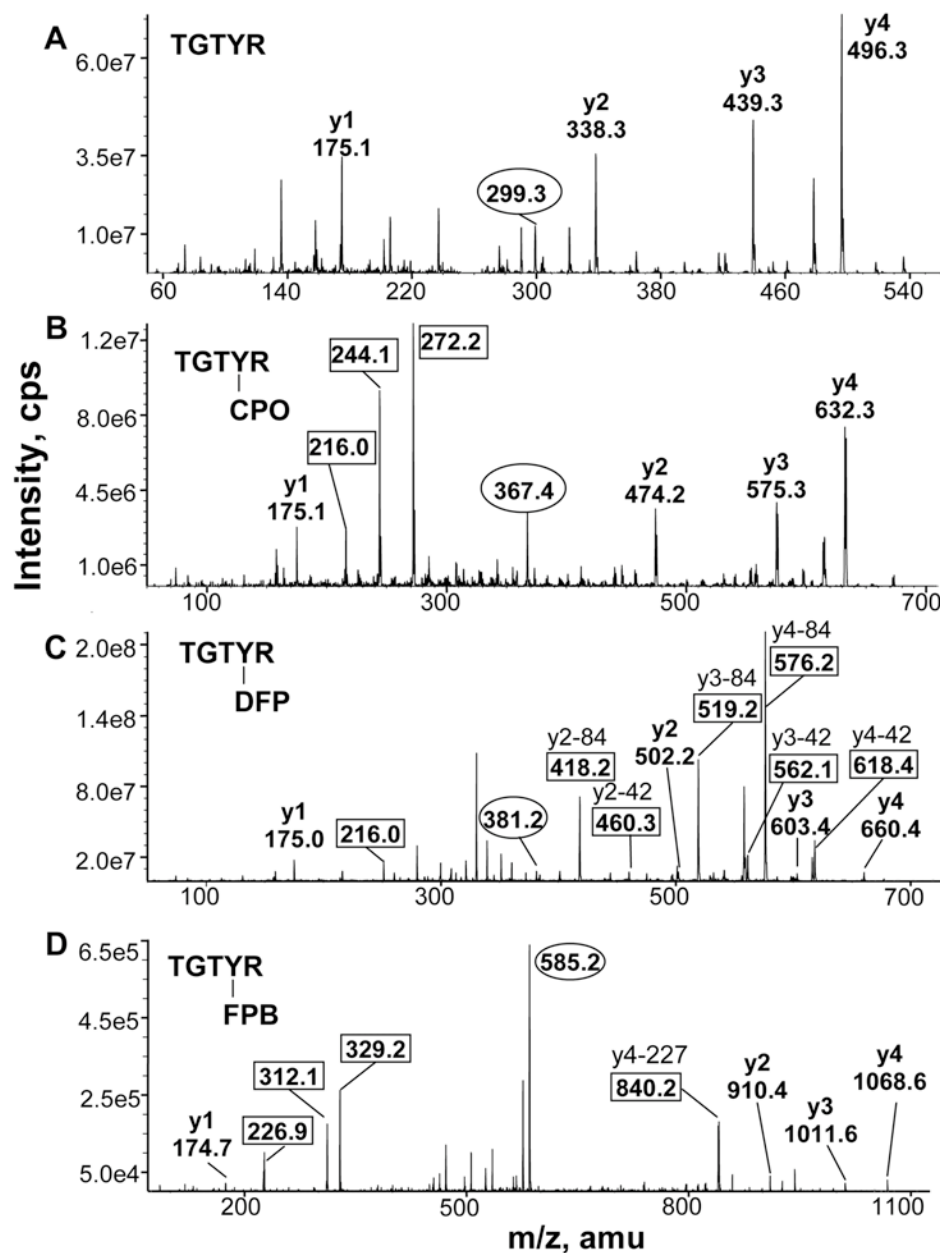
Figure 3.3. MS/MS spectra of the TGTYR peptide of alpha tubulin. A) Singly charged y ions derived from the doubly-charged, unlabeled parent ion at 299.3 m/z are shown. B) CPO-labeled TGTYR has a doubly charged parent ion of 367.4 m/z. The y ion masses are consistent with diethylphosphate attached to tyrosine. The mass at 244 m/z is phosphotyrosine, the mass at 216 m/z is the immonium ion of phosphotyrosine, and the mass at 272 m/z is monoethylphosphotyrosine. C) DFP-labeled TGTYR has a doubly charged parent ion of 381.2 m/z. The y ion masses are consistent with diisopropylphosphate attached to tyrosine. Masses enclosed in boxes are y ions that have lost one (42 amu) or both (84 amu) isopropyl groups. The ion at 216 m/z is the immonium ion of phosphotyrosine. D) FP-biotin labeled TGTYR has a doubly charged parent ion of 585.2 m/z. The y ion masses are consistent with FP-biotin attached to tyrosine. The ions at 227, 312, and 329 m/z are fragments of FP-biotin. The ion at 840.2 m/z is the y4 ion that has lost 227 amu from FP-biotin.
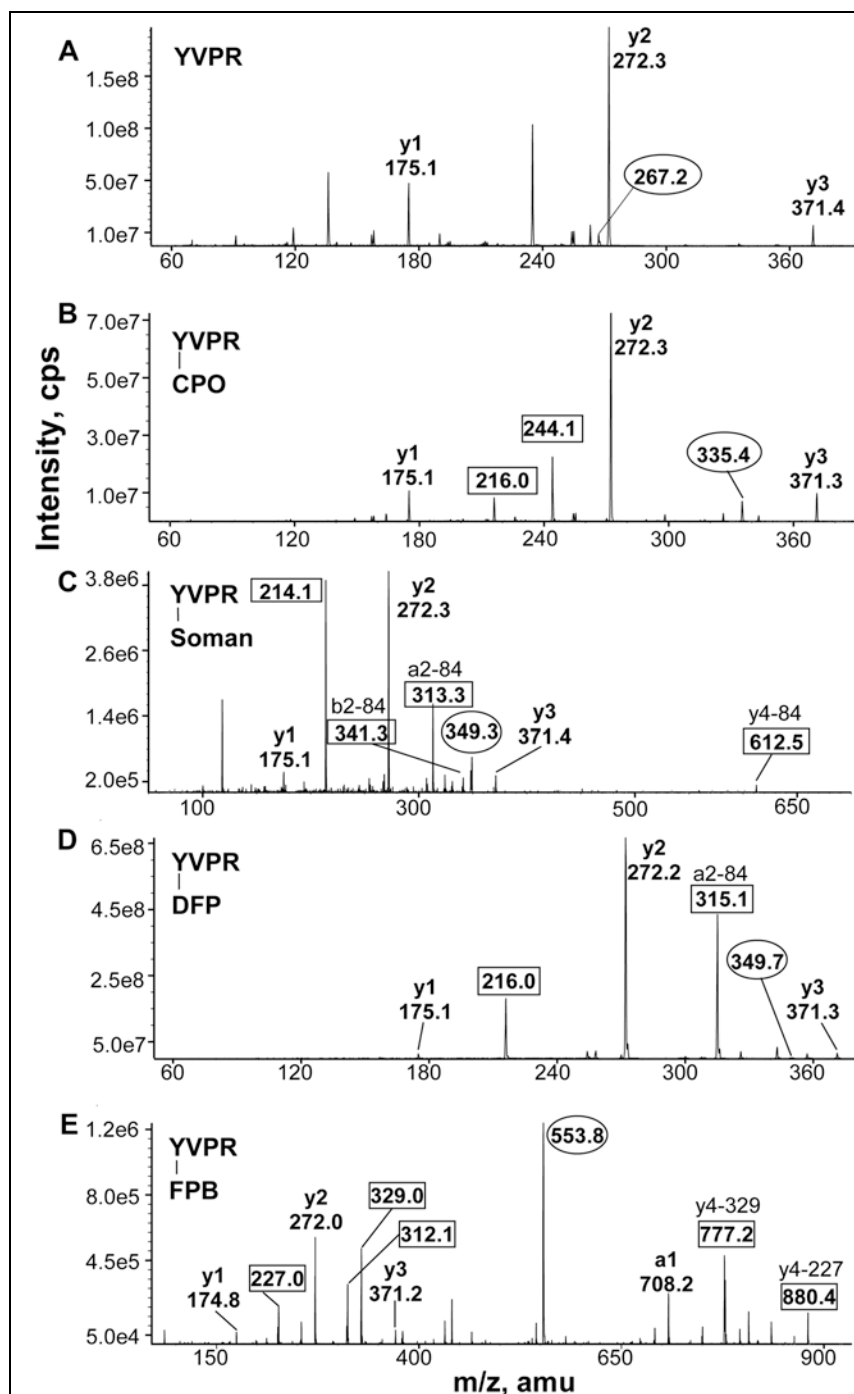
48

Figure 3.4. MS/MS spectra of the YVPR peptide of beta tubulin. A) Singly charged y ions derived from the doubly charged, unlabeled parent ion at 267.2 m/z are shown. B) CPO-labeled YVPR has a doubly charged parent ion of 335.4 m/z. The y ion masses are consistent with diethyl phosphate attached to tyrosine. The 216 m/z ion is the immonium ion of phosphotyrosine. The 244.1 ion is phosphotyrosine. C) Soman labeled YVPR had a doubly charged parent ion at 349 m/z. The 214 m/z ion is the immonium ion of methylphosphotyrosine. Loss of the pinacolyl group of soman reduces the mass of the singly charged parent ion by 84 amu to yield the 612 m/z, ion. Loss of the pinacolyl group also yields the b2 ion at 341 m/z, and the a2 ion at 313.3 m/z. D) DFP-labeled YVPR has a doubly charged parent ion at 349.7 m/z. The a2 ion has lost both isopropyl groups (84 amu) to yield 315.1 m/z. E) FP-biotin labeled YVPR has a doubly charged parent ion at 553.8 m/z. Ions at 227, 312, and 329 m/z are fragments of FP-biotin. The ions at 777.2 and 880.4 m/z are the parent ion that has lost 329 or 227 amu from FP-biotin.
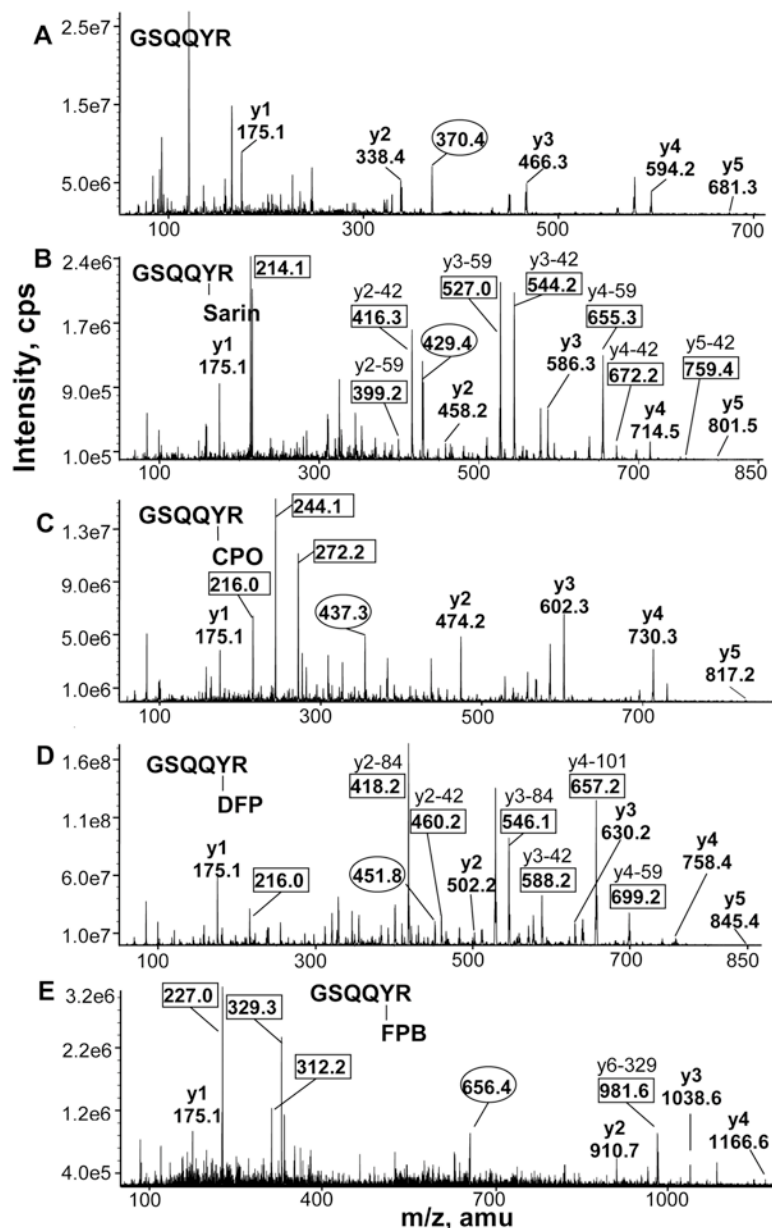
Figure 3.5. MS/MS spectra of the GSQQYR peptide of beta tubulin. A) Singly charged y ions derived from the doubly charged, unlabeled parent ion at 370.4 m/z are shown. B) Sarin-GSQQYR had a doubly charged parent ion at 429.4 m/z and the immonium methylphospho tyrosine ion at 214 m/z. Loss of the isopropyl group reduces the y ion masses by 42 amu. Loss of the isopropyl group plus loss of an NH_3 group reduces the y ion masses by 59 amu. C) CPO-GSQQYR had a doubly charged parent ion at 437.3 m/z. The immonium ion of phosphotyrosine is at 216 m/z. The phosphotyrosine ion is at 244.1 m/z. The monoethylphosphotyrosine ion is at 272.2 m/z. D) DFP-GSQQYR has a doubly charged parent ion at 451.8 m/z and the immonium phosphotyrosine ion at 216 m/z. Loss of one or both isopropyl groups from diisopropylphosphate yields y ions whose masses are reduced by 42 or 84 amu. An additional loss of 17 amu yields y ions that have lost 101 or 59 amu. E) FP-biotin-GSQQYR had a doubly charged parent ion at 656.4 m/z. Fragments derived from FP-biotin are at 227, 312, and 329 m/z. The singly charged ion at 981.6 m/z is consistent with the parent ion after loss of 329 amu from FP-biotin.
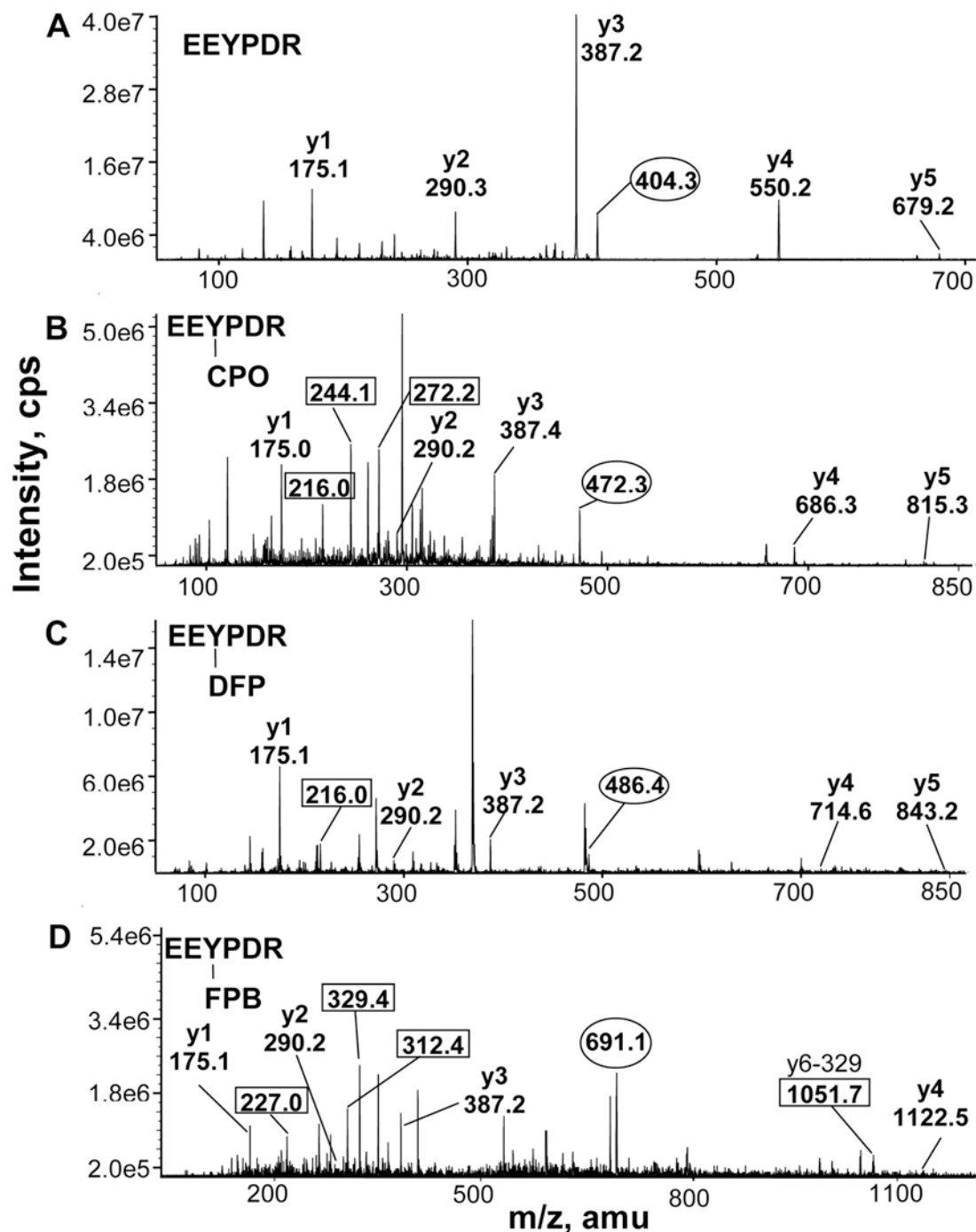
50

Figure 3.6. MS/MS spectra of the EEYPDR peptide of beta tubulin. A) Singly charged y ions derived from the doubly charged, unlabeled parent at 404.3 m/z are shown. B) CPO-EEYPDR has a doubly charged parent ion at 472.3 m/z. The immonium phosphotyrosine ion is at 216 m/z. Phosphotyrosine is at 244 m/z and monoethylphosphotyrosine is at 272 m/z. C) DFP-EEYPDR has a doubly charged parent ion at 486.4 m/z and an immonium phosphotyrosine ion at 216 m/z. D) FP-biotin EEYPDR has a doubly charged parent ion at 691.1 m/z. Fragment ions of FP-biotin are present at 227, 312, and 329 m/z. The singly charged parent ion that has lost 329 amu from FP-biotin is at 1051.7 m/z.

Fragmentation patterns characteristic of a particular OP. The data from Figures 3.3, 3.4, 3.5 and 3.6 reveal collision induced fragmentation patterns that are characteristic of particular OP. For example, DFP-peptides readily release one or both isopropyl to yield y ions missing either 42 or 84 amu. CPO-labeled peptides yield intense peaks at 216, 244 and 272 m/z that are consistent with phosphotyrosine immonium ion, phosphotyrosine and monoethylphospho tyrosine, respectively. The FP-biotinylated peptides release the characteristic fragments of FP-biotin at 227, 312, and 329 m/z. Singly charged ions missing either 227 or 329 amu were common. The pinacolyl group of soman was released from soman labeled YVPR peptide (Fig 4C) to yield ions missing 84 amu. The isopropyl group of sarin was released from sarin labeled GSQQYR peptide (Fig 5B) to yield ions missing 42 amu. Peptides that had lost 42 amu fragmented further to release NH_3 (17 amu), yielding an ion pair characteristic of sarin labeling.

In no case was the entire OP released from tyrosine. The phosphate group remained bound to tyrosine during collision induced fragmentation. This contrasts with OP bound to serine where the fragmentation process releases the entire bound OP, leaving no trace of the OP behind, and yielding dehydroAlanine in place of the OP-labeled serine (Fidder et al., 2002).

No aging. When soman, sarin, or DFP are bound to acetylcholinesterase or butyrylcholinesterase they rapidly lose an alkyl group in a process called aging (Michel et al., 1967; Millard et al., 1999; Nachon et al., 2005). An aged soman labeled peptide would have an added mass of 78 amu rather than 162; an aged sarin labeled peptide would have an added mass of 78 amu rather than 120; an aged DFP labeled peptide would have an added mass of 122 amu rather than 164 in the MS spectrum. No evidence of aging was found in OP labeled tubulin peptides as no masses representing aged OP-peptides were found in MS scans. We conclude that tubulin OP adducts on tyrosine do not age.

DISCUSSION
Tyrosine as a motif for OP labeling. The literature overwhelmingly supports the fact that OP bind covalently to an active site serine within the consensus sequence GXSXG. Enzymes are defined as serine hydrolases when their activity is inhibited by OP. On the other hand, covalent binding of OP to tyrosine has previously been reported only for albumin (Means and Wu, 1979; Li et al., 2007; Williams et al., 2007), papain (Chaiken and Smith, 1969) and bromelain (Murachi et al., 1965). Our previous mass spectrometry work identified the OP binding site in human albumin as Tyr 411, and in bovine albumin as Tyr 410 (Schopfer et al., 2005; Li et al., 2007). The present report of OP binding to tyrosine in alpha and beta tubulin is novel. No covalent attachment site for OP binding to tubulin has previously been reported.

No obvious consensus binding site can be deduced from the 4 peptides reported here, though each target peptide contains a positively charged arginine within 3 residues of the labeled tyrosine which may serve to reduce the pKa of the tyrosine hydroxyl group, and thereby activate it.

Significance of OP-labeling of tubulin. The crystal structure of tubulin shows that each of the OP-labeled tyrosines is located in a region where protofilaments interact laterally, or bind GTP (Nogales et al., 1998; Lowe et al., 2001). OP-binding to tubulin could therefore alter tubulin conformation or GTP binding. A change in tubulin conformation or GTP binding could explain the observation of Prendergast et al that CPO inhibits tubulin polymerization (Prendergast et al.,

2007). When tubulin does not polymerize, microtubules do not form, and nutrient transportation from the nerve cell body to the nerve synapse is disrupted. It is concluded that OP bind covalently to tubulin, and that this binding could explain the axonal transport deficits and cognitive impairment previously associated with OP exposure (Terry et al., 2003; Terry et al., 2007).

Additional progress on Milestones 3, 4, and 5

Pseudo-esterase activity of human albumin: slow turnover on Tyr 411 and stable acetylation of 82 residues including 59 lysines

ABSTRACT
Human albumin is thought to hydrolyze esters because multiple equivalents of product are formed for each equivalent of albumin. Esterase activity with p-nitrophenyl acetate has been attributed to turnover at tyrosine 411. However, p-nitrophenyl acetate creates multiple, stable, acetylated adducts, a property contrary to turnover. Our goal was to identify the residues that become acetylated by p-nitrophenyl acetate and determine the relationship between stable adduct formation and turnover. Fatty acid free human albumin 1 mg/mL in 10 mM TrisCl pH 8.0 was treated with 0.5 mM p-nitrophenyl acetate for 5 min to two weeks, or with 10 mM p-nitrophenyl acetate for 48 h to two weeks. Aliquots were digested with pepsin, trypsin, or GluC and analyzed by mass spectrometry to identify labeled residues. Only Y411 was acetylated within the first 5 min of reaction with 0.5 mM p-nitrophenyl acetate. After 0.5-6 h there was partial acetylation of 16-17 residues including D1, K4, K12, Y411, K413, and K414. Treatment with 10 mM p-nitrophenyl acetate resulted in acetylation of 59 lysines, 10 serines, 8 threonines, 4 tyrosines, and Asp1. When Y411 was blocked with diisopropylfluorophosphate or chlorpyrifos oxon, albumin had normal "esterase" activity with beta-naphthyl acetate as visualized on a nondenaturing gel. However, after 82 residues had been acetylated, esterase activity was almost completely inhibited. The half-life for deacetylation of Tyr 411 at pH 8.0, 22°C was 61±4 h. Acetylated lysines formed adducts that were even more stable. In conclusion, the pseudo-esterase activity of albumin is the result of irreversible acetylation of 82 residues and is not the result of turnover.

INTRODUCTION
Human albumin has esterase activity with p-nitrophenyl acetate (Tildon and Ogilvie, 1972; Means and Bender, 1975), alpha-naphthyl acetate, phenyl acetate, 1-naphthyl N-methylcarbamate (Casida and Augustinsson, 1959), beta-naphthyl acetate (Morikawa et al., 1979), aspirin (Rainsford et al., 1980), ketoprofen glucuronide (Dubois-Presle et al., 1995), carprofen acylglucuronide (Georges et al., 2000), cyclophosphamide (Kwon et al., 1987), nicotinate esters (Salvi et al., 1997), long- and short-chain fatty acid esters (Tove, 1962), octanoyl ghrelin (De Vriese et al., 2007), organophosphorus pesticides (Sogorb et al., 1998), carbaryl (Sogorb et al., 2004), o-nitroacetanilide (Manoharan and Boopathy, 2006), o-nitrotrifluoroacetanilide (Masson et al., 2007), and nerve agents (Li et al., 2008).

One site in albumin is rapidly acetylated by p-nitrophenyl acetate, showing a burst of product, but up to 5.2 molar equivalents are incorporated when albumin is treated with a 9-fold excess of p-nitrophenyl ^{14}C-acetate (Means and Bender, 1975). The 5 equivalents of label are not removable by extensive dialysis. The esteratic site has been identified as Tyr 411 based on site directed mutagenesis studies (Watanabe et al., 2000). Mass spectrometry has identified Tyr 411 as the residue labeled by organophosphorus esters including diisopropylfluorophosphate (DFP), soman, sarin, dichlorvos, FP-biotin, and chlorpyrifos oxon (Li et al., 2007; Li et al., 2008) confirming the report by Sanger that a tyrosine in albumin is labeled by DFP (Sanger, 1963), and reports that a tyrosine in albumin is labeled by the nerve agents soman, sarin, cyclosarin, and tabun (Williams et al., 2007). When albumin is labeled with 1 mole of DFP, albumin loses the fast phase of its esterase activity (the burst), supporting the conclusion that DFP and p-nitrophenyl acetate bind to the same site, namely to Tyr 411 (Means and Wu, 1979).

Our goal was to identify the additional sites labeled by p-nitrophenyl acetate. We wanted an explanation for the apparently inconsistent observation that albumin hydrolyzes p-nitrophenyl acetate at measurable rates, yet the ^{14}C-acetylated albumin formed by p-nitrophenyl acetate is a stable adduct.

METHODS

Materials. A 1 mg/mL solution of fatty acid free human albumin (Fluka 05418, via Sigma) was dissolved in 10 mM TrisCl pH 8.0. A 1 mg/mL solution of porcine pepsin (Sigma P6887) in 10 mM HCl was stored at -80˚C. Sequencing grade modified trypsin (Promega V5113) at a concentration of 20 µg in 50 µL of 50 mM acetic acid was stored at -80˚C. Endoproteinase GluC (S. Aureus protease V8) was from Worthington Biochemical Corp (Lakewood, N.J.; #LS003608). One mg of GluC powder was dissolved in 210 µL water, aliquoted into microfuge tubes each containing 10 µL (50 µg), dried in a vacuum centrifuge, and stored at -80˚C. A 10 mg/mL solution of alpha-cyano-4-hydroxycinnamic acid matrix (CHCA) (Applied Biosystems) in 50% acetonitrile, 0.1% trifluoroacetic acid was stored at room temperature. A 0.1 M solution of p-nitrophenyl acetate (Sigma N8130) in acetonitrile was stored at -20˚C. Diisopropylfluorophosphate (DFP), a liquid with a concentration of 5.73 M, was from Sigma (D0879). Chlorpyrifos oxon (ChemService Inc. West Chester, PA; MET-674B) was dissolved in methanol to make a 1 M solution and stored at -80˚C. Beta-naphthyl acetate, Fast Blue RR, and fluorodinitrobenzene (>99% pure) were from Sigma. Albumin samples were concentrated in a Microcon centrifugal device with a YM10 membrane whose molecular weight cutoff was 10,000 (Millipore 42406).

Pure albumin labeled with p-nitrophenyl acetate, digested with pepsin while albumin disulfides were intact. One mL of a 1 mg/mL solution of fatty acid free human albumin (15 µM) in 10 mM TrisCl pH 8.0 was treated with a 33-fold molar excess of p-nitrophenyl acetate (5 mL of 0.1 M in acetonitrile) at 22˚C. One mL of control albumin solution was treated with 5 µL of acetonitrile. A 50 µL aliquot was removed into 50 µL of 1% trifluoroacetic acid containing 2 µL of 1 mg/mL pepsin after 5, 10, 15, 20, 30, 40, 50, 60 min, 6 h, 24 h, 9 days and 14 days. The drop in pH to 1.4 stopped the reaction with p-nitrophenyl acetate. Digestion with pepsin was at 37˚C for 1 to 2 hours. A 0.5 µL aliquot of the digest was spotted on a MALDI target plate, dried, and overlaid with 0.5 µL of CHCA matrix, for analysis in a MALDI-TOF/TOF 4800 mass spectrometer.

Absorbance at 400 nm to measure p-nitrophenolate produced by albumin hydrolysis of p-nitrophenyl acetate. One mL of 1 mg/mL human albumin in 10 mM TrisCl pH 8.0 was incubated with 5 µL of 0.1 M p-nitrophenyl acetate at 22˚C. At various times after mixing a 50 µL aliquot was withdrawn and diluted to 2 mL for measurement of absorbance at 400 nm. The reaction was followed until all of the p-nitrophenyl acetate was consumed. A control sample, without albumin, was followed in a similar manner to measure spontaneous hydrolysis of p-nitrophenyl acetate, in 10 mM TrisCl pH 8.0. The amount of p-nitrophenylate ion formed in the albumin reaction was corrected for spontaneous hydrolysis.

The extinction coefficient for the p-nitrophenolate ion at pH 8.0 is 16,900 M^{-1} cm^{-1} at 400 nm (Means and Bender, 1975). Therefore, the completely hydrolyzed 500 µM p-nitrophenyl acetate should have an absorbance at 400 nm of 8.45.

Albumin incubated with potassium acetate. To determine whether acetylation of lysines was accomplished by reaction with p-nitrophenyl acetate or by reaction with free acetate we measured acetylated lysines after incubation of albumin with potassium acetate. One mL of 1 mg/mL albumin in 10 mM TrisCl pH 8.0 was incubated with 500 µM potassium acetate for 15 h at 22˚C. A 50 µL aliquot of the reaction mixture was removed into 50 µL of 1% trifluoroacetic acid containing 2 µL of 1 mg/mL pepsin and incubated for 2 h at 37˚C. The digest was analyzed with a MALDI-TOF-TOF 4800 mass spectrometer, with CHCA matrix.

Mass spectrometry with a MALDI-TOF-TOF 4800 (Applied Biosystems, Foster City, CA). Essentially salt-free 0.5 µL samples were spotted on a MALDI target plate, air dried, and overlaid with 0.5 µL of 10 mg/mL CHCA in 50% acetonitrile, 0.1% trifluoroacetic acid. MS spectra were acquired with laser power at 3000 volts in positive reflector mode. Each spectrum was the average of 500 laser shots. The percentage of acetylation was calculated by dividing the cluster area of the unlabeled peptide by the sum of the cluster areas for the unlabeled and labeled peaks. The mass spectrometer was calibrated against des-Arg-Bradykinin (904.468 Da), Angiotensin 1 (1296.685 Da), Glu-Fibrinopeptide B (1570.677 Da) and neurotensin (1672.918 Da) (Cal Mix 1 from Applied Biosystems).

LC/MS/MS with the QTRAP 2000 and LCQ Deca XP mass spectrometers. Human albumin treated with p-nitrophenyl acetate was denatured by boiling 10 min in the presence of 10 mM dithiothreitol, carbamidomethylated with 90 mM iodoacetamide, and dialyzed against 2 x 4 L of 10 mM ammonium bicarbonate. A 500 µg aliquot was digested with 10 µg of Promega trypsin overnight at 37˚C, or with 50 µg of GluC. The digest was dried in a vacuum centrifuge and dissolved in 5% acetonitrile, 0.1% formic acid to make 6.7 pmol/µL. A 10 µL aliquot was injected into the HPLC nanocolumn (#218MS3.07515 Vydac C18 polymeric rev-phase, 75 mm i.d. x 150 mm long; P.J. Cobert Assoc, St. Louis, MO). Peptides were separated with a 90 min linear gradient from 0% to 60% acetonitrile at a flow rate of 0.3 µL/min and electrosprayed through a fused silica emitter (360 mm o.d., 75 mm i.d., 15 mm taper, New Objective) directly into the QTRAP 2000 (Applied Biosystems, Foster City, CA), a hybrid quadrupole linear ion trap mass spectrometer. An ion-spray voltage of 1900 volts was maintained between the emitter and the mass spectrometer. Information-dependent acquisition was used to collect MS, enhanced MS and MS/MS spectra for the 3 most intense peaks in each cycle, having a charge of +1 to +4, a mass between 200 and 1700 m/z, and an intensity >10,000 cps. All spectra were collected in

the enhanced mode, using the trap function. Precursor ions were excluded for 30 seconds after one MS/MS spectrum had been collected. The collision cell was pressurized to 40 mTorr with pure nitrogen and collision energies between 20 and 40 eV were determined automatically by the software based on the mass and charge of the precursor ion. The mass spectrometer was calibrated on selected fragments from the MS/MS spectrum of Glu-Fibrinopeptide B. The MS/MS data were processed using Analyst 1.4.1 software and submitted to Mascot for identification of peptide sequences (Perkins et al., 1999).

A pepsin digest of the same carbamidomethylated preparation was analyzed on the LCQ Deca XP mass spectrometer (Thermo-Finnigan, San Jose, CA) coupled to the Ultimate 3000 HPLC system (Dionex, Sunnyvale, CA). The 75 µm i.d. C18 column was from LCPackings. HPLC solvents were A) 0.1 M acetic acid and B) 80% acetonitrile, 0.1 M acetic acid. Peptides were eluted with a gradient from 0 to 55% B in 90 min. Data were collected with Xcalibur 2.0 and analyzed with OMMSA search engine (Geer et al., 2004).

Infusion in the QTRAP 4000 mass spectrometer. Pepsin digests dissolved in 50% acetonitrile, 0.1% formic acid were infused into the QTRAP 4000 (Applied Biosystems, Foster City, CA) mass spectrometer at a flow rate of 0.3 µL/min through an 8 µm emitter (#FS360-50-8-D, New Objective) via a 25 µL Hamilton syringe mounted on a Harvard syringe pump. 500 MS/MS spectra were accumulated for each parent ion.

Deacetylation of Tyr 411. The production and disappearance of acetylated Tyr 411 was followed by MALDI-TOF mass spectrometry. A 15 µM solution of human albumin in 10 mM TrisCl pH 8.0 was treated with an equimolar concentration of p-nitrophenyl acetate at 22˚C. After various times, a 10 µL aliquot was mixed with 10 µL of 1% trifluoroacetic acid and 1 µL of 1 mg/mL pepsin. After 1-2 h at 37˚C a 0.5 µL aliquot of the digest was spotted on a MALDI target plate. Cluster areas for the unlabeled peptides at 1717 and 1830 amu and the labeled peptides at 1759 and 1872 amu were used to calculate % labeling on Tyr 411.

Percentage of acetylated lysines calculated from amino acid composition analysis.
Quantitation of the acetylated lysine was obtained by the use of fluorodinitrobenzene (Allfrey et al., 1984). Fluorodinitrobenzene reacts with un-acetylated lysine to form e-N-dinitrobenzylated lysine. Acid hydrolysis, in preparation for amino acid composition analysis hydrolyzes the e-N-acetyl lysines to yield free lysine, but the dinitrobenzylated lysines are relatively stable to acid hydrolysis. The amount of free lysine appearing in the amino acid composition analysis, corrected for hydrolysis of dinitrobenzylated lysine, represents the amount of lysine that was originally acetylated.

Fluorodinitrobenzylation employs the method originally described by Sanger (Sanger, 1945). Acetylated and control albumin were dialyzed into $NaHCO_3$ (20 mg/mL). Two hundred micrograms of dialyzed albumin were adjusted to 1 mL with $NaHCO_3$ and mixed with 2 mL of absolute ethanol. The mixture was shaken at room temperature for 1 hour, at which time 30 mL of fluorodinitrobenzene was added and that mixture shaken for an additional 2 hours. The insoluble yellow product was washed twice with water, twice with absolute ethanol, twice with diethyl ether, air dried and submitted for amino acid composition analysis.

Nondenaturing gel electrophoresis. Albumin esterase activity was demonstrated on a nondenaturing 4-30% polyacrylamide gradient gel, stained for esterase activity with beta-

naphthyl acetate and Fast Blue RR (Li et al., 2005). Gels were shaken in 100 mL of 0.05 M TrisCl pH 7.4 containing 50 mg of beta-naphthylacetate in 1 mL ethanol, and 50 mg of solid Fast Blue RR. Though most of the Fast Blue RR does not dissolve, pink bands of esterase activity appear within 15 to 30 min. The gel was counterstained with Coomassie Blue to show protein concentration.

        The positive control samples, not acetylated on any residues, were 5 µL of human serum and 200 µg of fatty acid free human albumin. The negative control was albumin that had been denatured in 8 M urea, reduced with 10 mM dithiothreitol, carbamidomethylated with iodoacetamide, dialyzed to remove salts, and concentrated to 10 µg/µL. Albumin acetylated on 100% of Tyr 411 only, was prepared by incubating 10 mg/mL albumin with 5 mM p-nitrophenyl acetate (33 fold excess) in 10 mM TrisCl pH 8.0 for 5 min, followed immediately by gel electrophoresis. Albumin acetylated on 100% Tyr 411 and 20% of the lysines was prepared by incubating 1 mg/mL albumin with 0.5 mM p-nitrophenyl acetate for 6 hours at 22˚C. Albumin with free Tyr 411 and 20% acetylated lysines was prepared by incubating 1 mg/mL albumin with 0.5 mM p-nitrophenyl acetate, 0.01% sodium azide for two weeks at 22˚C, during which time Tyr 411 was completely deacetylated as shown by mass spectrometry. Albumin with 100% acetylated Tyr 411 and 60-100% acetylated lysines was prepared by incubating 1 mg/mL albumin with 10 mM p-nitrophenyl acetate for 48 h. Percent acetylation of Tyr 411 and lysines was determined by mass spectrometry as described above, and by amino acid composition analysis after reaction with fluorodinitrobenzene.

        Albumin labeled with DFP on 80% of Tyr 411 was prepared by treating 2 mg/mL albumin with a 20-fold excess of DFP in 10 mM TrisCl pH 8.0 for 2 h at 22˚C. Albumin labeled with chlorpyrifos oxon on 95% of Tyr 411 was prepared by treating 1 mg/mL albumin in 10 mM TrisCl pH 8.0 with a 7.5 -fold excess of chlorpyrifos oxon for 48 h at 22˚C. The percent free and modified Tyr 411 was determined by mass spectrometry. No lysines were labeled by DFP or chlorpyrifos oxon.

RESULTS
Tyrosine 411 is rapidly acetylated by p-nitrophenyl acetate. A 5 min reaction of albumin (15 µM) with p-nitrophenyl acetate (500 µM) results in complete acetylation of Tyr 411. This is indicated by the mass shift of +42 amu for peptic peptides VRYTKKVPQVSTPTL and LVRYTKKVPQVSTPTL (missed cleavage), which have masses of 1717 and 1830 amu in the control albumin digest (Figure 4.1A), but masses of 1759 and 1872 amu after treatment with p-nitrophenyl acetate (Figure 4.1B). No unlabeled masses at 1717 and 1830 amu remain after treatment with p-nitrophenylacetate, indicating 100% labeling. No other peptides were found to have a mass shift at this time point.
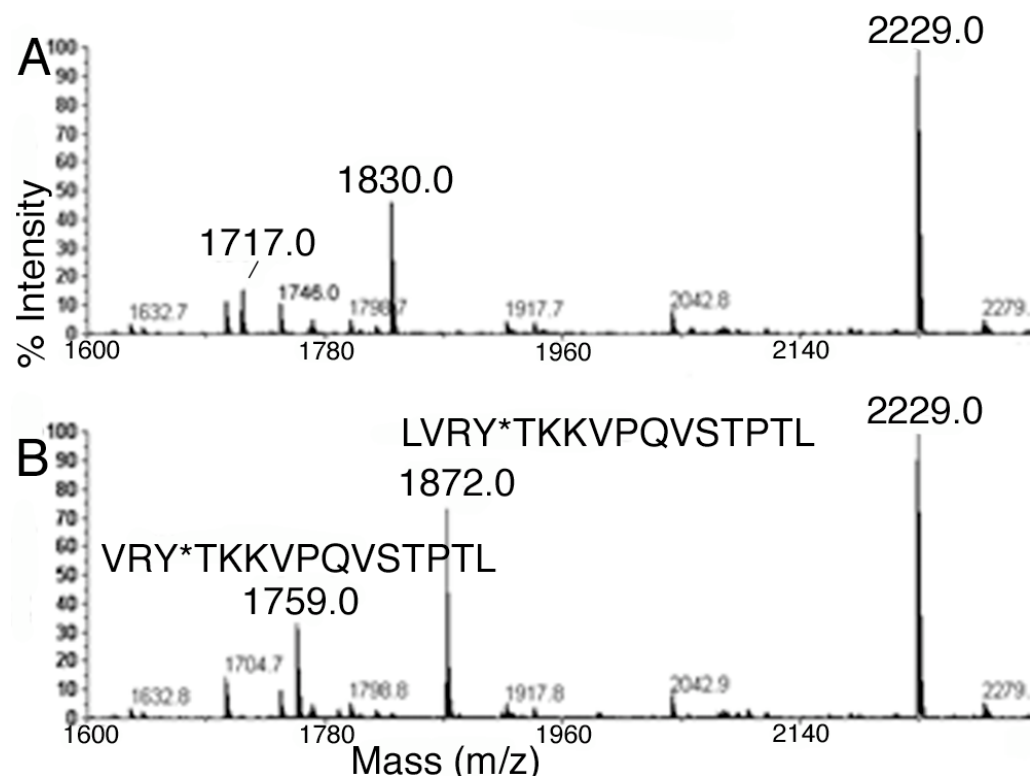
Figure 4.1. MALDI-TOF mass spectra of peptic peptides of human albumin before (A) and after (B) 5 min reaction with 0.5 mM p-nitrophenyl acetate. The mass of peptides at 1717 and 1830 amu increased by +42 amu due to acetylation of Tyr 411.

The labeled residue was identified as Tyrosine 411 by fragmentation of the doubly-charged parent ions 879.8 and 936.5 m/z (corresponding to the singly charged 1759 and 1872 amu ions) in the QTRAP mass spectrometer. Figure 4.2A shows fragmentation of the parent ion, 879.8 m/z. All of the major peaks are assigned to fragments of VRYTKKVPQVSTPTL. The presence of the b4 ion (representing residues VRY*T plus acetyl) at 562.2 amu indicates acetylation of this fragment. Of the residues in this fragment, tyrosine is the most likely candidate for acetylation. All of the fragments in the remainder of the b-ion series, b5 to b12, are 42 amu larger than predicted from the amino acid sequence alone, supporting acetylation of tyrosine in peptide VRYTKKVPQVSTPTL. Figure 4.2B shows fragmentation of parent ion 936.5 m/z. Again, all major peaks are assigned, this time to fragments of LVRYTKKVPQVSTPTL. The presence of the b4 ion (representing residues LVRY* plus acetyl) at 574.3 amu indicates acetylation of that fragment. The most likely candidate for acetylation is again the tyrosine. The b4-17 ion at 557.3 amu, and the b-ion fragments b5 ion at 675.3 amu through b13-18 at 1524.8 amu are all 42 amu larger than predicted from the amino acid sequence, further supporting acetylation of tyrosine in LVRYTKKVPQVSTPTL.

Taken together, the data indicate that Tyr411 is the first albumin residue to be acetylated by p-nitrophenyl acetate.
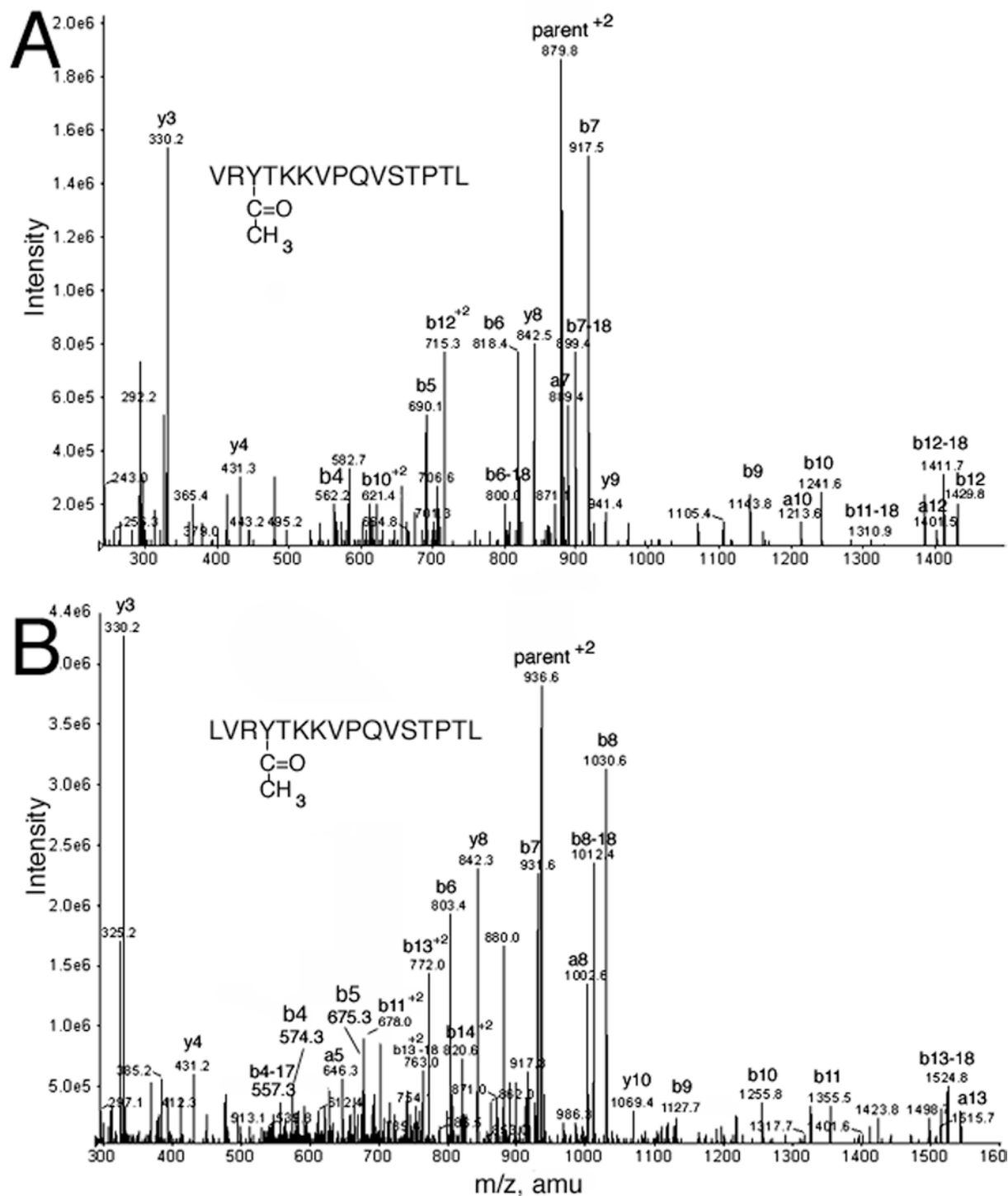
Figure 4.2. MS/MS spectra to identify the residue acetylated after 5 min reaction of 1 mg/mL albumin with 0.5 mM p-nitrophenyl acetate. (A) Fragmentation of the doubly-charged form of peptide 1759 identifies acetylated Tyr 411 in peptide VRY*TKKVPQVSTPTL. (B) Fragmentation of the doubly charged form of peptide 1872 identifies acetylated Tyr 411 in LVRY*TKKVPQVSTPTL.

Lysine 413 and lysine 414 are slowly acetylated by p-nitrophenyl acetate. After 6 hours reaction of 15 µM albumin with 500 µM p-nitrophenyl acetate, a second and third site on peptides VRYTKKVPQVSTPTL and LVRYTKKVPQVSTPTL was acetylated, as indicated by peaks with mass shifts of +42, +84 and +126 amu. The 1717 amu peak (Figure 4.3A) shifted to 1759 amu, 1801 amu, and 1843 amu (Figure 4.3B), while the 1830 amu peak shifted to 1872 amu, 1914 amu, and 1956 amu (Figure 4.3B). At 6 hours, about 50% of peptides VRYTKKVPQVSTPTL and LVRYTKKVPQVSTPTL were labeled with one acetate, about 50% with 2 acetates, and 1-2% with 3 acetates (percentage estimates are based on the cluster areas of the peaks). The percentage of acetylated peptides did not increase after 6 h because 90% of the p-nitrophenyl acetate had been hydrolyzed by that time.

 The possibility that acetate (rather than p-nitrophenyl acetate) might be acetylating lysines was ruled out by the finding that no mass shifts occurred when 1 mg/mL albumin was treated with 0.5 mM potassium acetate.

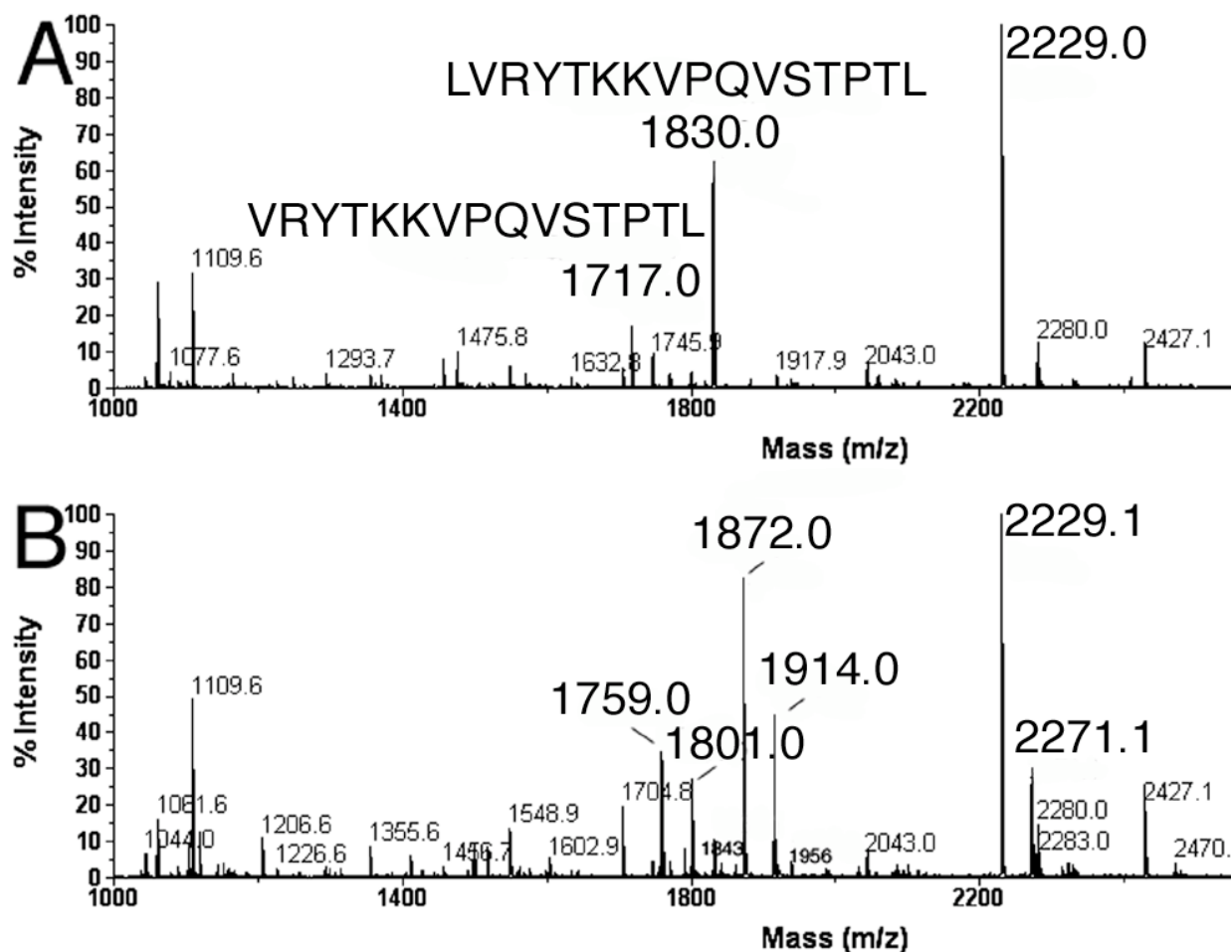Figure 4.3. MALDI-TOF mass spectra of pepsin digested human albumin (15 µM) before (A) and after (B) treatment with 0.5 mM p-nitrophenyl acetate for 6 h. The 1717 amu peak for VRYTKKVPQVSTPTL in panel A has acquired +42, +84, and +126 amu masses at 1759, 1801, and 1843 amu in panel B. The 1830 amu peak for LVRYTKKVPQVSTPTL in panel A has acquired +42, +84, and +126 amu masses in panel B at 1872, 1914, and 1956 amu.
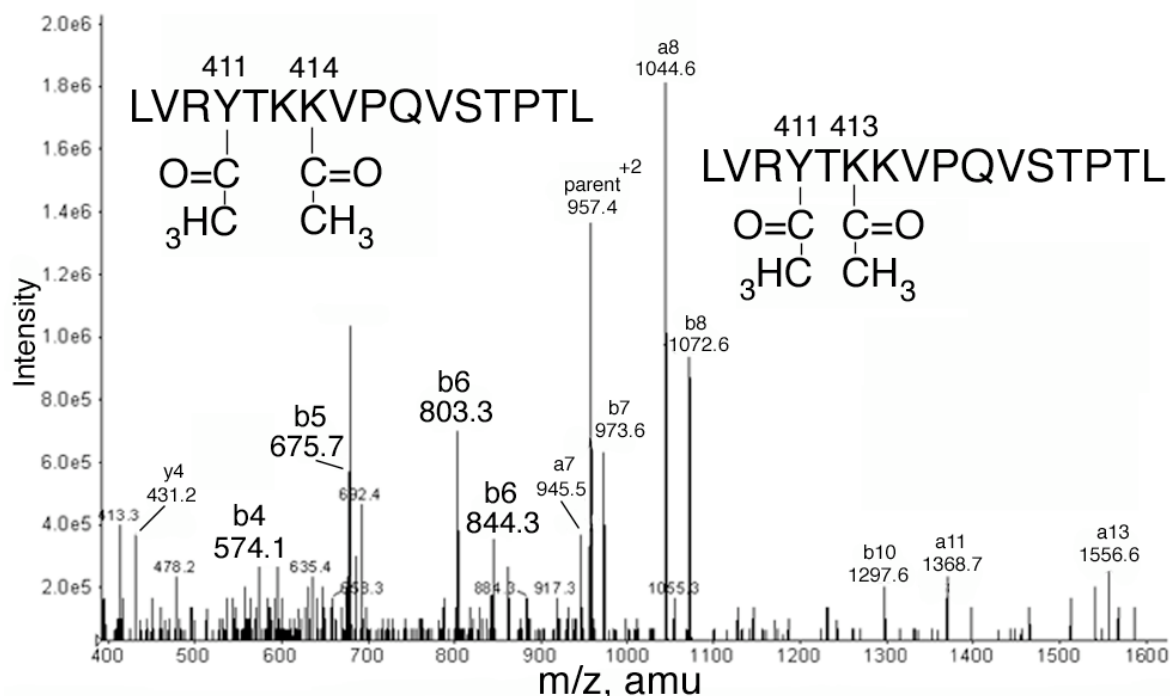
Figure 4.4. MS/MS spectrum to identify acetylated sites in LVRYTKKVPQVSTPTL after 6 h reaction of 1 mg/mL albumin with 0.5 mM p-nitrophenyl acetate. The doubly charged parent ion at 957.4 m/z, representing the singly charged 1914 amu ion, carries two acetyl groups. The acetyl groups are distributed between Y411/K414 and Y411/K413. The dominant ion is acetylated on Y411 and K414, while a less abundant ion is acetylated on Y411 and K413.

Peptides VRYTKKVPQVSTPTL and LVRYTKKVPQVSTPTL with a mass shift of +84 amu were acetylated on Tyr 411 and Lys 413, or on Tyr 411 and Lys 414. Figure 4.4 shows the MS/MS spectrum for doubly charged parent ion 957.5 of peptide LVRYTKKVPQVSTPTL at the 6 h time point. The b4 ion at 574.1 amu (representing residues LVRY* plus 1 acetyl) and the b5 ion at 675.7 amu (representing residues LVRY*T plus 1 acetyl) support acetylation of Tyr 411. The b6 ion at 844.3 amu (representing residues LVRY*TK* plus 2 acetyls) supports acetylation of Lys 413 in addition to Tyr 411. The existence of the b6 ion mass at 803.3 amu (representing residues LVRY*TK plus 1 acetyl) suggests that Lys 413 can appear without being acetylated. The appearance of an un-acetylated form of Lys 413 together with acetylated b7 to b11 ions is consistent with the second acetyl group on Lys 414. Other +84 ions were found (data not shown) where the second acetyl group was exclusively on Lys 413 or on Lys 414. Based on the relative intensities of the peaks at 803.3 and 844.3 amu, acetylated Lys 414 was more abundant than acetylated Lys 413.

From the above analysis, it follows that triply-acetylated peptides, with a mass shift of +126 amu, were acetylated on Tyr 411, Lys 413, and Lys 414.

The N-terminus of albumin, lysine 4, lysine 12, and serine 5 are slowly acetylated by p-nitrophenyl acetate. Another prominent peptide in pepsin digested albumin was DAHKSEVAHRFKDLGEENF at 2229 amu (Figure 4.3A). After 6 h reaction of 15 μM

62

albumin with 500 µM p-nitrophenyl acetate, 20% of this peak had acquired a mass of +42 amu (Figure 4.3B), 2% had acquired a mass of +84 amu, and about 0.5 % had increased in mass by +126 amu. Incubation with 10 mM p-nitrophenyl acetate for 48 h resulted in complete disappearance of the 2229 and 2271 amu peaks and appearance of +84, +126 and +168 amu ions at 2313, 2355, and 2397 amu (data not shown). MS/MS spectra showed that the +42 amu parent ion was acetylated on Asp 1, the N-terminus of albumin, the +84 amu parent ion was acetylated on Asp1 and Lys 12, and the +126 amu ion was acetylated on Asp 1, Lys 12 and Lys 4 (data not shown).

The +168 amu ion was acetylated on Asp 1, Lys 4, Ser 5, and Lys 12 (Figure 4.5). Most of the major peaks in the spectrum could be assigned to the DAHKSEVAHRFKDLGEENF peptide. The 366.1 amu mass was consistent with the b3 ion (representing D*AH plus 1 acetyl). Though histidine is a potential candidate for acetylation, N-acetylhistidine is unstable (Macdonald et al., 1999).   Therefore, acetylation is on the N-terminus. The mass at 536.2 amu is consistent with the b4 ion (representing D*AHK* plus 2 acetyls).   The 665.2 amu mass is consistent with the b5 ion (representing D*AHK*S* plus 3 acetyls). Additional b-ions at 794.4 amu (b6), 893.0 amu (b7), and 964.3 amu (b8) support the presence of 3 acetyls. The mass at 1296.5 amu is consistent with the y10 ion (representing RFK*DLGEENF plus 1 acetyl) where acetylation is on the lysine.
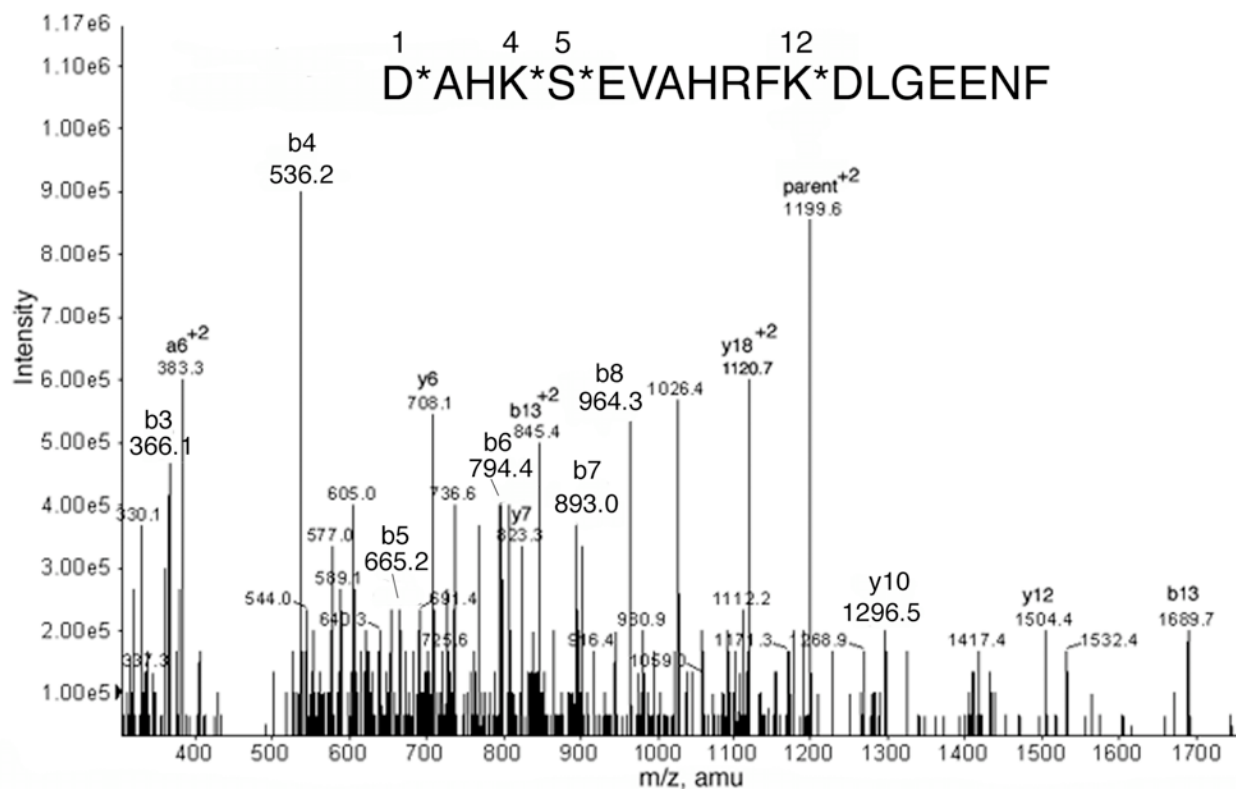

Figure 4.5. MS/MS spectrum to identify 4 acetylation sites on DAHKSEVAHRFKDLGEENF. Human albumin (15 µM) was incubated with 10 mM p-nitrophenyl acetate for 48 h at pH 8.0, before digestion with pepsin. The 4 acetylated residues in ion 2397 are D1, K4, S5, and K12.

Analysis of cluster areas in the MALDI-TOF spectra showed that the N-terminal Asp 1 and Lys 12 were 100% acetylated, consistent with the disappearance of peaks at 2229 and 2271 amu. About 65% of Lys 4 and 6% of Ser 5 residues were acetylated, indicating that serine is not nearly as reactive with p-nitrophenyl acetate as lysine.

Residues acetylated by 0.5 mM p-nitrophenyl acetate. Within the first 5 min of reaction of 15 µM albumin with 0.5 mM p-nitrophenyl acetate, Tyr 411 was acetylated 99-100%. No other residue was significantly acetylated within 5 min. Six hours after addition of p-nitrophenyl acetate, residues D1, K12, K413, and K414 were acetylated about 20-25% while Tyr 411 was still acetylated 100%. An additional 19 peptides had a mass shift of +42 amu as observed by MALDI-TOF, however peak intensities were low, and the peptide sequences could not be determined. After 50 hours, all of the p-nitrophenol had been exhausted and half of the Tyr 411 was free. By two weeks, none of the Tyr 411 was labeled. The albumin still carried a lot of label, but the label was on lysines and on the N-terminal Asp1.

Residues acetylated by 10 mM p-nitrophenyl acetate. Table 4.1 lists the residues in human albumin acetylated by treatment of 15 µM albumin with 10 mM p-nitrophenyl acetate at pH 8.0, 22˚C for 48 h. The Mascot search engine matched 215 peptides to albumin in accession # gi:3212456, yielding 76% coverage in the tryptic digest, and matched 331 peptides for 85% coverage in the GluC digest. Three peptides from a pepsin digest are included in Table 4.1. MS/MS spectra were manually evaluated before a labeled peptide was included in Table 4.1. MS/MS spectra positively identified acetylation of 59 lysines, 10 serines, 8 threonines, 4 tyrosines and the N-terminal aspartate. Albumin has 59 lysines; every lysine was at least partially acetylated. The 10 acetylated serines were S5, S65, S192, S202, S287, S312, S419, S427, S435, and S454. The 8 acetylated threonines were T68, T76, T79, T83, T467, T474, T527, and T540. The 4 acetylated tyrosines were Y84, Y161, Y401, and Y411. The N-terminal aspartate D1 was acetylated.

Both chemical and in vivo e-N-acetylation of lysines has precedent (Gershey et al., 1968; Allfrey et al., 1984; Violand et al., 1994; Macdonald et al., 1999; Lapko et al., 2001). Chemical O-acetylation of tyrosines also has precedent (Riordan and Vallee, 1972). Reports on acetylation of serines, and threonines are more rare, though indirect evidence has been reported for bovine growth hormone treated with acetic anhydride (Oikawa et al., 1967).

The peptides in Table 4.1 do not have an acetylated Lys at the C-terminus, with the exception of K162. The vast majority of acetylated lysines appear as missed cleavages within the peptide. This confirms reports in the literature (Violand et al., 1994) that trypsin generally does not recognize acetylated lysine as a cleavage site.

Carbamylation by ammonium cyanate, a degradation product of urea, would add a mass of +43, a value close to the mass of +42 from acetylation. To avoid carbamylation artifacts, we did not use urea in our protocol.

Table 4.1. Mass spectrometry identification of residues in human albumin (gi: 3212456) acetylated by 10 mM p-nitrophenyl acetate.

Start - End	Mr	Sequence	Acetylated
1 - 19	2396.06	DAHKSEVAHRFKDLGEENF	D1 K4 S5 K12
1 - 20	2482.19	DAHKSEVAHRFKDLGEENFK	D1 K4 K12
7 - 17	1341.67	VAHRFKDLGEE	K12
11 - 20	1267.61	FKDLGEENFK	K12
18 - 45	3417.74	NFKALVLIAFAQYLQQCPFEDHVKLVNE	K20 K41

18 - 45	3375.73	NFKALVLIAFAQYLQQCPFEDHVKLVNE	K41
42 - 64	2670.18	LVNEVTEFAKTCVADESAENCDK	K51
49 - 57	1081.47	FAKTCVADE	K51
49 - 60	1368.59	FAKTCVADESAE	K51
61 - 82	2661.29	NCDKSLHTLFGDKLCTVATLRE	K64 K73
61 - 82	2619.28	NCDKSLHTLFGDKLCTVATLRE	K73
61 - 82	2661.29	NCDKSLHTLFGDKLCTVATLRE	S65 K73
65 - 81	2015.05	SLHTLFGDKLCTVATLR	S65 K73
65 - 81	2015.05	SLHTLFGDKLCTVATLR	T68 K73
65 - 81	1973.04	SLHTLFGDKLCTVATLR	T76
65 - 81	1973.04	SLHTLFGDKLCTVATLR	K73
74 - 98	3171.36	LCTVATLRETYGEM$_{ox}$ADCCAKQEPER	T76 T79 T83 K93
74 - 98	3197.38	LCTVATLRETYGEMADCCAKQEPER	T76 T79 T83 Y84 K93
82 - 98	2114.83	ETYGEMADCCAKQEPER	K93
87 -100	1778.70	MADCCAKQEPERNE	K93
101 - 119	2389.20	CFLQHKDDNPNLPRLVRPE	K106
133 - 141	1245.66	TFLKKYLYE	K137
133 - 141	1287.68	TFLKKYLYE	K136 K137
137 - 144	1096.59	KYLYEIAR	K137
146 - 162	2315.18	HPYFYAPELLFFAKRYK	K159 Y161 K162
154 - 167	1745.95	LLFFAKRYKAAFTE	K159
154 - 167	1745.95	LLFFAKRYKAAFTE	Y161
154 - 167	1787.96	LLFFAKRYKAAFTE	Y161 K162
154 - 167	1787.96	LLFFAKRYKAAFTE	K159 K162
161 - 174	1703.73	YKAAFTECCQAADK	K162
161 - 181	2499.16	YKAAFTECCQAADKAACLLPK	K162 K174
161 - 186	3167.51	YKAAFTECCQAADKAACLLPKLDELR	K162 K174 K181
163 - 181	2165.99	AAFTECCQAADKAACLLPK	K174
168 - 184	2003.91	CCQAADKAACLLPKLDE	K174
168 - 184	2045.92	CCQAADKAACLLPKLDE	K174 K181
168 - 188	2517.17	CCQAADKAACLLPKLDELRDE	K174
168 - 188	2559.18	CCQAADKAACLLPKLDELRDE	K174 K181
175 - 186	1439.78	AACLLPKLDELR	K181
175 - 195	2313.20	AACLLPKLDELRDEGKASSAK	K190
182 - 197	1885.95	LDELRDEGKASSAKQR	K190 K195
182 - 197	1927.96	LDELRDEGKASSAKQR	K190 S192 K195
189 - 208	2319.20	GKASSAKQRLKCASLQKFGE	K190 K195 K199
189 - 208	2361.21	GKASSAKQRLKCASLQKFGE	K190 K195 K199 K205
198 - 209	1519.78	LKCASLQKFGER	K199 K205
198 - 209	1561.79	LKCASLQKFGER	K199 S202 K205
210 - 218	1060.58	AFKAWAVAR	K212
223 - 233	1293.66	FPKAEFAEVSK	K225
223 - 240	2106.12	FPKAEFAEVSKLVTDLTK	K225 K233
234 - 257	2898.29	LVTDLTKVHTECCHGDLLECADDR	K240
245 - 266	2725.12	CCHGDLLECADDRADLAKYICE	K262
253 - 266	1740.74	CADDRADLAKYICE	K262
258 - 274	1982.93	ADLAKYICENQDSISSK	K262
258 - 276	2266.12	ADLAKYICENQDSISSKLK	K262 K274
263 - 276	1725.82	YICENQDSISSKLK	K274
267 - 277	1289.65	NQDSISSKLKE	K274
267 - 277	1331.66	NQDSISSKLKE	K274 K276
275 - 286	1629.81	LKECCEKPLLEK	K276 K281
286 - 292	927.41	KSHCIAE	K286 S287
312 - 321	1296.57	SKDVCKNYAE	S312 K317
312 - 321	1296.57	SKDVCKNYAE	K313 K317
318 - 336	2341.11	NYAEAKDVFLGMFLYEYAR	K323
322 - 333	1473.72	AKDVFLGMFLYE	K323

349 - 359	1337.71	LAKTYETTLEK	K351
349 - 372	2913.30	LAKTYETTLEKCCAAADPHECYAK	K351 K359
359 - 376	2211.90	KCCAAADPHECYAKVFDE	K359
359 - 376	2253.91	KCCAAADPHECYAKVFDE	K359 K372
369 - 376	1072.45	CYAKVFDE	K372
377 - 393	2127.07	FKPLVEEPQNLIKQNCE	K378
377 - 393	2169.08	FKPLVEEPQNLIKQNCE	K378 K389
390 - 410	2640.30	QNCELFEQLGEYKFQNALLVR	K402
390 - 410	2640.30	QNCELFEQLGEYKFQNALLVR	Y401
401 - 425	3047.67	YKFQNALLVRYTKKVPQVSTPTLVE	Y401 K402 K413
408 - 423	1997.08	LVRYTKKVPQVSTPTL	Y411 K413 K414 S419
409 - 423	1883.99	VRYTKKVPQVSTPTL	Y411 K413 K414 S419
411 - 428	2115.16	YTKKVPQVSTPTLVEVSR	K413 K414
411 - 428	2157.17	YTKKVPQVSTPTLVEVSR	K413 K414 S419
414 - 428	1680.94	KVPQVSTPTLVEVSR	K414
414 - 428	1722.95	KVPQVSTPTLVEVSR	K414 S419
426 - 442	2039.00	VSRNLGKVGSKCCKHPE	K432 K436
426 - 442	2081.01	VSRNLGKVGSKCCKHPE	K432 K436 K439
426 - 442	2081.01	VSRNLGKVGSKCCKHPE	S427 K436 K439
426 - 442	2123.03	VSRNLGKVGSKCCKHPE	K432 S435 K436 K439
429 - 439	1333.65	NLGKVGSKCCK	K432 K436
429 - 444	1937.95	NLGKVGSKCCKHPEAK	K432 K436 K439
440 - 466	3293.60	HPEAKRM$_{OX}$PCAEDYLSVVLNQLCVLHEK	K444
446 - 466	2575.21	M$_{OX}$PCAEDYLSVVLNQLCVLHEK	S454
446 - 472	3214.55	MPCAEDYLSVVLNQLCVLHEKTPVSDR	K466
446 - 472	3230.54	M$_{OX}$PCAEDYLSVVLNQLCVLHEKTPVSDR	T467
446 - 472	3256.56	MPCAEDYLSVVLNQLCVLHEKTPVSDR	S454 K466
466 - 479	1721.81	KTPVSDRVTKCCTE	T467
466 - 479	1763.82	KTPVSDRVTKCCTE	K466 K475
473 - 484	1507.71	VTKCCTESLVNR	K475
473 - 484	1549.72	VTKCCTESLVNR	T474 K475
496 - 505	1238.58	TYVPKEFNAE	K500
501 - 521	2586.17	EFNAETFTFHADICTLSEKER	K519
506 - 520	1839.83	TFTFHADICTLSEKE	K519
521 - 531	1396.80	RQIKKQTALVE	K524 K525
522 - 534	1580.95	QIKKQTALVELVK	K524 K525
526 - 534	1041.61	QTALVELVK	T527
532 - 542	1403.81	LVKHKPKATKE	K534 K538 K541
535 - 557	2798.43	HKPKATKEQLKAVMDDFAAFVEK	K536 K538 T540 K545
539 - 557	2224.11	ATKEQLKAVMDDFAAFVEK	K541 K545
539 - 560	2772.28	ATKEQLKAVMDDFAAFVEKCCK	T540 K541 K545 K557
543 - 556	1624.78	QLKAVMDDFAAFVE	K545
546 - 560	1847.79	AVMDDFAAFVEKCCK	K557
558 - 574	2158.90	CCKADDKETCFAEEGKK	K560 K564
558 - 574	2200.91	CCKADDKETCFAEEGKK	K560 K564 K573
561 - 573	1540.64	ADDKETCFAEEGK	K564
561 - 574	1710.74	ADDKETCFAEEGKK	K564 K573
561 - 585	2705.32	ADDKETCFAEEGKKLVAASQAALGL	K573 K574
565 - 585	2276.14	ETCFAEEGKKLVAASQAALGL	K573 K574
572 - 585	1367.81	GKKLVAASQAALGL	K573
572 - 585	1409.82	GKKLVAASQAALGL	K573 K574
574 - 585	1182.70	KLVAASQAALGL	K574

The added mass from acetate is 42, and from carbamidomethylation is 57. All 59 lysines are acetylated. 10 serines are acetylated: S5, S65, S192, S202, S287, S312, S419, S427, S435, S454. 8 threonines are acetylated: T68, T76, T79, T83, T467, T474, T527, T540. 4 tyrosines are acetylated: Y84, Y161, Y401, Y411.

Lysines are stably acetylated. An estimate of the stability of acetylated lysines was obtained by measuring % acetylation of Lys 225 in peptide SQRFPK*AEF with time. After 6 hours reaction of 15 μM albumin with 0.5 mM p-nitrophenyl acetate, 9% of K225 was acetylated. No change in % acetylation of this peptide was observed for up to 9 days. The lack of an increase in % acetylation with time is explained by the fact that 90% of the p-nitrophenyl acetate had been consumed after 6 hours. The absence of a loss in % acetylation supports the conclusion that acetylated lysine is stable at pH 8.0. A peptide with 9% acetylated lysines was chosen for this example to make the point that a particular residue may be only partially acetylated.

A second example of stable acetylation was obtained by MALDI-TOF analysis of peptide D*AHK*S*EVAHRFK*DLGEENF. After 48 hours reaction of 15 μM albumin with 10 mM p-nitrophenyl acetate, followed by dialysis to remove excess reagent, 100% of the N-terminus (D1), 100% of K12, 78% of K4 and 5% of S5 were acetylated. After 18 days, the % acetylations were unchanged. We conclude that acetylated lysines, as well as the acetylated N-terminus and acetylated serine, are stable at pH 8.0 and 22˚C.

Deacetylation of Tyr 411. Treatment of 15 μM albumin with 15 μM p-nitrophenyl acetate in 10 mM TrisCl pH 8.0 resulted in exclusive acetylation of Tyr 411. No other residues were significantly acetylated. Tyr 411 was maximally acetylated after 1 h. Figure 4.6 shows the maximum acetylation level of 80% and loss of the acetyl group with time. The half-life for deacetylation of Tyr 411 at pH 8.0, 22˚C was 61±4 hours. This very slow deacetylation rate (k = 0.0002 min^{-1}) confirms a previous report that deacetylation is the rate limiting step for reaction of human albumin with p-nitrophenyl acetate (Masson et al., 2007). On the other hand, turnover with o-nitrotrifluoroacetanilide is explained by the instability of the trifluoroacetyl adduct due to the electronic effect of the fluorine atoms (Masson et al., 2007).
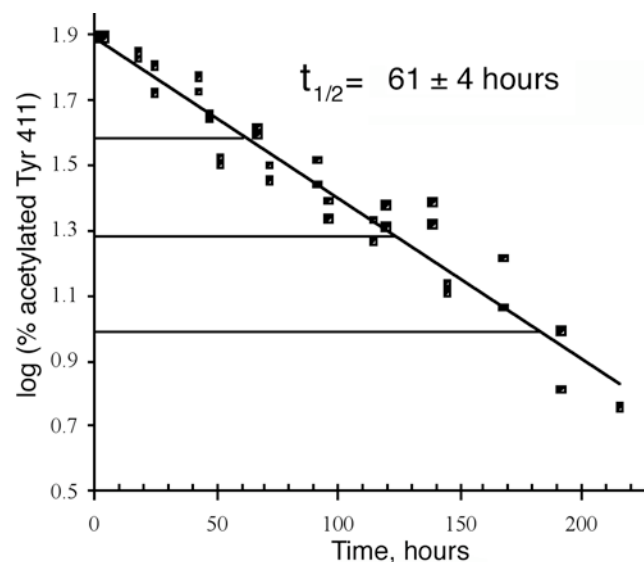

Figure 4.6. Deacetylation rate of Tyr 411. At time zero Tyr 411 was acetylated 80%. After 61 hours at pH 8.0, 22˚C, Tyr 411 was acetylated 40%. Deacetylation was monitored for 3.5 half-lives until only 5% of Tyr 411 was still acetylated. The 3 horizontal lines mark 3 half-lives. % acetylation was calculated from cluster areas in the MALDI-TOF mass spectrometer for peptides VRYTKKVPQVSTPTL and LVRYTKKVPQVSTPTL.

Location of ester-reactive residues. The location of the reactive residues in the crystal structure of human albumin is shown in Figure 4.7. All acetylated lysines, serines, and threonines are exposed to the surface. Tyr 411 is in a pocket 4.5 Angstroms from Arg 410. Acetylated Tyr 84, 161, and 401 may also have been activated by interaction with nearby arginines.
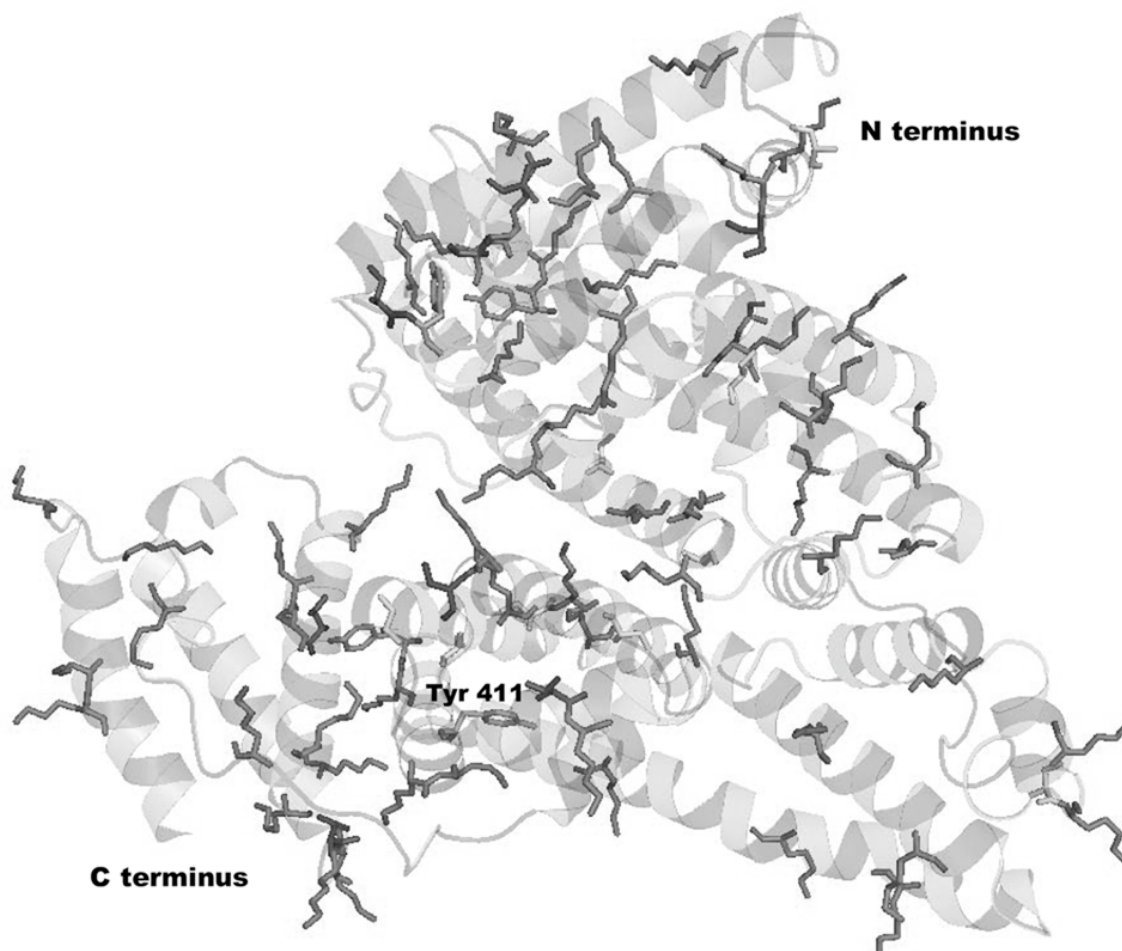

Figure 4.7. Surface location of acetylated residues in human albumin. The crystal structure of human albumin (PDB code 1bm0) shows side-chains for acetylated lysines, tyrosines, serines, and threonines. Asp 1 and Lys 4 are missing from the structure (Sugio et al., 1999).

Time to complete hydrolysis of 0.5 mM p-nitrophenyl acetate. Six hours after addition of p-nitrophenyl acetate to 15 μM albumin in 10 mM TrisCl pH 8.0, 22°C, 90% of the 0.5 mM p-nitrophenyl acetate had been consumed, and the rate of p-nitrophenol production by albumin had slowed so it was indistinguishable from the rate by buffer alone. By 24 hours, the endpoint absorbance of 8.42, at 400 nm, was reached and no further change in absorbance was obtained. The theoretical endpoint calculated from the extinction coefficient of 16,900 M^{-1} cm^{-1} for p-nitrophenolate ion at pH 8.0 was 8.45 (Means and Bender, 1975), a value in close agreement with the observed endpoint.

Percent acetylated lysines. About 50% of the hydrolysis of 0.5 mM p-nitrophenyl acetate was due to reaction with 15 µM albumin, and about 50% to reaction with pH 8.0 buffer. Assuming that the 250 µM of p-nitrophenyl acetate that reacted with 15 µM albumin resulted in stable acetylation of albumin, one can calculate about 16 to 17 molar equivalents of acetate bound per mole of albumin. If 16 out of 59 lysines are acetylated, then on average 27% of each lysine was acetylated. This value is close to the 20-25% acetylation calculated for K414.

  A third method was used to calculate % acetylated lysines. This method is based on the principle that lysines labeled with fluorodinitrobenzene are relatively stable to acid hydrolysis, whereas acetylated lysines are deacetylated to free lysines. Standard acid hydrolysis followed by amino acid composition analysis allows an estimate of the number of acetylated lysines (Allfrey et al., 1984). It was found that 27% of the lysines were acetylated in albumin treated with 0.5 mM p-nitrophenyl acetate, while 67% of the lysines were acetylated in albumin treated with 10 mM p-nitrophenyl acetate.

Esterase activity of albumin. The esterase activity of human albumin can be visualized on a nondenaturing gel stained for esterase activity with beta-naphthyl acetate and Fast Blue RR. The beta-naphthol reacts with the diazonium salt of Fast Blue RR to produce a pink, insoluble azodye, which precipitates at the site where naphthol is released.
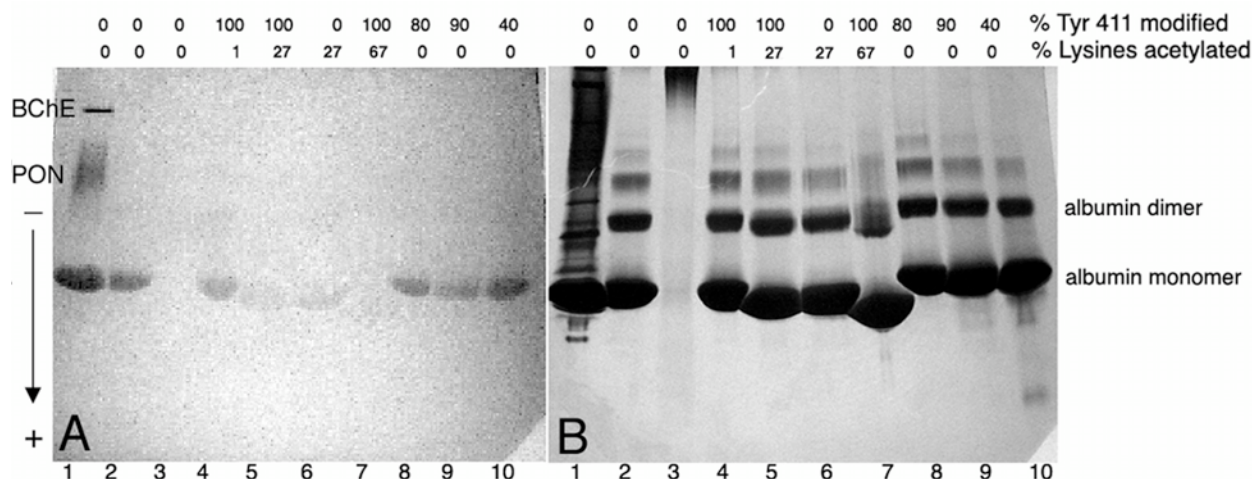

Figure 4.8. Nondenaturing gel stained for (A) esterase activity and counterstained with (B) Coomassie blue. Lane 1, 5 µL of human serum where the esterase bands are butyrylcholinesterase (BChE), paraoxonase (PON), and albumin. Lane 2, 200 µg of 99% pure fatty acid free human albumin. Lane 3, 200 µg denatured, carbamidomethylated albumin. Lane 4, 200 µg albumin treated 5 min with 0.5 mM p-nitrophenyl acetate to acetylate 100% of Tyr 411. Lane 5, 200 µg albumin treated with 0.5 mM p-nitrophenyl acetate for 6 h. Lane 6, 200 µg albumin treated with 0.5 mM p-nitrophenyl acetate for 2 weeks. Lane 7, 200 µg albumin treated with 10 mM p-nitrophenyl acetate for 48 h. Lane 8, 200 µg albumin treated with DFP to label 80% of Tyr 411. Lane 9, 200 µg albumin treated with chlorpyrifos oxon to label 90% of Tyr 411. Lane 10, 200 µg albumin treated with chlorpyrifos oxon to label 40% of Tyr 411. Percent labeling of Tyr 411 was estimated from cluster areas of peaks in the MADLI-TOF mass spectrometer. Percent labeling of lysines was estimated from amino acid composition analysis. The arrow indicates the direction of migration of proteins on the gel.

The gel in Figure 4.8A shows naphthol production by the albumin present in 5 µL of human plasma (lane 1), as well as by 200 µg of pure human albumin (lane 2). Additional esterase bands in lane 1 are from butyrylcholinesterase and paraoxonase. The question of interest was how much of the apparent esterase activity of albumin was due to Tyr 411 and how much to irreversible acetylation of lysines? To answer this question, albumin preparations with various percent acetylation of Tyr 411 and lysines were loaded on the gel. The esterase activity in lane 4 where 100% of Tyr 411 was acetylated, was similar to that in lane 2 where none of the Tyr 411 was acetylated. The esterase activity in lane 5 where 100% of the Tyr 411 was acetylated, and 27% of the lysines were acetylated, was substantially decreased. The albumin in lane 6 was acetylated only on lysines because Tyr 411 had completely deacetylated during two weeks incubation; the esterase activity in lane 6 was similar to that in lane 5, showing that lysines contributed more to albumin esterase activity than Tyr 411. The albumin in lane 7 was maximally acetylated by 10 mM p-nitrophenyl acetated, corresponding to the 82 residues acetylated in Table 4.1. The esterase activity in lane 7 was nearly abolished. Blocking Tyr 411 by covalent modification with DFP (lane 8) or chlorpyrifos oxon (lanes 9 and 10) had little effect on the apparent esterase activity.

The gel was counterstained with Coomassie blue in Figure 4.8B to show that protein loading per lane was equivalent. Slower migrating bands are consistent with higher molecular weight forms of albumin. Pure albumin is predominantly monomeric, but also forms dimers, and higher multimers. Figure 4.8B clearly shows that the highly acetylated albumin (67%) in lane 7 migrated substantially further than native albumin in lane 2. Albumin that was 27% acetylated migrated slightly further than native. This behavior is consistent with elimination of positive charge from the protein by acetylation of the e-N-amino groups of the lysines, thus giving the acetylated protein a greater net negative charge so that it would be attracted more readily to the positively-charged electrode at the bottom of the gel.

The esterase activity of albumin is characterized by an initial burst of product formation that is equal to one equivalent of albumin, followed by slower formation of multiple equivalents of product (Means and Bender, 1975). The fast phase has been attributed to initial acetylation of Tyr 411 (Means and Wu, 1979), which is consistent with the rapid labeling of Tyr 411 described in Figure 4.1. From the activity shown in Figure 4.8, it can be concluded that the apparent slow phase esterase activity of albumin is due to release of p-nitrophenol upon acetylation of 59 lysines, and to some extent the surface accessible serines, threonines and other tyrosines. This myriad of acetylations creates the appearance of enzymatic turnover, but it is not a true turnover process. Lysine, serine and threonine are acetylated but do not release the acetate. Acetylated Tyr 411 does release the bound acetate (that is, it turns over), but the release rate is too slow to account for a significant part of the apparent esterase activity of albumin in a 30 min assay. Albumin must therefore be regarded as a pseudo-esterase, not an enzymatic esterase.

DISCUSSION
Albumin esterase activity. In our previous reports we had identified Tyr 411 as the residue in albumin that is labeled by soman, sarin, DFP, chlorpyrifos oxon, FP-biotin, and dichlorvos (Li et al., 2007; Li et al., 2008). Others have also identified tyrosine as the site of covalent binding of soman, sarin, cyclosarin, and tabun to albumin (Williams et al., 2007). Organophosphorus agents inhibit the esterase activity of butyrylcholinesterase and other serine esterases by covalent binding to the active site serine (Nachon et al., 2005). By analogy, we had expected that OP binding to albumin would inhibit the esterase activity of albumin because it is commonly

assumed that Tyr 411 is the active site residue on albumin that is responsible for esterase activity. The burst activity of albumin with p-nitrophenyl acetate is indeed inhibited by labeling Tyr 411 with an organophosphorus agent (Means and Wu, 1979). However our results show that the slow steady state esterase activity of albumin is not inhibited by binding OP to Tyr 411, but instead is inhibited by acetylation of lysines. These results lead to a revised model of the esterase activity of albumin.

      In this revised model of the esterase activity of albumin up to 82 residues participate. The most reactive residue is Tyr 411. Deacetylation of Tyr 411 occurs with a half-life of 61±4 h, which means the p-nitrophenolate product formed in a 30 min reaction cannot come from turnover on Tyr 411. The majority of the "esterase" activity of albumin is due to a half-reaction with lysines, serines, threonines and tyrosines. These acetylated residues do not turnover but form stable adducts. At high p-nitrophenyl acetate concentration a total of 59 lysines, 10 serines, 8 threonines, 4 tyrosines and the N-terminal aspartate are acetylated.

      The lysines of albumin are acetylated by p-nitrophenyl acetate, but are not labeled by organophosphorus esters. We have found no evidence for labeling of lysines by organophosphorus agents (manuscript in preparation).

Confirmation of the prediction of Means and Bender. When Means and Bender (Means and Bender, 1975) found stable incorporation of ^{14}C-acetate into albumin they concluded that accelerated formation of p-nitrophenolate ion in the presence of serum albumin was not due to increased hydrolysis, but to rapid acetylation of serum albumin by p-nitrophenyl acetate. Means and Bender did not identify the residues involved and therefore their conclusion has been overlooked during the past 30 years while investigators focused on Tyr 411 as the esteratic site (Sakurai et al., 2004). With the availability of mass spectrometry we have identified the specific residues in albumin that become acetylated by p-nitrophenyl acetate and therefore provide proof for the concept introduced by Means and Bender to explain albumin esterase activity. Our results support their conclusion that the overall reaction rate, as reflected by appearance of p-nitrophenolate ion, corresponds to the sum of a large number of simultaneous reactions at different sites on the protein plus spontaneous hydrolysis.

      Additional support for the conclusion that lysines and tyrosine participate in the esterase activity of albumin comes from studies of chemically modified albumin (Georges et al., 2000). Modification of tyrosine and lysine suppressed hydrolysis of carprofen glucuronide, leading to the conclusion that Tyr and Lys have roles in hydrolysis.

Significance. It is expected that other esters will also acetylate albumin. Acetyl salicylic acid (aspirin) has been shown to acetylate up to 3 residues on human albumin, though only one acetylation site has been identified to date, namely Lys 199 (Hawkins et al., 1968; Walker, 1976; Yang et al., 2007).

      Albumin is unusual in the family of plasma proteins because it has no carbohydrates. This makes the amino acids of albumin more accessible to acetylation than those of a protein like butyrylcholinesterase whose surface is sugar coated. Nevertheless, it is possible that other proteins including butyrylcholinesterase are acetylated by carboxylic acid esters on multiple sites. Several lysines on ubiquitin are acetylated by aspirin (Macdonald et al., 1999).

      In some cases, chemical acetylation has an important physiological consequence. For example, the anti-inflammatory action of aspirin is explained by acetylation of the N-terminal serine of prostaglandin synthetase (Roth and Siok, 1978).

KEY RESEARCH ACCOMPLISHMENTS
• A new motif for OP binding to proteins has been identified. OP make a covalent bond with tyrosine.
• Albumin, transferrin, and tubulin bind OP covalently on tyrosine. This finding is contrary to the expectation that OP bind exclusively to serine.
• Synthetic peptides bind OP on tyrosine.
• The OP reactive tyrosines are near a positively charged residue that stabilizes the ionized hydroxyl group of tyrosine. The ionized form of tyrosine reacts with OP.
• OP-labeled tyrosines are stable at pH 7.4. This means the OP will not dissociate from tyrosine when OP-tyrosine labeled protein is injected into an animal for the purpose of producing an antibody.
• Albumin is a pseudo-esterase because esters acylate its 59 lysines to form stable derivatives on lysine. Tyrosine 411 slowly turns over with esters but forms a stable covalent bond with OP.

REPORTABLE OUTCOMES
• Published paper (pdf copy attached)
   Li B, Nachon F, Froment MT, Verdier L, Debouzy JC, Brasme B, Gillon E, Schopfer LM, Masson P (2008) Binding and hydrolysis of soman by human serum albumin. *Chem Res Toxicol* 21: 421-431.
• Submitted paper
   Lockridge O, Xue W, Gaydess A, Grigoryan H, Ding SJ, Schopfer LM, Hinrichs SH, Masson P. Pseudo-esterase activity of human albumin: slow turnover on Tyr 411 and stable acetylation of 82 residues including 59 lysines.
• Submitted paper
   Dins SH, Carr J, Carlson JE, Tong L, Xue W, Li Y, Schopfer LM, Li B, Nachon F, Asojo O, Thompson CM, Hinrichs SH, Masson P, Lockridge O. Five tyrosines and two serines in human albumin are labeled by the organophosphorus agent FP-biotin

CONCLUSION
Our mass spectrometry results contradict the dogma that serine esterases and serine proteases are the only class of proteins modified by exposure to OP. We have found 5 tyrosines in human albumin, 2 tyrosines in human transferrin, and 4 tyrosines in tubulin that are labeled by OP. The significance of this finding is in diagnosis of OP exposure. It now becomes possible to look for several proteins in human tissues, in addition to butyrylcholinesterase and acetylcholinesterase, for evidence of OP exposure.

PERSONNEL
Oksana Lockridge, Ph.D.
Lawrence M. Schopfer, Ph.D.
Shi-Jiang Ding, Ph.D.
Bin Li, Ph.D.
He Li, Ph.D.
Ellen G. Duysen, BS
Weihua Xue, BS

REFERENCES

Adams TK, Capacio BR, Smith JR, Whalley CE and Korte WD (2004) The application of the fluoride reactivation process to the detection of sarin and soman nerve agent exposures in biological samples. *Drug Chem Toxicol* **27**:77-91.

Aldridge JE, Seidler FJ, Meyer A, Thillai I and Slotkin TA (2003) Serotonergic systems targeted by developmental exposure to chlorpyrifos: effects during different critical periods. *Environ Health Perspect* **111**:1736-1743.

Allfrey VG, Di Paola EA and Sterner R (1984) Protein side-chain acetylations. *Methods Enzymol* **107**:224-240.

Atkins WM, Wang RW, Bird AW, Newton DJ and Lu AY (1993) The catalytic mechanism of glutathione S-transferase (GST). Spectroscopic determination of the pKa of Tyr-9 in rat alpha 1-1 GST. *J Biol Chem* **268**:19188-19191.

Ballinger P and Long FA (1960) Acid ionization constants of alcohols. II. Acidities of some substituted methanols and related compounds. *J Am Chem Soc* **82**:795-798.

Bates GW and Schlabach MR (1973) The reaction of ferric salts with transferrin. *J Biol Chem* **248**:3228-3232.

Bomser JA and Casida JE (2001) Diethylphosphorylation of rat cardiac M2 muscarinic receptor by chlorpyrifos oxon in vitro. *Toxicol Lett* **119**:21-26.

Carter DC, He XM, Munson SH, Twigg PD, Gernert KM, Broom MB and Miller TY (1989) Three-dimensional structure of human serum albumin. *Science* **244**:1195-1198.

Carter WG, Tarhoni M, Rathbone AJ and Ray DE (2007) Differential protein adduction by seven organophosphorus pesticides in both brain and thymus. *Hum Exp Toxicol* **26**:347-353.

Casida JE and Augustinsson KB (1959) Reaction of plasma albumin with 1-naphthyl N-methylcarbamate and certain other esters. *Biochim Biophys Acta* **36**:411-426.

Casida JE and Quistad GB (2004) Organophosphate toxicology: safety aspects of nonacetylcholinesterase secondary targets. *Chem Res Toxicol* **17**:983-998.

Chaiken IM and Smith EL (1969) Reaction of a specific tyrosine residue of papain with diisopropylfluorophosphate. *J Biol Chem* **244**:4247-4250.

Cuatrecasas P, Fuchs S and Anfinsen CB (1968) The tyrosyl residues at the active site of staphylococcal nuclease. Modifications by tetranitromethane. *J Biol Chem* **243**:4787-4798.

Curry S, Mandelkow H, Brick P and Franks N (1998) Crystal structure of human serum albumin complexed with fatty acid reveals an asymmetric distribution of binding sites. *Nat Struct Biol* **5**:827-835.

De Vriese C, Hacquebard M, Gregoire F, Carpentier Y and Delporte C (2007) Ghrelin interacts with human plasma lipoproteins. *Endocrinology*.

Derst C, Wehner A, Specht V and Rohm KH (1994) States and functions of tyrosine residues in Escherichia coli asparaginase II. *Eur J Biochem* **224**:533-540.

Dubois-Presle N, Lapicque F, Maurice MH, Fournel-Gigleux S, Magdalou J, Abiteboul M, Siest G and Netter P (1995) Stereoselective esterase activity of human serum albumin toward ketoprofen glucuronide. *Mol Pharmacol* **47**:647-653.

Fidder A, Hulst AG, Noort D, de Ruiter R, van der Schans MJ, Benschop HP and Langenberg JP (2002) Retrospective detection of exposure to organophosphorus anti-cholinesterases: mass spectrometric analysis of phosphylated human butyrylcholinesterase. *Chem Res Toxicol* **15**:582-590.

Gearhart DA, Sickles DW, Buccafusco JJ, Prendergast MA and Terry AV, Jr. (2007) Chlorpyrifos, chlorpyrifos-oxon, and diisopropylfluorophosphate inhibit kinesin-dependent microtubule motility. *Toxicol Appl Pharmacol* **218**:20-29.

Geer LY, Markey SP, Kowalak JA, Wagner L, Xu M, Maynard DM, Yang X, Shi W and Bryant SH (2004) Open mass spectrometry search algorithm. *J Proteome Res* **3**:958-964.

Georges H, Presle N, Buronfosse T, Fournel-Gigleux S, Netter P, Magdalou J and Lapicque F (2000) In vitro stereoselective degradation of carprofen glucuronide by human serum albumin. Characterization of sites and reactive amino acids. *Chirality* **12**:53-62.

Gershey EL, Vidali G and Allfrey VG (1968) Chemical studies of histone acetylation. The occurrence of epsilon-N-acetyllysine in the f2a1 histone. *J Biol Chem* **243**:5018-5022.

Grigoryan H, Schopfer LM, Thompson CM, Terry AV, Masson P and Lockridge O (2008) Mass spectrometry identifies covalent binding of soman, sarin, chlorpyrifos oxon, diisopropyl fluorophosphate, and FP-biotin to tyrosines on tubulin; OP-binding to tubulin may explain cognitive deficits associated with OP exposure. *Chem Biol Interact*.

Hagag N, Birnbaum ER and Darnall DW (1983) Resonance energy transfer between cysteine-34, tryptophan-214, and tyrosine-411 of human serum albumin. *Biochemistry* **22**:2420-2427.

Hawkins D, Pinckard RN and Farr RS (1968) Acetylation of human serum albumin by acetylsalicylic acid. *Science* **160**:780-781.

Jansz HS, Brons D and Warringa MG (1959) Chemical nature of the DFP-binding site of pseudocholinesterase. *Biochim Biophys Acta* **34**:573-575.

Ji Y, Neverova I, Van Eyk JE and Bennett BM (2006) Nitration of tyrosine 92 mediates the activation of rat microsomal glutathione s-transferase by peroxynitrite. *J Biol Chem* **281**:1986-1991.

Kassa J, Krocova Z, Sevelova L, Sheshko V, Kasalova I and Neubauerova V (2003) Low-level sarin-induced alteration of immune system reaction in inbred BALB/c mice. *Toxicology* **187**:195-203.

Katz EJ, Cortes VI, Eldefrawi ME and Eldefrawi AT (1997) Chlorpyrifos, parathion, and their oxons bind to and desensitize a nicotinic acetylcholine receptor: relevance to their toxicities. *Toxicol Appl Pharmacol* **146**:227-236.

Kohli RM and Massey V (1998) The oxidative half-reaction of Old Yellow Enzyme. The role of tyrosine 196. *J Biol Chem* **273**:32763-32770.

Kwon CH, Maddison K, LoCastro L and Borch RF (1987) Accelerated decomposition of 4-hydroxycyclophosphamide by human serum albumin. *Cancer Res* **47**:1505-1508.

Lamotte-Brasseur J, Dubus A and Wade RC (2000) pK(a) calculations for class C beta-lactamases: the role of Tyr-150. *Proteins* **40**:23-28.

Lapko VN, Smith DL and Smith JB (2001) In vivo carbamylation and acetylation of water-soluble human lens alphaB-crystallin lysine 92. *Protein Sci* **10**:1130-1136.

Lein PJ and Fryer AD (2005) Organophosphorus insecticides induce airway hyperreactivity by decreasing neuronal M2 muscarinic receptor function independent of acetylcholinesterase inhibition. *Toxicol Sci* **83**:166-176.

Li B, Nachon F, Froment MT, Verdier L, Debouzy JC, Brasme B, Gillon E, Schopfer LM, Lockridge O and Masson P (2008) Binding and Hydrolysis of Soman by Human Serum Albumin. *Chem Res Toxicol* **21**:421-431.

Li B, Schopfer LM, Hinrichs SH, Masson P and Lockridge O (2007) Matrix-assisted laser desorption/ionization time-of-flight mass spectrometry assay for organophosphorus toxicants bound to human albumin at Tyr411. *Anal Biochem* **361**:263-272.

Li B, Sedlacek M, Manoharan I, Boopathy R, Duysen EG, Masson P and Lockridge O (2005) Butyrylcholinesterase, paraoxonase, and albumin esterase, but not carboxylesterase, are present in human plasma. *Biochem Pharmacol* **70**:1673-1684.

Lockridge O, Schopfer LM, Winger G and Woods JH (2005) Large scale purification of butyrylcholinesterase from human plasma suitable for injection into monkeys; a potential new therapeutic for protection against cocaine and nerve agent toxicity. *J Med CBR Def* **3**:online publication.

London L, Flisher AJ, Wesseling C, Mergler D and Kromhout H (2005) Suicide and exposure to organophosphate insecticides: cause or effect? *Am J Ind Med* **47**:308-321.

Lowe J, Li H, Downing KH and Nogales E (2001) Refined structure of alpha beta-tubulin at 3.5 A resolution. *J Mol Biol* **313**:1045-1057.

Macdonald JM, LeBlanc DA, Haas AL and London RE (1999) An NMR analysis of the reaction of ubiquitin with [acetyl-1-13C]aspirin. *Biochem Pharmacol* **57**:1233-1244.

MacGillivray RT, Mendez E, Sinha SK, Sutton MR, Lineback-Zins J and Brew K (1982) The complete amino acid sequence of human serum transferrin. *Proc Natl Acad Sci U S A* **79**:2504-2508.

Manoharan I and Boopathy R (2006) Diisopropylfluorophosphate-sensitive aryl acylamidase activity of fatty acid free human serum albumin. *Arch Biochem Biophys* **452**:186-188.

Masson P, Froment MT, Darvesh S, Schopfer LM and Lockridge O (2007) Aryl acylamidase activity of human serum albumin with o-nitrotrifluoroacetanilide as the substrate. *J Enzyme Inhib Med Chem* **22**:463-469.

Maxwell DM, Brecht KM, Koplovitz I and Sweeney RE (2006) Acetylcholinesterase inhibition: does it explain the toxicity of organophosphorus compounds? *Arch Toxicol* **80**:756-760.

McDonough JH, Jr. and Shih TM (1997) Neuropharmacological mechanisms of nerve agent-induced seizure and neuropathology. *Neurosci Biobehav Rev* **21**:559-579.

Means GE and Bender ML (1975) Acetylation of human serum albumin by p-nitrophenyl acetate. *Biochemistry* **14**:4989-4994.

Means GE and Wu HL (1979) The reactive tyrosine residue of human serum albumin: characterization of its reaction with diisopropylfluorophosphate. *Arch Biochem Biophys* **194**:526-530.

Michel HO, Hackley BE, Jr., Berkowitz L, List G, Hackley EB, Gillilan W and Pankau M (1967) Ageing and dealkylation of Soman (pinacolylmethylphosphonofluoridate)-inactivated eel cholinesterase. *Arch Biochem Biophys* **121**:29-34.

Millard CB, Kryger G, Ordentlich A, Greenblatt HM, Harel M, Raves ML, Segall Y, Barak D, Shafferman A, Silman I and Sussman JL (1999) Crystal structures of aged phosphonylated acetylcholinesterase: nerve agent reaction products at the atomic level. *Biochemistry* **38**:7032-7039.

Morikawa M, Inoue M, Tsuboi M and Sugiura M (1979) Studies on aspirin esterase of human serum. *Jpn J Pharmacol* **29**:581-586.

Moser VC (1995) Comparisons of the acute effects of cholinesterase inhibitors using a neurobehavioral screening battery in rats. *Neurotoxicol Teratol* **17**:617-625.

Murachi T, Inagami T and Yasui M (1965) Evidence for alkylphosphorylation of tyrosyl residues of stem bromelain by diisopropylphosphorofluoridate. *Biochemistry* **4**:2815-2825.

Nachon F, Asojo OA, Borgstahl GE, Masson P and Lockridge O (2005) Role of water in aging of human butyrylcholinesterase inhibited by echothiophate: the crystal structure suggests two alternative mechanisms of aging. *Biochemistry* **44**:1154-1162.

Nogales E, Wolf SG and Downing KH (1998) Structure of the alpha beta tubulin dimer by
        electron crystallography. *Nature* **391**:199-203.
Oikawa A, Dellacha JM and Sonenberg M (1967) Chemical analysis of acetylated bovine growth
        hormone, a growth-hormone inhibitor. *Biochem J* **104**:947-952.
Peeples ES, Schopfer LM, Duysen EG, Spaulding R, Voelker T, Thompson CM and Lockridge
        O (2005) Albumin, a new biomarker of organophosphorus toxicant exposure, identified
        by mass spectrometry. *Toxicol Sci* **83**:303-312.
Perkins DN, Pappin DJ, Creasy DM and Cottrell JS (1999) Probability-based protein
        identification by searching sequence databases using mass spectrometry data.
        Electrophoresis **20**:3551-3567.
Pope CN (1999) Organophosphorus pesticides: do they all have the same mechanism of toxicity?
        J Toxicol Environ Health B Crit Rev **2**:161-181.
Prendergast MA, Self RL, Smith KJ, Ghayoumi L, Mullins MM, Butler TR, Buccafusco JJ,
        Gearhart DA and Terry Jr AV (2007) Microtubule-associated targets in chlorpyrifos oxon
        hippocampal neurotoxicity. *Neuroscience*.
Quistad GB, Klintenberg R and Casida JE (2005) Blood acylpeptide hydrolase activity is a
        sensitive marker for exposure to some organophosphate toxicants. *Toxicol Sci* **86**:291-
        299.
Quistad GB, Nomura DK, Sparks SE, Segall Y and Casida JE (2002) Cannabinoid CB1 receptor
        as a target for chlorpyrifos oxon and other organophosphorus pesticides. *Toxicol Lett*
        135:89-93.
Rainsford KD, Ford NL, Brooks PM and Watson HM (1980) Plasma aspirin esterases in normal
        individuals, patients with alcoholic liver disease and rheumatoid arthritis: characterization
        and the importance of the enzymic components. *Eur J Clin Invest* **10**:413-420.
Richards PG, Johnson MK and Ray DE (2000) Identification of acylpeptide hydrolase as a
        sensitive site for reaction with organophosphorus compounds and a potential target for
        cognitive enhancing drugs. *Mol Pharmacol* **58**:577-583.
Riordan JF and Vallee BL (1972) O-Acetyltyrosine. *Methods Enzymol* **25**:500-506.
Roldan-Tapia L, Parron T and Sanchez-Santed F (2005) Neuropsychological effects of long-term
        exposure to organophosphate pesticides. *Neurotoxicol Teratol* **27**:259-266.
Roth GJ and Siok CJ (1978) Acetylation of the NH2-terminal serine of prostaglandin synthetase
        by aspirin. *J Biol Chem* **253**:3782-3784.
Sakurai Y, Ma SF, Watanabe H, Yamaotsu N, Hirono S, Kurono Y, Kragh-Hansen U and Otagiri
        M (2004) Esterase-like activity of serum albumin: characterization of its structural
        chemistry using p-nitrophenyl esters as substrates. *Pharm Res* **21**:285-292.
Salvi A, Carrupt PA, Mayer JM and Testa B (1997) Esterase-like activity of human serum
        albumin toward prodrug esters of nicotinic acid. *Drug Metab Dispos* **25**:395-398.
Sanger F (1945) The free amino groups of insulin. *Biochem J* **39**:507-515.
Sanger F (1963) Amino-acid sequences in the active centers of certain enzymes. *Proc Chem Soc*
        5:76-83.
Sargent PJ, Farnaud S and Evans RW (2005) Structure/function overview of proteins involved in
        iron storage and transport. *Curr Med Chem* **12**:2683-2693.
Schopfer LM, Champion MM, Tamblyn N, Thompson CM and Lockridge O (2005)
        Characteristic mass spectral fragments of the organophosphorus agent FP-biotin and FP-
        biotinylated peptides from trypsin and bovine albumin (Tyr410). *Anal Biochem* **345**:122-
        132.

Schuh RA, Lein PJ, Beckles RA and Jett DA (2002) Noncholinesterase mechanisms of chlorpyrifos neurotoxicity: altered phosphorylation of Ca2+/cAMP response element binding protein in cultured neurons. *Toxicol Appl Pharmacol* **182**:176-185.

Schwartz M (1982) A serine protease activity of human serum albumin towards 4-methylumbelliferyl-guanidinobenzoate (MUGB) and diisopropyl fluorophosphate (DEP): implications for the use of MUGB reactivity in amniotic fluid in prenatal diagnosis of cystic fibrosis. *Clin Chim Acta* **124**:213-223.

Smulders CJ, Bueters TJ, Vailati S, van Kleef RG and Vijverberg HP (2004) Block of neuronal nicotinic acetylcholine receptors by organophosphate insecticides. *Toxicol Sci* **82**:545-554.

Sogorb MA, Carrera V and Vilanova E (2004) Hydrolysis of carbaryl by human serum albumin. *Arch Toxicol* **78**:629-634.

Sogorb MA, Diaz-Alejo N, Escudero MA and Vilanova E (1998) Phosphotriesterase activity identified in purified serum albumins. *Arch Toxicol* **72**:219-226.

Sogorb MA and Vilanova E (2002) Enzymes involved in the detoxification of organophosphorus, carbamate and pyrethroid insecticides through hydrolysis. *Toxicol Lett* **128**:215-228.

Song X, Seidler FJ, Saleh JL, Zhang J, Padilla S and Slotkin TA (1997) Cellular mechanisms for developmental toxicity of chlorpyrifos: targeting the adenylyl cyclase signaling cascade. *Toxicol Appl Pharmacol* **145**:158-174.

Stephens R, Spurgeon A, Calvert IA, Beach J, Levy LS, Berry H and Harrington JM (1995) Neuropsychological effects of long-term exposure to organophosphates in sheep dip. *Lancet* **345**:1135-1139.

Sugio S, Kashima A, Mochizuki S, Noda M and Kobayashi K (1999) Crystal structure of human serum albumin at 2.5 A resolution. *Protein Eng* **12**:439-446.

Sultatos LG, Basker KM, Shao M and Murphy SD (1984) The interaction of the phosphorothioate insecticides chlorpyrifos and parathion and their oxygen analogues with bovine serum albumin. *Mol Pharmacol* **26**:99-104.

Terry AV, Jr., Gearhart DA, Beck WD, Jr., Truan JN, Middlemore ML, Williamson LN, Bartlett MG, Prendergast MA, Sickles DW and Buccafusco JJ (2007) Chronic, intermittent exposure to chlorpyrifos in rats: protracted effects on axonal transport, neurotrophin receptors, cholinergic markers, and information processing. *J Pharmacol Exp Ther* **322**:1117-1128.

Terry AV, Jr., Stone JD, Buccafusco JJ, Sickles DW, Sood A and Prendergast MA (2003) Repeated exposures to subthreshold doses of chlorpyrifos in rats: hippocampal damage, impaired axonal transport, and deficits in spatial learning. *J Pharmacol Exp Ther* **305**:375-384.

Tildon JT and Ogilvie JW (1972) The esterase activity of bovine mercaptalbumin. The reaction of the protein with p-nitrophenyl acetate. *J Biol Chem* **247**:1265-1271.

Tove SB (1962) The esterolytic activity of serum albumin. *Biochim Biophys Acta* **57**:230-235.

Van Der Schans MJ, Polhuijs M, Van Dijk C, Degenhardt CE, Pleijsier K, Langenberg JP and Benschop HP (2004) Retrospective detection of exposure to nerve agents: analysis of phosphofluoridates originating from fluoride-induced reactivation of phosphylated BuChE. *Arch Toxicol* **78**:508-524.

Violand BN, Schlittler MR, Lawson CQ, Kane JF, Siegel NR, Smith CE, Kolodziej EW and Duffin KL (1994) Isolation of Escherichia coli synthesized recombinant eukaryotic proteins that contain epsilon-N-acetyllysine. *Protein Sci* **3**:1089-1097.

Walker JE (1976) Lysine residue 199 of human serum albumin is modified by acetylsalicyclic acid. *FEBS Lett* **66**:173-175.

Wally J, Halbrooks PJ, Vonrhein C, Rould MA, Everse SJ, Mason AB and Buchanan SK (2006) The crystal structure of iron-free human serum transferrin provides insight into inter-lobe communication and receptor binding. *J Biol Chem* **281**:24934-24944.

Watanabe H, Tanase S, Nakajou K, Maruyama T, Kragh-Hansen U and Otagiri M (2000) Role of arg-410 and tyr-411 in human serum albumin for ligand binding and esterase-like activity. *Biochem J* **349 Pt 3**:813-819.

Welch S and Skinner A (1989) A comparison of the structure and properties of human, rat and rabbit serum transferrin. *Comp Biochem Physiol B* **93**:417-424.

Williams NH, Harrison JM, Read RW and Black RM (2007) Phosphylated tyrosine in albumin as a biomarker of exposure to organophosphorus nerve agents. *Arch Toxicol* **81**:627-639.

Yang F, Bian C, Zhu L, Zhao G, Huang Z and Huang M (2007) Effect of human serum albumin on drug metabolism: structural evidence of esterase activity of human serum albumin. *J Struct Biol* **157**:348-355.

Binding and Hydrolysis of Soman by Human Serum Albumin

Bin Li,[†] Florian Nachon,[‡,§] Marie-Thérèse Froment,[‡,§] Laurent Verdier,[#]
Jean-Claude Debouzy,[‡,△] Bernardo Brasme,[‡,⊥] Emilie Gillon,[‡,§] Lawrence M. Schopfer,[†]
Oksana Lockridge,[†] and Patrick Masson*,[‡,§]

*University of Nebraska Medical Center, Eppley Institute, Omaha, Nebraska 68198-6805, Centre de Recherches
du Service de Santé des Armées, Département de Toxicologie, Unité d'Enzymologie, Unité de Biophysique,
Service de Biospectroscopie, BP 87, 38702 La Tronche cédex, France, 3, and Département Analyse Chimique,
Centre d'Etudes du Bouchet, BP 3, 91710 Vert-le-Petit, France*

Received September 15, 2007

Human plasma and fatty acid free human albumin were incubated with soman at pH 8.0 and 25 °C. Four methods were used to monitor the reaction of albumin with soman: progressive inhibition of the aryl acylamidase activity of albumin, the release of fluoride ion from soman, ^{31}P NMR, and mass spectrometry. Inhibition (phosphonylation) was slow with a bimolecular rate constant of 15 ± 3 M^{-1} min^{-1}. MALDI-TOF and tandem mass spectrometry of the soman–albumin adduct showed that albumin was phosphonylated on tyrosine 411. No secondary dealkylation of the adduct (aging) occurred. Covalent docking simulations and ^{31}P NMR experiments showed that albumin has no enantiomeric preference for the four stereoisomers of soman. Spontaneous reactivation at pH 8.0 and 25 °C, measured as regaining of aryl acylamidase activity and decrease of covalent adduct (pinacolyl methylphosphonylated albumin) by NMR, occurred at a rate of 0.0044 h^{-1}, indicating that the adduct is quite stable ($t_{1/2} = 6.5$ days). At pH 7.4 and 22 °C, the covalent soman–albumin adduct, measured by MALDI-TOF mass spectrometry, was more stable ($t_{1/2} = 20$ days). Though the concentration of albumin in plasma is very high (about 0.6 mM), its reactivity with soman (phosphonylation and phosphotriesterase activity) is too slow to play a major role in detoxification of the highly toxic organophosphorus compound soman. Increasing the bimolecular rate constant of albumin for organophosphates is a protein engineering challenge that could lead to a new class of bioscavengers to be used against poisoning by nerve agents. Soman-albumin adducts detected by mass spectrometry could be useful for the diagnosis of soman exposure.

1. Introduction

Albumin is an abundant protein that represents 50–60% of the total protein in human plasma and body fluids. Its concentration in plasma is about 0.6 mM. Albumin displays both an esterase activity (*1*) and an aryl acylamidase activity (*2, 3*). The topology of the esterase/amidase active site of albumin has been probed by site-directed mutagenesis (*4*) and X-ray structure determination of several drug–albumin complexes (*5*). Tyr411 was determined to be the catalytic nucleophile in these reactions.

Albumin is also known to bind organophosphates (OPs[1]) and carbamates (*6–8*) and to react with them (*9–11*). OPs and certain carbamates are actually hydrolyzed by albumin through transient phosphylation/alkylation of its active site (*12–17*). The residue that reacts with OPs was proven to be a tyrosine (*9–11, 14, 18*). DF^{32}P-labeling of human albumin followed by peptide sequencing showed that the labeled tyrosine is in the tetrapeptide

sequence Arg-*Tyr*-Thr-Lys (*9*). Arg and Tyr were subsequently identified as Arg 410 and Tyr 411, the key residues of the esteratic site of HSA (*4*). Recently, DFP-inhibition of the aryl acylamidase (AAA) activity of FAF-HSA confirmed that Tyr 411 is also the nucleophilic pole of the albumin AAA activity (*2*). Finally, MALDI-TOF mass spectrometry provided direct evidence that the OPs chlorpyrifos-oxon, dichlorvos, DFP, and sarin bind covalently to human albumin at Tyr 411 (*19*).

In the present work, we investigated the reaction of human albumin with soman. MALDI-TOF and quadrupole tandem MS/ MS mass spectrometry of the soman–albumin adduct showed that Tyr411 was phosphonylated. Unlike soman adducts of butyrylcholinesterase, the albumin–soman adduct did not age, that is, lose its pinacolyl chain. Covalent docking simulations and ^{31}P NMR experiments indicated that there was no enantiomeric preference of albumin for the stereoisomers of soman. Kinetic parameters of albumin phosphonylation by soman and subsequent dephosphonylation were determined.

Our results could have application for the detection of soman exposure in humans. Mass spectrometry could be used to detect soman–albumin adducts. In addition, antibodies to the soman– albumin adduct could be generated for use in a rapid antibody-based assay of soman exposure. Lastly, mutants of albumin could lead to a new class of scavengers against OP poisoning.

2. Experimental Procedures

2.1. Chemicals. Fatty acid-free human albumin (FAF-HSA) and porcine pepsin were from Sigma Chemical Co. (Saint Quentin

* To whom correspondence should be addressed. Patrick Masson, CRSSA, Département de Toxicologie, Unité d'Enzymologie, BP 87, 38702 La Tronche cédex, France. Tel: +33 (0)4 76 63 69 59. Fax: +33 (0)4 76 63 69 62. E-mail: pmasson@unmc.edu.
† Eppley Institute.
‡ Centre de Recherches du Service de Santé des Armées.
§ Département de Toxicologie, Unité d'Enzymologie.
# Centre d'Etudes du Bouchet.
△ Unité de Biophysique.
⊥ Service de Biospectroscopie.
[1] Abbreviations: AAA, aryl acylamidase; AChE, acetylcholinesterase; BuChE, butyrylcholinesterase; DFP, diisopropylfluorophosphate; FAF-HSA, fatty acid-free human serum albumin; HSA, human serum albumin; MP, methylphosphonate; PMP, pinacolyl methylphosphonate; o-NTFNAC, *N*-(*o*-nitrophenyl)trifluoroacetamide; OP, organophosphorus ester.

Fallavier, France). o-NTFNAC was a gift from Dr. Sultan Darvesh (Dalhousie University, Halifax, Canada). Racemic soman (pinacolyl methylfluorophosphate) dissolved in isopropanol was from CEB (Vert-le-Petit, France). All other chemicals were of biochemical grade.

The concentration of racemic soman in the stock solution was determined by programmed temperature gas chromatography after hydrolysis into methylpinacolyl phosphonic acid and derivatization with pentafluorobenzyl bromide (20). It was 4.73 mg/mL (26 mM). ^{31}P NMR spectra of 2 mM soman in deuterated dimethylsulfoxide were recorded at 27 °C on a Bruker spectrometer (AM400, 9.4 T). The spectra showed that the four stereoisomers are present in nearly equimolar amounts. Soman has two chiral centers. The absolute configuration of the four diastereoisomers is known. P_S, P_R, C_S, and C_R correspond to the old notation P−, P+, C+, and C−, respectively. Thus, isomers P_SC_S = P−C+, P_SC_R = P−C−, P_RC_R = P+C−, and P_RC_S = P+C+. Stereoisomers P_SC_S and P_SC_R are the most active toward the biological target acetylcholinesterase (21).

2.2. Aryl Acylamidase Enzymatic Assay of Albumin. The AAA activity of albumin was assayed with o-NTFNAC (2 mM) as the substrate in 60 mM Tris/HCl buffer at pH 8.0 at 25 °C. A 60 mM stock solution of o-NTFNAC was prepared in 50% water/acetonitrile (v/v). Because isopropanol is the solvent for soman, isopropanol was also added to the buffer in the control assay for the AAA activity of albumin in the absence of soman. The final concentration of acetonitrile in the assay was 3.3% and that of isopropanol was 2%. The release of the phenolic product (o-nitroaniline) was monitored for 5 min at 430 nm (ε = 3954 M^{-1} cm^{-1}) according to Darvesh et al. (22). Because of the low enzymatic activity of albumin with o-NTFNAC (3), high concentrations of FAF-HSA were used in assays (0.075 mM final). Measured rates were corrected for spontaneous hydrolysis of o-NTFNAC.

2.3. Mass Spectrometry (MALDI-TOF and Quadrupole MS/MS) of the Soman−Albumin Adduct from Human Plasma. One hundred microliters of human plasma was mixed with 2.3 μL of stock soman (26 mM in isopropanol) to give a reaction mixture containing 600 μM soman (in 2.3% isopropanol). The mixture was incubated at room temperature for 3–7 days before processing. No buffer was added to the plasma during this step. The pH of a 10 μL aliquot was reduced to pH 2.3 by adding 10 μL of 1% trifluoroacetic acid. Proteins were digested with 0.5 μg of pepsin for 2 h at 37 °C. At pH 2.3, selective proteolysis at the C-terminal side of the leucine and phenylalanine residues is expected. There was no need to denature the proteins or to reduce and alkylate the disulfide bonds because the peptides of interest were released without these added steps. Peptides were separated on a C18 reverse phase column on a Waters 625 LC system with a 40 min gradient starting with 85% buffer A (0.1% trifluoroacetic acid in water), 15% buffer B (acetonitrile containing 0.07% trifluoroacetic acid), and ending with 65% buffer A and 35% buffer B. One milliliter fractions were reduced in volume to 200 μL in a vacuum centrifuge, and 1 μL was analyzed by MALDI-TOF with a 2,5-dihydroxybenzoic acid matrix. Mass spectra were acquired with the Applied Biosystems Voyager DE-PRO MALDI-TOF mass spectrometer in linear positive ion mode. The spectrometer was calibrated using standard peptides (Applied Biosystems Mixture 1). A control plasma sample was identically treated, except that it was incubated with 3.1% isopropanol rather than with soman.

MS/MS spectra were acquired on a Q-Trap 2000 triple quadrupole linear ion trap mass spectrometer (Applied Biosystems, MDS Sciex, Foster City, CA) with a nano electrospray ionization source. Samples were infused into the mass spectrometer at 0.35 μL/min via a fused silica emitter (360 μm o.d., 20 μm i.d., 15 μm taper, New Objective, Woburn, MA) using a Harvard syringe pump to drive a 25 μL Hamilton syringe equipped with an inline 0.25 μm filter. Samples were sprayed with 50% acetonitrile and 0.1% formic acid. Mass spectra were calibrated using fragment ions generated from collision-induced dissociation of Glu fibrinopeptide B (Sigma). Enhanced product ion scans were obtained with a collision energy of 50 ± 5 V and a pure nitrogen gas pressure of 4 × 10^{-5} Torr.

The final enhanced product ion scan was the average of 105 scans. Ions were identified by manual sequencing.

2.4. ^{31}P NMR Spectroscopy. ^{31}P NMR spectra for the reaction between albumin (0.78 mM or 1.3 mM) and soman (1.3 mM) in 60 mM Tris/HCl buffer at pH 8.0 were recorded at 27 °C on a Bruker AM400NB spectrometer operating at 162 MHz. The spectra were acquired using successive 8 acquisition blocks of 5,000 accumulated scans (acquisition time: 3 h/spectrum) using 30 kHz spectral width, 32,000 acquisition points, and a composite pulse proton decoupling (CPD mode). The external reference for chemical shifts was 85% (w/v) H$_3$PO$_4$. Spectra were compared to the spectrum of soman in buffer and the spectrum of methyl pinacolyl phosphonate (MPP) in the presence and absence of albumin. MPP was made by the complete hydrolysis of soman in 5 N sodium hydroxide.

2.5. Kinetic Studies of the Reaction of Albumin with Soman. 2.5.1. Residual AAA Activity. FAF-HSA (780 μM) was incubated with 120 to 1300 μM concentrations of racemic soman in 60 mM Tris/HCl buffer at pH 8.0 at 25 °C. The time dependence of the inhibition of albumin by soman was monitored by following the residual AAA activity of albumin. Measurements of the AAA residual activity were performed on 100 μL aliquots of reaction mixture, using the sampling method (23).

2.5.2. Monitoring the Release of Fluoride from Soman. The release of fluoride, that is, the leaving group of soman, upon the reaction of soman with albumin and spontaneous hydrolysis was monitored by ionometry using a thermostatted ionometer (Radiometer IONcheck 45) equipped with an ion-selective electrode for fluoride (ISE 301F). FAF-HSA (780 μM) was incubated with 520, 780, and 1300 μM concentrations of racemic soman in 60 mM Tris/HCl buffer at pH 8.0 at 25 °C, and the concentration of released fluoride was assayed. The spontaneous hydrolysis of soman was determined under the same conditions.

2.5.3. Kinetic ^{31}P NMR Spectroscopy. To follow the phosphonylation reaction, 1.33 mM FAF-HSA was incubated with 1.35 mM soman in 60 mM Tris/HCl buffer at pH 8.0 at 25 °C in the presence of deuterated DMSO (10% v/v final). The successive spectra were recorded every 20 min (800 scans) over 4 h. Concentrations of the different species were plotted as a function of time. To follow the reactivation of phosphonylated albumin, 1.3 mM FAF-HSA was reacted with one equivalent of racemic soman in 60 mM Tris/HCl buffer at pH 8.0. Then, the phosphonylated albumin solution was maintained at 25 °C, and spectra were recorded every 2 h over 60 h. Kinetic constants for the spontaneous hydrolysis of soman, phosphonylation of albumin, and reactivation of albumin (dephosphonylation) were determined by fitting data against the numeric solution of differential equations that describe Scheme 1, using Mathematica 5 (Wolfram Research).

2.5.4. Kinetic Mass Spectrometry. The stability of the covalent soman−albumin adduct was measured on a MALDI-TOF-TOF 4800 mass spectrometer (Applied Biosystems). Human albumin was labeled by incubating a 1 mg/mL solution (15 μM) in 10 mM Tris/HCl at pH 8.0 with 200 μM soman for 24 h at room temperature. After this time, the concentration of active soman was negligible as determined by measuring the inhibition of human butyrylcholinesterase. The albumin solution was diluted to 0.1 mg/mL with 0.01% sodium azide in water and the pH adjusted to 7.4. The 200 μL solution was stored at 22 °C. Every 2 or 3 days, a 10 μL aliquot was acidified with 10 μL of 1% trifluoroacetic acid and digested with 2 μL of 1 mg/mL porcine pepsin (dissolved in 10 mM HCl). The digest was incubated at 37 °C for 1–4 h, and then 0.5 μL was spotted on a MALDI target plate. The dry spot was overlaid with 0.5 μL of 10 mg/mL α-cyano-4-hydroxycinnamic acid in 50% acetonitrile and 0.1% trifluoroacetic acid. MS scans in reflector mode were acquired at 3000 V by summing 500 laser shots per scan. The percent label on Tyr 411 was calculated from cluster areas. Peptide masses acquired in reflector mode are monoisotopic, which makes their mass about 1 amu lower than the average mass acquired in linear mode.

2.6. Molecular Modeling. 2.6.1. Noncovalent Docking. Docking calculations were carried out using two programs: (1) Autodock, version 3.0.5, with the Lamarckian genetic algorithm (LGA (*24*)) and (2) Gold, version 3.1 (CCDC Software, Ltd). Docking with Autodock employed the following procedure. The molecular models of the four diastereoisomers of soman were built and minimized with the MM2 force field of Chem3D (Cambridge soft.). The structure of HSA was prepared from the crystal structure of its complex with indoxyl sulfate (pdb code 2bxh) or warfarin (pdb code 2bxd) to take into account the heterogeneity of conformation of Val433. Molecules of water and ligands were removed from the model. Soman and HSA were further prepared using Autodock Tools 1.4 (*25*). The 3D affinity grid box was designed to include the full pocket near Tyr411. The number of grid points in the *x*-, *y*-, and *z*-axes was 60, 60, and 60 with grid points separated by 0.375 Å. Docking calculations were set to 100 runs. At the end of the calculation, Autodock performed cluster analysis. Docking solutions with ligand all-atom root-mean-square deviation (rmsd) within 1.0 Å of each other were clustered together and ranked by the lowest energy representative. The lowest-energy solution was accepted as the one most representative of the soman−HSA complex. Docking with Gold employed the following procedure. Protein structures were protonated and minimized by conjugate gradients using Gromacs 3.3 (*26, 27*) and the parameter set 53A6 (*28*). Ligands were built into the Sybyl 7.2 package (Tripos Inc.). The Mopac-PM3 (*29*) semiempirical method was chosen for geometry optimization and calculation of atomic charges. The cavity was defined as residues having atoms up to 15 Å from the Tyr411 hydroxyl group. We used long search settings for the Gold GA: 40 docking with parameters corresponding to the default 200% search efficiency settings. The final selection of conformers was based on the two scoring functions, Goldscore (*30*) and Chemscore (*31*).

2.6.2. Covalent Docking. This simulation was carried out using Gold, version 3.1 with GA settings similar to those for noncovalent docking. We used the same proteins as before, and the results were scored using both Goldscore and Chemscore functions. The fluorine atom from each of the four soman stereoisomers was replaced by a hydroxyl group, and the phosphorus stereochemistry was inverted to get the right configuration when the phosphorus atom binds to the Tyr411 Oγ. The highest score isomers were chosen as the ones giving the lowest ΔH_f when estimating the energy of the system with Mopac-PM3. To reduce the number of atoms in our system, we removed residues having all atoms further than 5 Å from any soman atoms.

3. Results

3.1. Mass Spectrometry to Identify the Covalent Binding of Soman to Tyrosine 411. Peptic digests of soman-labeled and control human plasma were separated by HPLC. Matched fractions from the two preparations were examined by MALDI-TOF mass spectrometry. MALDI-TOF signals for soman−albumin and control albumin peptides are shown in Figure 1. A peptide with mass 1880 amu is present in fraction 21 from the soman-labeled preparation (Figure 1, panel B). This mass is consistent with the peptide (L)VRY*TKKVPQVSTPTL(V) (1718 amu, from residues 409–423 of the mature albumin sequence) with an added mass of 162 amu from soman. A peptide with mass 1993 amu is present in fraction 23 from the soman-labeled preparation (Figure 1, panel D). This mass is consistent with the peptide (L)LVRY*TKKVPQVSTPTL(V) (1831 amu, from residues 408–423 of the mature albumin sequence, representing a missed peptic cleavage) with an added mass of 162 amu from soman. The parallel fractions from control human plasma do not have peptides of these masses (Figure 1, panels A and C). However, other prominent peaks are present at identical masses in both the control and soman-labeled spectra (compare panels A to B, and C to D), confirming that the fractions are matched with regard to HPLC elution and relative mass spectral
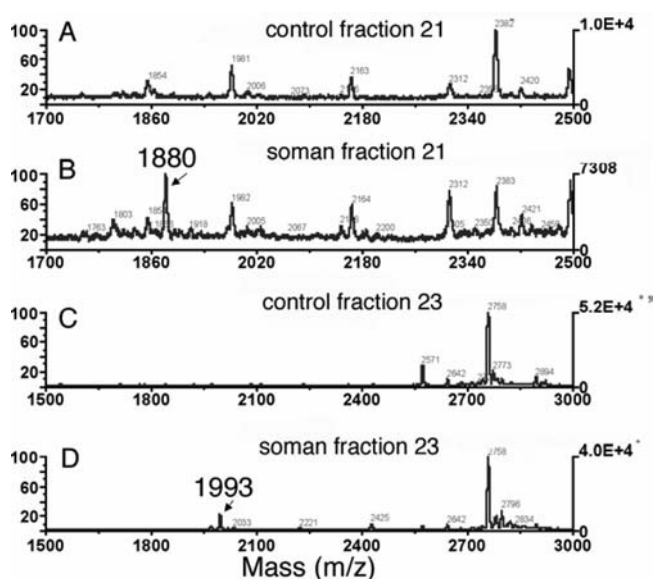

Figure 1. MALDI-TOF mass spectra of peptic peptides from the soman−albumin adduct. Panels A and C, control human plasma digested with pepsin and fractionated by HPLC, but not treated with soman. Panels B and D, human plasma treated with soman before digestion with pepsin and fractionation by HPLC. Soman-labeled albumin peptides of 1880 and 1993 amu include 162 amu from soman.

sensitivity. Tyr411 is present in both peptides (indicated by the star), supporting the proposal that soman binds covalently to Tyr411 of human albumin in plasma. Peptides with an added mass of 162 from soman, but not with an added mass of 78 were found. This indicates that the soman adduct does not lose the pinacolyl group when soman is bound to albumin. Thus, the soman−albumin adduct does not age.

An additional experiment was performed to demonstrate by a second mass spectrometry method that soman was covalently bound to Tyr 411 of human albumin. HPLC fraction 21 containing the soman-labeled albumin peptide at 1880 *m/z* was infused into the Q-Trap, quadrupole mass spectrometer. The enhanced mass spectrum showed a peak at 940.7 *m/z*, which is consistent with the doubly charged form of the 1880 peptide. This peptide was subjected to collision-induced dissociation. The resulting enhanced product ion spectrum yielded amino acid sequence information consistent with the sequence VRYT-KKVPQVSTPTL, with soman covalently bound to tyrosine (see Figure 2).

The prominent peak at 898.6 *m/z* is a doubly charged ion, 42 mass units less than the parent ion at 940.7 *m/z*. This is consistent with the loss of the pinacolyl group (84 mass units) from the doubly charged parent to form a doubly charged product retaining methylphosphonic acid. A comparable 42 amu loss from the parent ion was seen in the enhanced product ion spectrum of the LVRYTKKVPQVSTPTL peptide (data not shown). Preferential loss of the pinacolyl group seems to be a characteristic feature of soman-labeled peptides when they are fragmented in the mass spectrometer, as the soman-labeled butyrylcholinesterase peptide also lost the pinacolyl group during the collision process (*32, 33*).

The 940.7 *m/z* parent ion in Figure 2 included the pinacolyl group of soman. This is a significant point because it demonstrates that soman had not lost the pinacolyl group while bound to intact albumin protein or during digestion and HPLC separation. The pinacolyl group only dissociated when the peptide was subjected to collision-induced dissociation in the
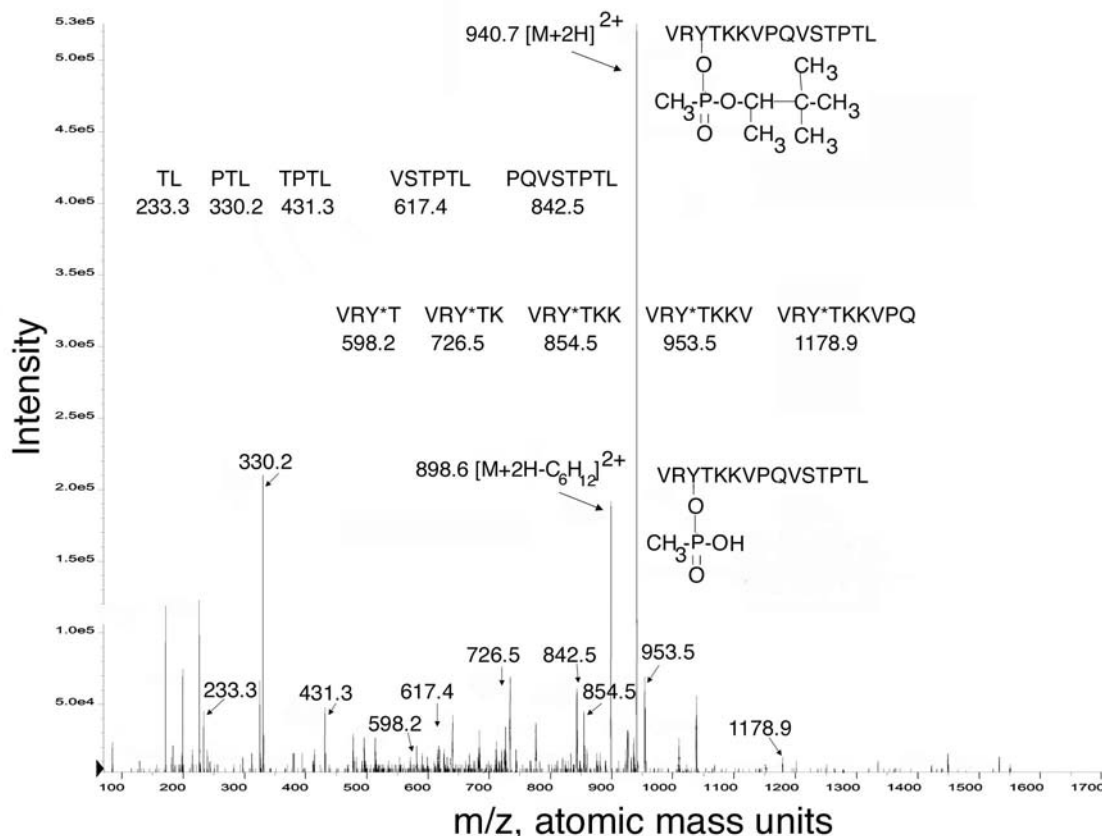
Figure 2. Product ion spectrum of the soman-labeled human albumin peptic peptide. The doubly charged parent ion at 940.7 *m/z* yielded fragments consistent with the sequence VRY*TKKVPQVSTPTL, where * indicates soman covalently bound to tyrosine 411. The accession number for human albumin is GI:28592. In this resource, Tyr 411 is given as Tyr 435 because the numbering begins with the 24-amino acid signal peptide.

mass spectrometer. The presence of the pinacolyl group in the parent ion demonstrates that soman did not age when bound to albumin.

At least four separate ion series from the VRYT-KKVPQVSTPTL peptide could be extracted from the spectrum in Figure 2. Only the y and b ion series are indicated in the Figure for the sake of clarity.

The peptide [VRY*T]KKV[PQ] was seen as part of the b-ion series. The masses of all five observed fragments were consistent with the indicated amino acid sequence plus 78 amu for the added mass of a methyl phosphonic acid. The only residue in this sequence capable of forming a methyl phosphonic acid adduct is the tyrosine, establishing this as the modified amino acid in the peptide. The presence of a 78 amu added mass on the observed fragments, rather than 162 amu, indicates that the pinacolyl group is dissociated from the peptide, in the collision chamber, prior to the onset of backbone fragmentation.

The peptide [PQ][VS]TP[TL] was seen as part of the y-ion series. The masses of the observed fragments were consistent with only the amino acids, unencumbered with any adduct mass. Thus, the potentially phosphonylated serine was not labeled, supporting the assignment of the tyrosine as the modified amino acid.

The complete amino acid sequence of peptide VRY*TKKV PQVSTPTL was represented by these two ions. These results confirm the conclusion that soman covalently binds to Tyr 411 of human albumin.

3.2. Kinetics for the Phosphonylation of Albumin by Soman and for the Reactivation of Phosphonylated Albumin.
**3.2.1. Phosphonylation of Albumin by Soman.** Because of the low reactivity of albumin with esters, aryl amides (*1, 3*),

and DFP (*10*), a low soman phosphonylation rate was expected. Therefore, the phosphonylation of albumin by soman was carried out under second-order conditions (*3, 34*), that is, the initial concentrations of soman, $[S]_0$, and albumin, $[A]_0$, were not very different. As a result, the concentrations of the uncomplexed forms of both reactants varied with time during the reaction.

Albumin (0.78 mM) was phosphonylated by sub and super-stoichiometric amounts of racemic soman (0.32 to 1.3 mM) that inhibited albumin's aryl acylamidase activity. Reaction was monitored by following albumin's aryl acylamidase (AAA) activity. Inspection of the inhibition time courses (Figure 3) indicated that less albumin was inhibited by soman than would have been expected from a stoichiometric reaction with the total amount of soman in the reaction. For example, in the presence of a 2-fold excess of soman, 100% inactivation of the AAA activity of albumin was never reached. The titration plot (not shown) for 0.78 mM albumin incubated with different concentrations of soman (0.38, 0.65, 0.81, and 1.30 mM) confirmed this observation. This suggests either that a large part of soman spontaneously hydrolyzed in the nucleophilic Tris/HCl buffer at pH 8.0 or that albumin reacted stereoselectively with specific stereoisomers of soman.

3.2.2. Determination of Fluoride Released during the Reaction of Soman with Albumin. In an effort to decide whether the substoichiometric reaction of soman with albumin was due to a competing spontaneous hydrolysis of soman or to a stereoselective reaction of albumin with soman, ionometric measurements of fluoride released from soman in the presence and absence of albumin were performed (Figure 4). It was found that spontaneous hydrolysis of soman in 60 mM Tris/HCl buffer at pH 8.0 at 25 °C was high. The rate constant for hydrolysis
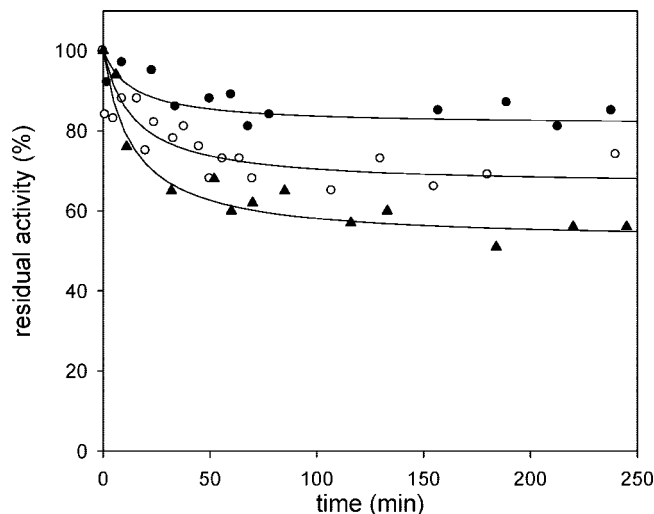
Figure 3. Progressive inhibition of the AAA activity of FAF-HSA ([E] = 0.78 mM) by different concentrations of racemic soman (●, 0.324 mM; ○, 0.520 mM; π, 0.780 mM) in 60 mM Tris/HCl buffer at pH 8.0 at 25 °C. A plot of % residual AAA activity of albumin vs time. The progress curves reach a plateau after consumption of the reactive soman.
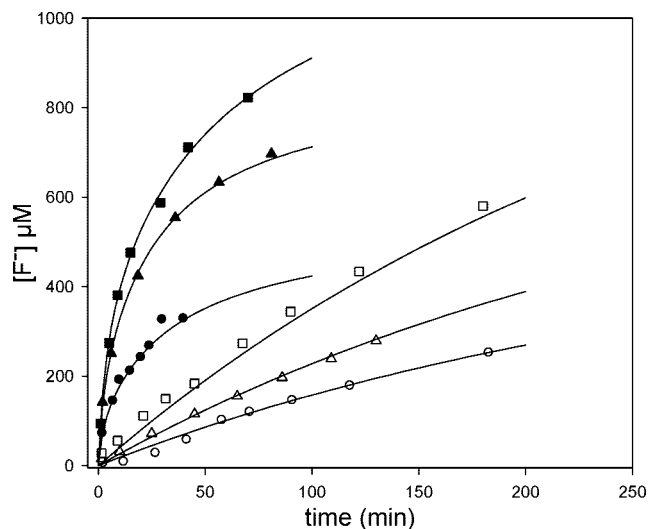
Figure 4. Time course of fluoride ions released from soman, in the presence and absence of FAF-HSA. Soman ([S]$_0$ = ●○, 0.52, ▲△, 0.78, ■□, 1.3 mM) was incubated with albumin ([E] = 0.78 mM) (filled symbols), or soman was incubated by itself through spontaneous hydrolysis (open symbols on continuous curves). Both reactions were in 60 mM Tris/HCl at pH 8.0.

of soman (k_{ho}) was 0.00342 ± 0.00007 min^{-1}. In the presence of albumin, the rate of fluoride release was significantly higher. Semiquantitative analysis of progress curves shows not only that spontaneous hydrolysis of soman occurred at rates comparable to the phosphonylation rates of albumin but also that albumin itself provides a physicochemical environment that enhances the spontaneous hydrolysis of soman. The following is an example of this semiquantitative analysis.

The filled squares in Figure 4 describe the release of fluoride after mixing 1.3 mM soman with 0.78 mM FAF-HSA. After 100 min of incubation, 0.3 mM albumin was inhibited (see Figure 3) so that the phosphonylation of albumin accounts for 0.3 mM of released fluoride. Over this time period, about 0.9 mM fluoride was released. Spontaneous hydrolysis of 1.3 mM soman (□ in Figure 4) accounts for about 0.35 mM of released fluoride. This leaves about 0.25 mM fluoride unaccounted for. Thus, the release of this extra fluoride suggests that the hydrolysis of soman at pH

8.0 is faster in the presence of albumin than in buffer alone. However, dephosphonylation of the Tyr411 adduct is far too slow (0.0044 ± 0.0008 h^{-1}; see section 3.2.5) to account for this albumin-dependent hydrolysis of soman. Thus, this suggests that this catalysis takes place at a different site. However, only one soman adduct on albumin was detected by MALDI-TOF. This finding is consistent with reports on the phosphonylation of bovine serum albumin by FP-biotin (*18*) and the phosphorylation of human serum albumin by diisopropylfluorophosphate (*9*). Therefore, it may be hypothesized that albumin-mediated hydrolysis of soman occurs via a mechanism that does not involve a covalent intermediate. Nevertheless, this catalytic effect is extremely weak, about 2 times higher than spontaneous hydrolysis, and may be tentatively regarded as a nonenzymatic, physicochemical interfacial reaction. However, we cannot rule out the existence of a second active center.

3.2.3. Is There Enantioselectivity in the Reaction of Albumin with Soman? Racemic soman is an equimolar mixture of four stereoisomers. Though experiments on the release of fluoride argue against the enantioselectivity of albumin for certain soman isomers, the possibility that albumin's reaction with soman is stereoselective was tested directly using ^{31}P NMR. Each of the intact isomers of soman (Ps− and Pr−) generates a doublet in ^{31}P NMR (Figure 5, panel A). Soman completely hydrolyzed in 5 N sodium hydroxide gives methylphosphonate (MP) (Figure 5, panel B); the hydrolysis of soman at pH 8.0 gives pinacolyl methylphosphonate PMP (Figure 5, panel D) (*35*).

The reaction between 1.3 mM racemic soman and 0.78 mM albumin was monitored over 24 h by recording ^{31}P NMR spectra. Initial spectra showed the progressive disappearance of the intact soman peaks with the concomitant appearance of three broader resonance peaks, of 80 Hz line width (Figure 5, panel C). After 2 h of incubation, signals for intact soman had vanished. At this point in the reaction, the spectrum of the products was compared to a spectrum of methylpinacolyl phosphonate (MPP). MPP, created under mild conditions of hydrolysis, showed a peak at 23.74 ppm. That peak was unaffected by the presence of albumin (Figure 5, panel D). The most prominent peak in the soman/albumin reaction mixture (the 23.74 ppm peak, f, in Figure 5, panel C) can therefore be assigned to MPP. For longer reaction times (up to 24 h), the MPP peak increased at the expense of the other two peaks in Figure 5, panel C. This strongly suggests that peaks e and d (at 25.59 and 27.56 ppm) correspond to the Ps− and Pr− covalent adducts of soman bound to albumin and that there is a slow, spontaneous release of MPP from the of phosphonlyated albumin. Such a release can be described as reactivation.

The fact that after 2 h of reaction between albumin and soman, adduct peaks d and e have the same intensity indicates that albumin reacted with the same probability with both the Ps− and Pr− soman enantiomers. Thus, there is no enantiomeric preference of albumin for the soman isomers.

3.2.4. Effect of MPP on Phosphonylation of Albumin by Soman. Because a large part of soman was hydrolyzed into MPP in Tris buffer at pH 8.0 during the time course of the phosphonylation reaction (Figure 5, panel C), we tested the hypothesis that MPP could compete with soman for noncovalent binding to the Tyr411 site and thereby slow down the phosphonylation reaction. We found that phosphonylation of (0.75 mM) albumin by soman (1.3 mM) in the presence of 1.3 mM MPP caused no change in the progressive inhibition of the AAA activity of albumin. Thus, MPP does not compete with soman.

3.2.5. Spontaneous Reactivation of Soman-Inhibited Albumin Monitored by ^{31}P NMR and MALDI-TOF. Fluoride has been shown to promote dephosphonylation of albumin (*36*).
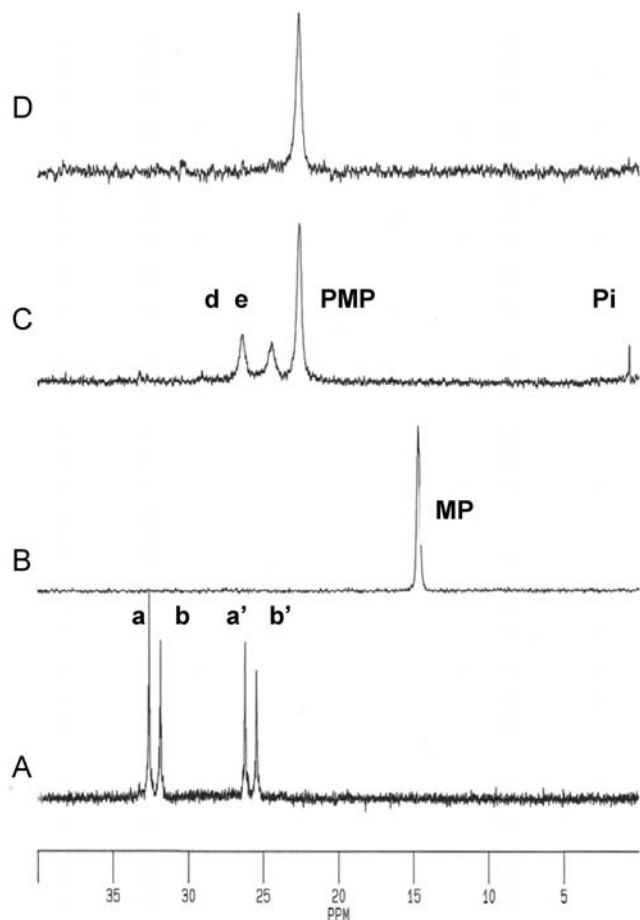
Figure 5. ^{31}P NMR spectra of soman in the presence and absence of albumin. Panel A shows 2 mM racemic soman in dimethylsulfoxide-d_6. The four stereoisomers are indistinguishable. The four resonance peaks correspond to the two doublets of the two pairs of diastereo-isomers (35). Panel B shows methyl phosphonate (MP) (a product of soman hydrolysis in 5 N NaOH). Panel C shows 1.3 mM racemic soman after reaction (2 h) with 0.78 mM albumin, in 60 mM Tris/HCl at pH 8; d and e correspond to the P_R and P_S adducts of albumin, and f is the product of the spontaneous hydrolysis of soman and methyl pinacolyl phosphonate (MPP). Panel D shows 1.3 mM methyl pinacolyl phosphonate (MPP) in the presence of 1.3 mM albumin. The observed peak is that of uncomplexed MPP (35).

However, because of the low nucleophilicity of fluoride ion, it seems unlikely that reactivation was mediated by the fluoride ions released during the phosphonylation step ([F$^-$] ≤ 1.3 mM for the highest soman concentration used). Following the reactivation rate by measuring the recovery of the AAA activity was not accurate; therefore, ^{31}P NMR spectral kinetics was used instead.

FAF-HSA (1.3 mM) was inhibited by 1.3 mM soman (10% isopropanol, final). We followed the decrease of the integrated area of the NMR peaks corresponding to the soman−albumin adduct (peaks d + e in Figure 5, panel C) from 10 to 60 h (Figure 6). Because no soman was left after 10 h of incubation, because of its spontaneous hydrolysis (S → S″ + F$^-$) and to its reaction with albumin (see Scheme 1), the change in the concentration of the soman−albumin conjugate (A−S′) was due only to reactivation (k_r). It was assumed that the process was uncompromised and followed pseudo-first-order kinetics (eq 1):

$$[A - S']_t = [A - S']_{10h} \cdot e^{-k_r(t-10)} \qquad (1)$$

The relative intensity at $t = 10$ h was 0.54 ± 0.01; this is equivalent to 0.700 ± 0.015 mM of conjugate. Fitting the data from Figure 6 to eq 1 provided the reactivation constant, $k_r =$
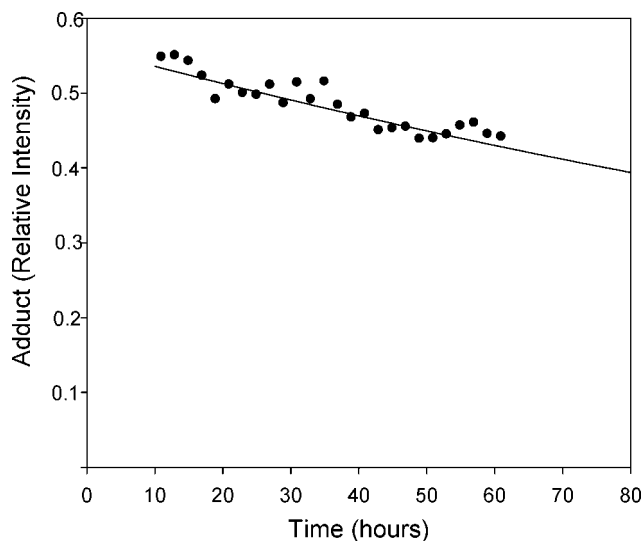
Figure 6. Reactivation kinetics by ^{31}P NMR. Each point represents the integrated area of the NMR peaks (d + e). The areas, in turn, correspond to the relative amounts of adduct. The line is from a fit of the data to eq 1.

Scheme 1
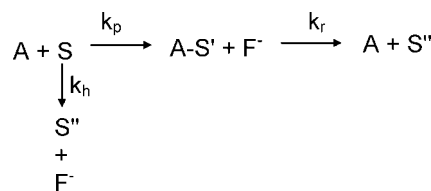
$0.0044 ± 0.0008$ h^{-1} = $0.000073 ± 0.000013$ min^{-1} = $0.74 ± 0.13$ week^{-1}. Thus the half-time for decay of the soman−albumin adduct at pH 8.0 and 25 °C is about 1 week.

The stability of the soman−albumin adduct was also measured by mass spectrometry. Soman-labeled albumin was digested with pepsin to release labeled and unlabeled Tyr411 peptides after various periods of incubation. The peptide masses and the area of each peak were determined by MALDI-TOF in reflector mode. Figure 7A shows a scan, after 24 h, where the highest peaks at 1992.1 and 1879.0 have soman bound to Tyr411 in peptides LVRYTKKVPQVSTPTL and VRYTKKVPQ-VSTPTL. At a later time point after the adduct had been incubated at pH 7.4 and 22 °C for 768 h, the unlabeled peptides at 1717.0 and 1830.1 have a higher intensity than the labeled peptides (Figure 7B). The % label on Tyr411 was calculated from cluster areas and plotted in Figure 7C as a function of time. The half-life for decay of the soman−albumin adduct at pH 7.4 and 22 °C was 20 days. The time course in Figure 7C is first order for nearly two half-lives, supporting the proposal that reactivation is a simple first order process. The difference in rate constants obtained from the mass spectrometry and the NMR experiments is consistent with expectation for the difference in pH.

3.2.6. Progressive Binding of Soman to Tyr411 of Albumin Monitored by ^{31}P NMR Kinetics. The complete reaction path of albumin (A) with soman (S) can be depicted by Scheme 1, which includes the competing spontaneous hydrolysis of soman, second-order phosphonylation of albumin, followed by hydrolytic dephosphonylation (reactivation of the AAA activity of albumin).

In Scheme 1, k_p is the rate constant of phosphonylation, k_r is the rate constant of dephosphonylation (spontaneous reactivation of phosphonylated albumin A-S′), and k_h is the rate of the
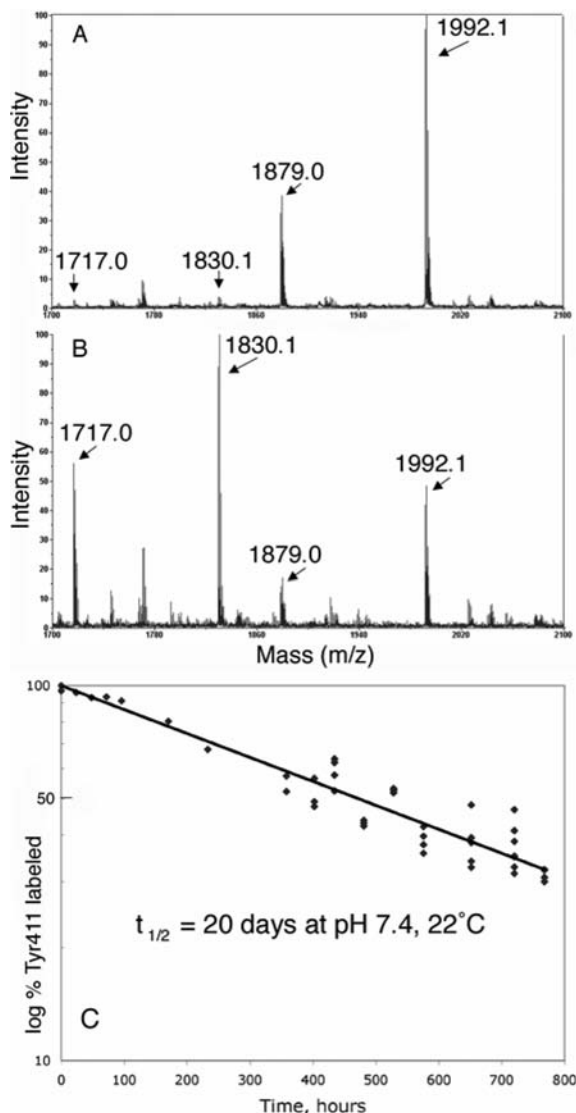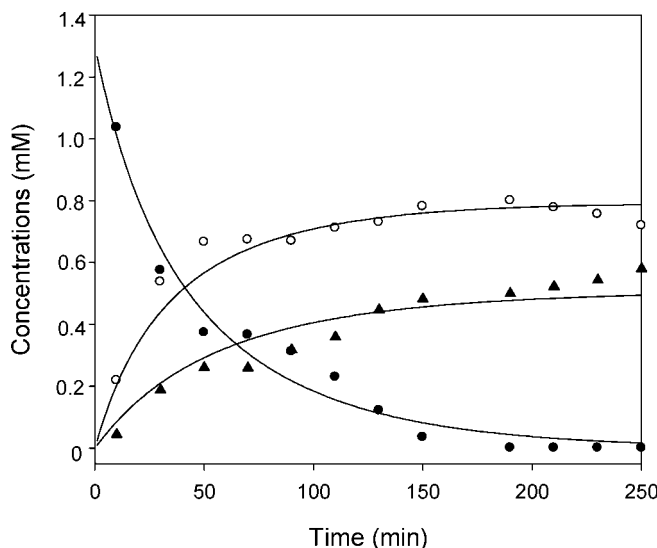
Figure 7. Stability of the soman−albumin adduct calculated from mass spectrometer data. Panels A and B are MALDI-TOF spectra of pepsin-digested, soman-labeled human albumin after 24 and 768 h incubation, respectively, at pH 7.4 and 22 °C. Panel C is a plot of % Tyr411 labeled by soman, as a function of time of incubation of the soman−albumin adduct. The soman−albumin adduct decays with a half-life of 20 days.

Figure 8. Time course of the reaction between 1.3 mM soman and 1.3 mM albumin monitored by ^{31}P NMR: ●, soman; ○, adduct; ▲, MPP. The points were measured data. The lines are from numerical fitting of the data to eq 2.

spontaneous hydrolysis of soman. F$^-$ is the fluoride leaving group and S″ the hydrolysis product, methyl pinacolyl phosphonate (MPP). It follows then that the concentration of all species as a function of time is described by a system of differential equations (eq 2) as sollows:

$$\frac{d[A]}{dt} = -k_p \cdot [A][S] + k_r \cdot [AS']$$

$$\frac{d[S]}{dt} = -k_p \cdot [A][S] + k_h \cdot [S]$$

$$\frac{d[AS']}{dt} = -\frac{d[A]}{dt} \qquad (2)$$

$$\frac{d[S'']}{dt} = -k_r \cdot [AS'] + k_h \cdot [S]$$

$$\frac{d[F^-]}{dt} = -\frac{d[S]}{dt}$$

Because the concentration of soman and albumin are of the same order of magnitude and because the rates of spontaneous hydrolysis of soman and phosphonylation of albumin are of the same order of magnitude, it is not possible to make assumptions allowing a simple integration of the system. However, a numerical solution of the system can be obtained using mathematical software such as Mathematica.

Following the residual AAA activity of albumin allows only the measurement of d[A]/dt = −d[AS′]/dt, while measuring the release of F$^-$ gives only d[F$^-$]/dt = d[S]/dt. However, following the reaction kinetics by ^{31}P NMR gives d[S]/dt = −d[F$^-$]/dt, d[AS′]/dt = −d[A]/dt, and d[S″]/dt in one single experiment (Figure 8). k_r was measured separately under the same experimental conditions ($k_r = 0.0044 \pm 0.0008$ h^{-1}; see section 3.2.4 and Figure 6).

Fitting the numerical solution of the differential equation system against ^{31}P NMR data gave $k_p = 15 \pm 3$ M^{-1} min^{-1} and $k_h = 0.0076 \pm 0.005$ min^{-1}. Thus, the rate constant for spontaneous hydrolysis of soman in the presence of albumin (k_h) is about 2 times the rate for the spontaneous hydrolysis of soman in the absence of albumin ($k_{h0} = 0.00342 \pm 0.00007$ min^{-1}, from section 3.2.2). This value for k_h is in agreement with the estimate for k_h made from the measurement of [F$^-$] release, as described in section 3.2.2.

3.3. Molecular Modeling. The crystal structure of HSA with numerous ligands has been described (5). A comparison between these structures shows that Val433 located in the pocket containing Tyr411 might adopt two different conformations depending on the occupant of the pocket. These alternate conformations change the diameter of the pocket and may affect the binding of soman in the pocket. Therefore, we docked soman with both representative crystal structures: 2bxd displaying a narrower pocket in absence of ligand and 2bxh displaying a wider pocket that develops when indoxyl sulfate is bound. The four diastereoisomers of soman were docked in both structures.

3.3.1. Noncovalent Docking by Autodock. Key values from the noncovalent docking results are summarized in Table 1. All four stereoisomers of soman bind better to HSA when the pocket is narrowed by the conformational change of Val433 (2bxd). A narrower pocket provides more stabilizing van der Waals interactions between soman and the residues of the pocket. Therefore, it is expected that the actual conformation of HSA when in complex with soman is similar to that of 2bxd. For 2bxd, the estimated affinity constants for all four stereoisomers

Table 1. Non Covalent Docking of Soman in the Tyr411 Pocket of HSA Performed by Autodock

soman isomer	HSA pdb structure	docked energy (kcal.mol^{-1})	estimated K_d (μM)
P_SC_R	2bxd	−5.69	148
	2bxh	−5.56	167
P_SC_S	2bxd	−5.76	115
	2bxh	−5.48	206
P_RC_R	2bxd	−5.69	147
	2bxh	−5.50	176
P_RC_S	2bxd	−5.73	128
	2bxh	−5.42	226

are virtually identical: $K_d = 134 \pm 16 \mu$M (Table 1). The pocket seems to be large enough to accommodate all enantiomers of soman (Figure 9). Soman binds with the pinacolyl group stacked against the disulfide bridge formed by Cys392-Cys438. The pinacolyl group makes many hydrophobic contacts with the side chains of Val433, Ile388, Ala449, Phe395, Phe403 and the main chain of Gly434. The binding conformation of soman is largely dictated by its carbon stereocenter. Indeed, P_SC_S and P_RC_S display the same binding conformation (rmsd = 0.07 Å), except that the positions of the fluoride and phosphonate oxygen are inverted as a result of the difference in stereochemistry at the phosphorus. The same applies to the P_SC_R and P_RC_R stereo-isomers (rmsd = 0.13 Å). This inversion between the fluoride and phosphonate oxygen does not cost much energy of binding because of the lack of specific interactions between these atoms and residues of the pocket. The phosphorus atom is separated from the hydroxyl of Tyr411 by a distance ranging from 6.80 Å (C_R enantiomers) to 7.24 Å (C_S enantiomers). This distance is not suitable for a nucleophilic attack of Tyr411 on the phosphorus and explains the slow reactivity of soman toward HSA. It looks like soman may randomly react with Tyr411 on its way in/out of the pocket.

3.3.2. Noncovalent Docking by Gold. In order to check the dependency of the results on the software, to test the robustness of the models obtained by Autodock, and also to generate as many conformers as possible, we decided to repeat the docking simulations using another software, Gold, version 3.1. Gold gave us the possibility of using two scoring functions, Goldscore (force-field-based like Autodock) and Chemscore (empirical, i.e., optimized on a test set of protein–ligand complexes). We performed the docking simulations using both the 2bxh and the 2bxd protein structures. Our results did not show any significant

Figure 9. Models of soman noncovalently docked into albumin. The various stereoisomers of soman were docked in the estero-amidase active center (Tyr411) of HSA using Autodock software.
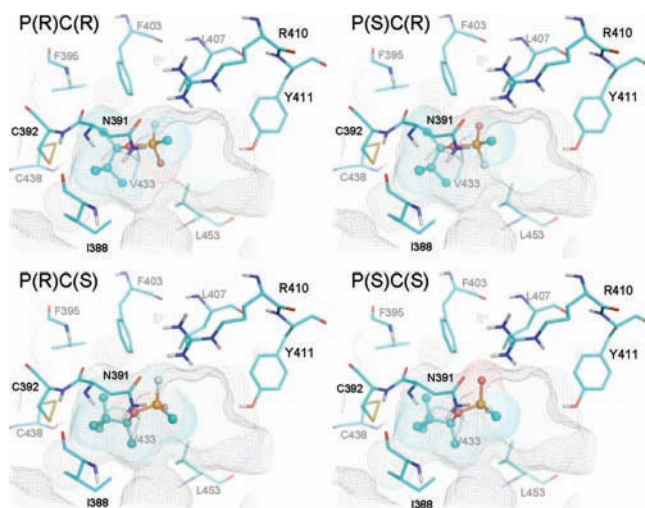
difference between the structures; therfore, we describe here only the results obtained with the minimized 2bxh protein.

We docked the four enantiomers of soman with the minimized 2bxh protein using Gold/Goldscore. The best conformers obtained were similar to the ones obtained by Autodock. The pinacolyl moiety is located at essentially the same place obtained by Autodock (Figure 9); the difference is only a small translation of Tyr411 in the direction of the phosphorus atom (P-OH$_{Y411}$ distances vary from 6.37 to 6.67 Å). As described for Autodock, the rotation of the P (O, F, Me) moiety is relatively free; this is not surprising because of the lack of specific interactions of these atoms with residues of the active site pocket. Again, the phosphorus atom is at a position that does not permit easy phosphonylation of Tyr411. The scores obtained were in the same range for all enantiomers: $P_SC_S = 39.93$, $P_SC_R = 40.09$, $P_RC_R = 41.28$, and $P_RC_S = 38.16$. We obtained very similar results in terms of conformers and energies when we used Autodock or Gold with either 2bxh or 2bxd, which clearly shows the robustness of the models in Figure 9.

The Chemscore function is empirical. It can potentially generate different binding modes because contributions of intermolecular interactions are not the same as those with Goldscore or Autodock. The docking using Gold/Chemscore gave different kinds of conformers than Goldscore, but with very small changes in energy. Within the different clusters, some models displayed a phosphorus atom close to Tyr411 (P-OH$_{Y411}$ distances: $P_RC_R = 4.33$ Å, $P_RC_S = 3.51$ Å, $P_SC_S = 3.98$ Å, and $P_SC_R = 3.41$ Å). The enantiomers with P_R configuration have a P-F in a favorable position for a nucleophilic attack (OH$_{Y411}$-P-F angle: $P_RC_R = 155°$, $P_RC_S = 138°$, $P_SC_S = 42°$, and $P_SC_R = 45°$). Chemscore docking simulation generated a prephosphonylation complex (fluorine opposite OH$_{Y411}$ and hydrogen bonding between P = O and OG$_{S489}$) for the two P_R enantiomers. These results suggest that the prephosphonylation step would be energetically more favorable for the P_R than for the P_S enantiomers. To compare these models with the previous ones, we rescored the prephosphonylation complexes with conformers P_RC_R and P_SC_S by the Goldscore function and obtained 10.78 and 27.07, respectively. Compared to the Gold/Goldscore results (41.28 and 38.16), the rescoring clearly indicates that the ligand positions in the prephosphonylation complexes are not energetically favorable. Therefore, the Chemscore results do not contradict the previous conclusions obtained from the Autodock and Gold/Goldscore dockings.

These docking results may explain why the reactivity of soman with HSA is so poor. First, the binding affinity is weak $\langle K_d \rangle = 134 \mu$M. Second, the phosphorus does not bind in a position that is favorable for reaction with Tyr411. The docking results also suggest that a higher bimolecular rate constant is probable in the case of P_R enantiomers. But because of the poor reactivity and the limited measurement accuracy, an increased reactivity of the P_R enantiomers was not experimentally observed.

3.3.3. Covalent Docking by Gold. The noncovalent docking of soman to the HSA protein showed a low enantioselectivity. In order to confirm this finding, we covalently docked the four enantiomers of soman to the 2bxh form of albumin and compared energies (or scores). We used the software Gold, version 3.1, which permits covalent docking. As done before, dockings were scored by the functions Goldscore and Chemscore. To discriminate the conformers obtained by Gold/Goldscore or Gold/Chemscore dockings, we calculated the energies of soman−protein complexes using mopac-pm3, a

Table 2. Covalent Docking of Soman in HSA Performed by Gold[a]

soman isomer	Goldscore/ΔH_f	Chemscore/ΔH_f
$P_S C_R$	11.68/489.8	15.95/519.3
$P_S C_S$	16.88/483.2	17.43/514.7
$P_R C_R$	15.67/529.0	16.46/497.8
$P_R C_S$	12.88/480.4	14.55/539.8

[a] Scores (Goldscore and Chemscore) have no units. Enthalpies of formation (ΔH_f) are in kcal·mol^{-1}.
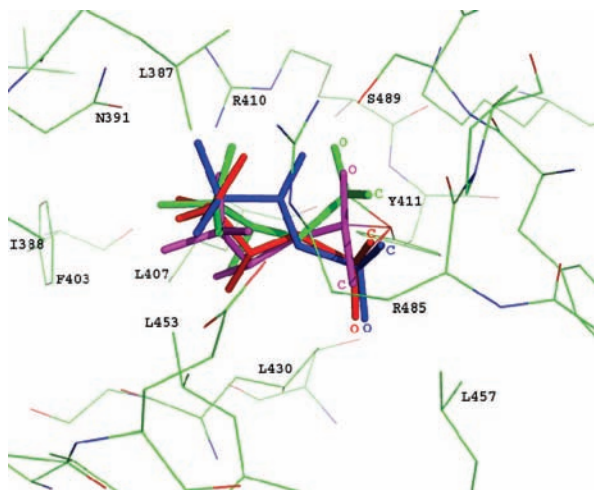
Figure 10. Models of soman covalently docked into albumin. Various enantiomers of soman were docked into Tyr 411 of HSA (form 2bxh) using Gold software, version 3.1. $P_S C_S$ (blue), $P_S C_R$ (red), $P_R C_R$ (magenta), and $P_R C_S$ (green).

semiempirical method, and selected those with the lowest ΔH_f. The results are summarized in Table 2.

The four models are superimposed in Figure 10. The position of the tertiary butyl group is well conserved for all enantiomers (it points to Leu387, Ile388, Asn391, and Phe403), while the $P = O$ points to Leu430 and Leu457 for $P_S C_R$ or $P_S C_S$ enantiomers, Ser489 (hydrogen bonding with OH) for $P_R C_R$, and R410 for $P_R C_S$. The conformers $P_S C_S$ and $P_S C_R$ are nearly perfect mirror images, the only difference being the position of the CH$_3$ bond to the asymmetric carbon that points to Leu430 for C_R and Arg410 for C_S. In the case of P_R, there are more differences between the two enantiomers because the $P_R C_R$ enantiomer is the only one that allows hydrogen bonding with Ser489 without having too many disfavored van der Waals interactions. (Arg410 constrains the position of the CH$_3$ bond to C*.) The mopac-pm3 ΔH_f values are in the same order of magnitude ($\sim$490 ± 10 kcal.mol^{-1}), showing no thermodynamic enantioselectivity.

4. Discussion

4.1. Roles for Albumin and Albumin/Soman Adducts in the Monitoring of and Protection against Soman Exposure.
4.1.1. Scavenging OP. The reaction of albumin with soman was found to be slow ($k_p = 15 \pm 3$ M^{-1} min^{-1} at pH 8.0). This is in agreement with the slow rate of reaction of albumin with the nerve agent simulant, DFP (75 M^{-1} min^{-1} at pH 8.2) (*10*). Combined with the high concentration of albumin present in plasma (0.6 mM), the apparent pseudo-first-order rate constant for the reaction of albumin with soman would be 0.009 min^{-1} ($t_{1/2} = 77$ min). Thus, despite its high concentration in blood, stoichiometric scavenging of soman by albumin is not expected to play a major role in protection against acute poisoning. Regardless of the low reactivity, significant amounts of OPs are bound to albumin upon in vivo exposure. For example, when

mice were injected with small amounts of the organophosphonate, FP-biotin (10-fluoroethoxyphosphinyl-*N*-biotinamido pentyldecanamide), amounts that produced no toxic signs, albumin was the most abundantly labeled protein in plasma (*46*), making it the dominant stoichiometric scavenger. In vitro pretreatment of plasma with a variety of organophosphates (malaoxon, paraoxon, chlorpyrifos oxon, methyl paraoxon, dichlorvos, diisopropylfluorophosphate, diazoxon, and echothiophate) reduced the subsequent reaction of FP-biotin with albumin, indicating that all of these other OPs also react with albumin (*46*). This strongly suggests that albumin will also be a scavenger for these OPs in vivo.

Although albumin displays a low reactivity toward OPs compared to that of cholinesterases and other known secondary biological targets of OPs (*37*), the large quantity of albumin in blood circulation and lymph may provide a substantial reservoir for sequestering OPs. We also found that phosphonylated albumin slowly self-reactivates. Though the catalytic OPase activity is associated with HSA, and Tyr411 is slow and thus toxicologically insignificant, it may be hypothesized that mutants of albumin capable of hydrolyzing OPs at high rate could be used for the detoxification of soman in vivo.

4.1.2. Biomarker. Phosphonylated albumin may prove to be a useful biological marker of soman exposure (*11*). The sensitive mass spectrometry methods used by Black et al. (*11*) and further developed in the present article could prove useful for the diagnosis of soman exposure. In particular, it has been shown that soman tyrosine adducts can be detected at least up to 7 days post exposure in guinea pigs (*38*). Advantages of a soman−albumin biomarker include its stability and the absence of aging. The half-life for spontaneous reactivation is estimated to be about 1 week at pH 8.0 and 25 °C, and 20 days at pH 7.4 and 22 °C, making the soman−albumin adduct suitable for retrospective studies. The absence of aging means that soman exposure can be unambiguously identified because the soman−albumin adduct does not lose the diagnostic pinacolyl group. Our finding that soman−albumin adducts do not age confirms the reports that there is no loss of alkoxy groups from soman−, sarin−, or DFP−albumin adducts (*11, 19, 36*). In addition, it has recently been shown that OP−albumin conjugates do not appear to be reactivatable by oximes used as antidotes of OP poisoning. Therefore, the detection of Tyr411 adducts in plasma may be possible, even though individuals exposed to OPs have received effective oxime therapy (*38*).

Another potential method of monitoring for soman exposure is through the use of antibodies. The information presented in this work raises interesting possibilities regarding the generation of antibodies to the soman−albumin adduct. The noteworthy aspect of the soman−albumin adduct in this regard is that Tyr411 is located on the surface of albumin. A soman−albumin adduct at Tyr411 therefore becomes a viable target for antibodies, unlike the soman adducts of cholinesterases, which are buried in a deep gorge well below the enzyme's surface. In addition, the surface location for the soman−albumin adduct suggests that people exposed to soman might normally produce antibodies against the soman−albumin adduct. This in turn suggests the possibility of monitoring exposure to soman by looking for those antibodies, long after the exposure incident has passed and long after the antigen has disappeared.

4.2. Perspectives: Would Mutant Albumins Be Good OP Scavengers? 4.2.1. Stoichiometric Scavenging. The bimolecular rate constant for the phosphonylation of albumin, k_p, 15 M^{-1} min^{-1}, is about 6×10^6 times slower than that for the inhibition of acetylcholinesterase and butyrylcholinesterase by

soman ($\sim 9 \times 10^7$ M^{-1} min^{-1}). Because the concentration of soman in the most severe cases of poisoning would be far less than that of albumin in plasma, for example, <11 nM (*39*), the reaction between albumin and soman would be pseudo-first-order. The pseudo-first-order rate expression can be rearranged (eq 3) so that the time, t, needed for a stoichiometric scavenger to reduce a concentration of a toxicant such as soman from $[S]_0$ to $[S]_t$ can be easily determined.

$$t = \frac{\ln([S]_0/[S]_t)}{k_p \cdot [E]} \quad (3)$$

Since the concentration of albumin in plasma is about 0.6 mM, it would take about 8.5 h to reduce the soman concentration by 100-fold (Ln $[S]_0/[S]_t$ = 4.6). Because, red blood cell acetylcholinesterase, plasma butyrylcholinesterase, and plasma paraoxonase react much faster than albumin with soman, the contribution of albumin to soman detoxification would take place only after the saturation of these enzymes (*36*).

4.2.2. Catalyic Scavenging. If we assume that the turnover of soman by albumin fits a Michael mechanism with a high K_m, then phosphonylation could appear to be second-order under our experimental conditions. If in addition, $k_r << k_p$, which is the case for the soman/albumin turnover, then k_{cat}/K_m is equal to k_p. Under these conditions, k_p defines the catalytic efficiency. Thus, the catalytic efficiency for the hydrolysis of soman by albumin, at Tyr411, is 15 M^{-1} min^{-1}. This value is about 4 to 5 orders of magnitude lower than that for the hydrolysis of soman by *Pseudomonas diminuta* phosphotriesterase (6×10^5 M^{-1} min^{-1}) (*40*) or allozyme Q192 of human paraoxonase (2.6×10^6 M^{-1} min^{-1}) (*41*). Eq 4 gives the time needed for a catalytic scavenger to drop the concentration of a toxicant from $[S]_0$ to $[S]_t$.

$$t = \frac{\ln([S]_0/[S]_t)}{(k_{cat}/K_m) \cdot [E]} \quad (4)$$

Thus, taking the estimated k_{cat}/K_m value, the time needed for the catalytic activity of albumin (0.6 mM) to decrease the soman concentration in blood by 100-fold would be about 9 h. It is therefore obvious that the reaction of soman at Tyr411 of HSA does not contribute significantly to the catalytic turnover of soman molecules in plasma. However, the in vitro observation that pure FAF-HSA promotes the hydrolysis of soman at a second site (k_h = 0.0076 min^{-1}) with a rate 100 times higher than the turnover at Tyr411 is important. The in vivo toxicological relevance of this chemical activity has to be demonstrated, but if proved, this process could contribute to the degradation of soman and other nerve agents in human plasma.

4.2.3. Mutant Albumin. Could mutants of recombinant human albumin be made into productive stoichiometric or catalytic scavengers for prophylaxis and treatment of OP poisoning? HSA is a nonglycosylated protein. Scaled-up production of recombinant human albumin (rHSA) in *Pichia pastoris* has been made possible for pharmaceutical purposes (*42*). This product exhibits good pharmacokinetics and biodistribution (*43*). Thus, rHSA would appear to be an ideal candidate for protein engineering.

To address the scavenger issue of rHSA, we have to first determine how much improvement in reactivity would be desired. As a reference, the reactivity of the currently accepted OP scavengers, serum butyrylcholinesterase and red cell acetylcholinesterase, were used. Comparison was made on the basis of the first-order rate constants. For the reaction of natural HSA with soman in plasma, the apparent pseudofirst order rate

constant, $k_p \cdot [E]$, is 0.009 min^{-1}. The sum of the first-order reaction rate constants for the reaction of soman with erythrocyte AChE and plasma BuChE is 4.5 min^{-1}. This number was arrived at by taking the concentration of AChE in blood to be about 2.5 nM, the concentration of BuChE to be 50 nM, and k_2/K_d to be about 9×10^7 M^{-1} min^{-1} for both enzymes. Thus, in blood, cholinesterases react with soman about 500 times faster than albumin does.

For an injected, mutated albumin to be used as a stoichiometric scavenger, it should react at least 500 times faster than the endogenous albumin to be competitive with the cholinesterases. There is a limit to the amount of plasma-derived albumin that can be put into the human body, that is, 25 g/100 mL (Albu Rx25) by slow infusion or 500 mg in 2 mL by intravenous injection. Injected into a human of 70 kg (3 L of plasma), 500 mg would give a final plasma concentration of mutant albumin of 166 mg/L (2.55×10^{-6} M). To react faster than cholinesterases, the bimolecular rate constant of this amount of mutant albumin should be at least 1.8×10^6 M^{-1} min^{-1}. Compared to endogenous albumin (15 M^{-1} min^{-1}), this is an efficiency improvement of about 5 orders of magnitude. Though there are few examples of evolved enzymes, showing enhancement of such a magnitude, site-directed mutagenesis and/or directed evolution can lead to dramatic improvement in the catalytic activity of enzymes. Improvements of 4 orders of magnitude for the glyphosate tolerance protein (*44*) and 5 orders of magnitude for α-lytic protease (*45*) have been reported. Therefore, improving the reactivity of albumin against OPs for the purpose of making a stoichiometric scavenger would be a challenge, but it is possible.

In addition, the observed catalysis of soman hydrolysis on the albumin surface at a site different from Tyr 411 could also be improved. Work is in progress to identify this area on the albumin surface. Thus, stoichiometric and catalytic bioscavengers based on modified human albumins have to be considered as possible candidates.

References

(1) Sakurai, Y., Ma, S. F., Watanabe, H., Yamaotsu, N., Hirono, S., Kurono, Y., Kragh-Hansen, U., and Otagiri, M. (2004) Esterase-like activity of serum albumin: characterization of its structural chemistry using p-nitrophenyl esters as substrates. *Pharm. Res. 21*, 285–292.

(2) Manoharan, I., and Boopathy, R. (2006) Diisopropylfluorophosphate-sensitive aryl acylamidase activity of fatty acid free human serum albumin. *Arch. Biochem. Biophys. 452*, 186–188.

(3) Masson, P., Froment, M.-T., Darvesh, S., Schopfer, L. M., and Lockridge, O. (2007) Aryl acylamidase activity of human serum albumin with o-nitrotrifluoroacetanilide as the substrate. *J. Enzyme Inhib. Med. Chem. 22*, 463–469.

(4) Watanabe, H., Tanase, S., Nakajou, K., Maruyama, T., Kragh-Hansen, U., and Otagiri, M. (2000) Role of arg-410 and tyr-411 in human serum albumin for ligand binding and esterase-like activity. *Biochem. J. 349*, 813–819.

(5) Ghuman, J., Zunszain, P. A., Petitpas, I., Bhattacharya, A. A., Otagiri, M., and Curry, S. (2005) Structural basis of the drug-binding specificity of human serum albumin. *J. Mol. Biol. 353*, 38–52.

(6) Mourik, J., and de Jong, L. P. (1978) Binding of the organophosphates parathion and paraoxon to bovine and human serum albumin. *Arch. Toxicol. 41*, 43–48.

(7) Maliwal, B. P., and Guthrie, F. E. (1981) Interaction of insecticides with human serum albumin. *Mol. Pharmacol. 20*, 138–144.

(8) Silva, D., Cortez, C. M., Cunha-Bastos, J., and Louro, S. R. (2004) Methyl parathion interaction with human and bovine serum albumin. *Toxicol. Lett. 147*, 53–61.

(9) Sanger, F. (1963) Amino-acid sequences in the active centers of certain enzymes. *Proc. Chem. Soc. 5*, 76–83.

(10) Means, G. E., and Wu, H. L. (1979) The reactive tyrosine residue of human serum albumin: characterization of its reaction with diisopropylfluorophosphate. *Arch. Biochem. Biophys. 194*, 526–530.

(11) Black, R. M., Harrison, J. M., and Read, R. W. (1999) The interaction of sarin and soman with plasma proteins: the identification of a novel phosphonylation site. *Arch. Toxicol. 73*, 123–126.

(12) De Bisschop, H. C., De Meerleer, W. A., Van Hecke, P. R., and Willems, J. L. (1987) Stereoselective hydrolysis of soman in human plasma and serum. *Biochem. Pharmacol. 36*, 3579–3585.

(13) Sogorb, M. A., Monroy, A., and Vilanova, E. (1998) Chicken serum albumin hydrolyzes dichlorophenyl phosphoramidates by a mechanism based on transient phosphorylation. *Chem. Res. Toxicol. 11*, 1441–1446.

(14) Sogorb, M. A., Carrera, V., and Vilanova, E. (2004) Hydrolysis of carbaryl by human serum albumin. *Arch. Toxicol. 78*, 629–634.

(15) Sogorb, M. A., Diaz-Alejo, N., Escudero, M. A., and Vilanova, E. (1998) Phosphotriesterase activity identified in purified serum albumins. *Arch. Toxicol. 72*, 219–226.

(16) Sogorb, M. A., and Vilanova, E. (2002) Enzymes involved in the detoxification of organophosphorus, carbamate and pyrethroid insecticides through hydrolysis. *Toxicol. Lett. 128*, 215–228.

(17) Sogorb, M. A., Alvarez-Escalante, C., Carrera, V., and Vilanova, E. (2007) An in vitro approach for demonstrating the critical role of serum albumin in the detoxication of the carbamate carbaryl at in vivo toxicologically relevant concentrations. *Arch. Toxicol. 81*, 113–119.

(18) Schopfer, L. M., Champion, M. M., Tamblyn, N., Thompson, C. M., and Lockridge, O. (2005) Characteristic mass spectral fragments of the organophosphorus agent FP-biotin and FP-biotinylated peptides from trypsin and bovine albumin (Tyr410). *Anal. Biochem. 345*, 122–132.

(19) Li, B., Schopfer, L. M., Hinrichs, S. H., Masson, P., and Lockridge, O. (2007) Matrix-assisted laser desorption/ionization time-of-flight mass spectrometry assay for organophosphorus toxicants bound to human albumin at Tyr411. *Anal. Biochem. 361*, 263–272.

(20) Riches, J., Morton, I., Read, R. W., and Black, R. M. (2005) The trace analysis of alkyl alkylphosphonic acids in urine using gas chromatography-ion trap negative ion tandem mass spectrometry. *J. Chromatogr., B 816*, 251–258.

(21) Ordentlich, A., Barak, D., Kronman, C., Benschop, H. P., De Jong, L. P., Ariel, N., Barak, R., Segall, Y., Velan, B., and Shafferman, A. (1999) Exploring the active center of human acetylcholinesterase with stereomers of an organophosphorus inhibitor with two chiral centers. *Biochemistry 38*, 3055–3066.

(22) Darvesh, S., McDonald, R. S., Darvesh, K. V., Mataija, D., Mothana, S., Cook, H., Carneiro, K. M., Richard, N., Walsh, R., and Martin, E. (2006) On the active site for hydrolysis of aryl amides and choline esters by human cholinesterases. *Bioorg. Med. Chem. 14*, 4586–4599.

(23) Kitz, R., and Wilson, I. B. (1962) Esters of methanesulfonic acid as irreversible inhibitors of acetylcholinesterase. *J. Biol. Chem. 237*, 3245–3249.

(24) Morris, G. M., Goodsell, D. S., Halliday, R. S., Huey, R., Hart, W. E., Belew, R. K., and Olson, A. J. (1998) Automated docking using a Lamarckian genetic algorithm and an empirical binding free energy function. *J. Comput. Chem. 19*, 1639–1662.

(25) Sanner, M. F. (1999) Python: a programming language for software integration and development. *J. Mol. Graphics 17*, 57–61.

(26) Berendsen, H. J. C., van der Spoel, D., and van Drunen, R. (1995) Gromacs: a message-passing parallel molecular dynamics implementation. *Comput. Phys. Commun. 91*, 43–56.

(27) Lindahl, E., Hess, B., and van der Spoel, D. (2001) Gromacs 3.0: a package for molecular simulation and trajectory analysis. *J. Mol. Model. 7*, 306–317.

(28) Oostenbrink, C., Villa, A., Mark, A. E., and van Gunsteren, W. F. (2004) A biomolecular force field based on the free enthalpy of hydration and solvation: the GROMOS force-field parameter sets 53A5 and 53A6. *J. Comput. Chem. 25*, 1656–1676.

(29) Stewart, J. J. P. (1989) Optimization of parameters for semiempirical methods I. Method. *J. Comput. Chem. 10*, 209–220.

(30) Jones, G., Willett, P., Glen, R. C., Leach, A. R., and Taylor, R. (1997) Development and validation of a genetic algorithm for flexible docking. *J. Mol. Biol. 267*, 727–748.

(31) Eldridge, M. D., Murray, C. W., Auton, T. R., Paolini, G. V., and Mee, R. P. (1997) Empirical scoring functions: I. The development of a fast empirical scoring function to estimate the binding affinity of ligands in receptor complexes. *J. Comput.-Aided Mol. Des. 11*, 425–445.

(32) Tsuge, K., and Seto, Y. (2006) Detection of human butyrylcholinesterase-nerve gas adducts by liquid chromatography-mass spectrometric analysis after in gel chymotryptic digestion. *J. Chromatogr., B 838*, 21–30.

(33) Fidder, A., Hulst, A. G., Noort, D., de Ruiter, R., van der Schans, M. J., Benschop, H. P., and Langenberg, J. P. (2002) Retrospective detection of exposure to organophosphorus anti-cholinesterases: mass spectrometric analysis of phosphylated human butyrylcholinesterase. *Chem. Res. Toxicol. 15*, 582–590.

(34) Frost, A. A., and Pearson, R. G. (1965) *Kinetics and Mechanisms: A Study of Homogeneous Chemical Reactions*, 2nd ed., John Wiley & Sons, New York.

(35) Segall, Y., Waysbort, D., Barak, D., Ariel, N., Doctor, B. P., Grunwald, J., and Ashani, Y. (1993) Direct observation and elucidation of the structures of aged and nonaged phosphorylated cholinesterases by 31P NMR spectroscopy. *Biochemistry 32*, 13441–13450.

(36) Adams, T. K., Capacio, B. R., Smith, J. R., Whalley, C. E., and Korte, W. D. (2004) The application of the fluoride reactivation process to the detection of sarin and soman nerve agent exposures in biological samples. *Drug Chem. Toxicol. 27*, 77–91.

(37) Casida, J. E., and Quistad, G. B. (2004) Organophosphate toxicology: safety aspects of nonacetylcholinesterase secondary targets. *Chem. Res. Toxicol. 17*, 983–998.

(38) Williams, N. H., Harrison, J. M., Read, R. W., and Black, R. M. (2007) Phosphylated tyrosine in albumin as a biomarker of exposure to organophosphorus nerve agents. *Arch. Toxicol. 81*, 627–639.

(39) Sweeney, R. E., and Maxwell, D. M. (2003) A theoretical expression for the protection associated with stoichiometric and catalytic scavengers in a single compartment model of organophosphorus poisoning. *Math Biosci. 181*, 133–143.

(40) Dumas, D. P., Durst, H. D., Landis, W. G., Raushel, F. M., and Wild, J. R. (1990) Inactivation of organophosphorus nerve agents by the phosphotriesterase from Pseudomonas diminuta. *Arch. Biochem. Biophys. 277*, 155–159.

(41) Davies, H. G., Richter, R. J., Keifer, M., Broomfield, C. A., Sowalla, J., and Furlong, C. E. (1996) The effect of the human serum paraoxonase polymorphism is reversed with diazoxon, soman and sarin. *Nat. Genet. 14*, 334–336.

(42) Kobayashi, K. (2006) Summary of recombinant human serum albumin development. *Biologicals 34*, 55–59.

(43) Matsushita, S., Chuang, V. T., Kanazawa, M., Tanase, S., Kawai, K., Maruyama, T., Suenaga, A., and Otagiri, M. (2006) Recombinant Human Serum Albumin Dimer has High Blood Circulation Activity and Low Vascular Permeability in Comparison with Native Human Serum Albumin. *Pharm. Res. 23*, 882–891.

(44) Castle, L. A., Siehl, D. L., Gorton, R., Patten, P. A., Chen, Y. H., Bertain, S., Cho, H. J., Duck, N., Wong, J., Liu, D., and Lassner, M. W. (2004) Discovery and directed evolution of a glyphosate tolerance gene. *Science 304*, 1151–1154.

(45) Bone, R., Fujishige, A., Kettner, C. A., and Agard, D. A. (1991) Structural basis for broad specificity in alpha-lytic protease mutants. *Biochemistry 30*, 10388–10398.

(46) Peeples, E. S., Schopfer, L. M., Duysen, E. G., Spaulding, R., Voelker, T., Thompson, C. M., and Lockridge, O. (2005) Albumin, a new biomarker of organophosphorous toxicant exposure, indentified by mass spectrometry. *Toxicol. Sci. 83*, 303–312.